JOURNAL OF GEOPHYSICAL RESEARCH, VOL. 102, NO. D24, PAGES 28,731–28,769, DECEMBER 26, 1997

BOREAS in 1997: Experiment overview, scientific results, and future directions

Piers J. Sellers,[1] Forrest G. Hall,[1] Robert D. Kelly,[2] Andrew Black,[3] Dennis Baldocchi,[4] Joe Berry,[5] Michael Ryan,[6] K. Jon Ranson,[1] Patrick M. Crill,[7] Dennis P. Lettenmaier,[8] Hank Margolis,[9] Josef Cihlar,[10] Jeffrey Newcomer,[1] David Fitzjarrald,[11] Paul G. Jarvis,[12] Stith T. Gower,[13] David Halliwell,[14] Darrel Williams,[1] Barry Goodison,[15] Diane E. Wickland,[16] and Florian E. Guertin[10]

Abstract. The goal of the Boreal Ecosystem-Atmosphere Study (BOREAS) is to improve our understanding of the interactions between the boreal forest biome and the atmosphere in order to clarify their roles in global change. This overview paper describes the science background and motivations for BOREAS and the experimental design and operations of the BOREAS 1994 and BOREAS 1996 field years. The findings of the 83 papers in this journal special issue are reviewed. In section 7, important scientific results of the project to date are summarized and future research directions are identified.

1. Introduction

Persuasive arguments indicate that there will be global warming resulting from the continuing increase in atmospheric CO_2 concentration [*Houghton et al.*, 1995; *Hasselmann*, 1997]. However, there are uncertainties about the magnitude and regional patterns of projected global change because of shortcomings in the atmospheric general circulation models (AGCMs) used for climate simulation. There is a real need to improve (1) our understanding of basic climatic physical and dynamic processes so that we can enhance the realism and accuracy of AGCMs and (2) our ability to quantify global-scale climate variables and parameters to better initialize and validate models. Success in these two research areas should result in improved climate models and data sets, which in turn should provide more credible and useful climate projections [*Trenberth*, 1992; *Sellers et al.*, 1997].

The exchanges of energy, water, and carbon between the atmosphere and the continents represent the lower boundary condition for the atmospheric physical climate system and the climatic forcing to terrestrial biota and biogeochemical cycles. The magnitudes and dynamics of these exchanges and many of their controlling processes are poorly understood for most of the Earth's ecosystems. The boreal forest is a good example: this ecosystem encircles the Earth above 48°N, is second in areal extent only to the world's tropical forests, occupies about 21% of the forested land surface [*Whittaker and Likins*, 1975], and contains 13% of the carbon stored in biomass and 43% of the carbon stored in soil [*Schlesinger*, 1991]. Several climate model projections indicate that the greatest warming will occur at these high latitudes (43°–65°N) with the most marked effects within the continental interiors [*Houghton et al.*, 1995; *Mitchell*, 1983; *Schlesinger and Mitchell*, 1987; *Sellers et al.*, 1996a]. Large perturbations in northern continental climates are expected to lead to changes in the carbon cycle and the ecological functioning of the boreal forest, which could feedback onto the global climate. Thus the size of the boreal forest, its sensitivity to relatively small climatic variations, and its importance to the climate of the northern hemisphere and the global carbon cycle combine to make it an important biome to understand and to represent correctly in global models.

The Boreal Ecosystem-Atmosphere Study (BOREAS) was initiated as a large-scale international investigation focused on improving our understanding of the exchanges of radiative energy, sensible heat, water, CO_2, and other radiatively active trace gases between the boreal forest and the lower atmosphere. A primary objective of BOREAS was to collect the data needed to improve computer simulation models of the important processes controlling these exchanges so that the effects of global change on the biome can be anticipated, in particular the effects of altered temperature and precipitation, as well as providing AGCMs with better land surface process submodels and data sets for the boreal zone. The field phase of the experiment extended from 1993 to 1997 and included two series of intensive field campaigns in 1994 and 1996. Monitoring of the BOREAS study area will continue on a reduced basis through at least 2001 and some infrastructure may be retained for possible follow-up studies. This journal special issue brings together results from field work conducted in 1994, and to a lesser extent in 1996, and some preliminary findings from modeling studies. A 2-year program of follow-on analyses of the

[1]NASA Goddard Space Flight Center, Greenbelt, Maryland.
[2]University of Wyoming, Laramie.
[3]University of British Columbia, Vancouver, Canada.
[4]National Oceanographic and Atmospheric Administration, Oak Ridge, Tennessee.
[5]Carnegie Institution, Stanford, California.
[6]United States Department of Agriculture, Fort Collins, Colorado.
[7]University of New Hampshire, Durham.
[8]University of Washington, Seattle.
[9]Centre de Recherche en Biologie Forestière, Sainte-Foy, Quebec, Canada.
[10]Canada Center for Remote Sensing, Ottawa.
[11]Atmospheric Sciences Resource Center, Albany, New York.
[12]University of Edinburgh, Edinburgh, Scotland.
[13]University of Wisconsin, Madison.
[14]Forestry Canada, Edmonton, Alberta, Canada.
[15]Atmospheric Environment Service, Downsview, Ontario, Canada.
[16]NASA Headquarters, Washington, D.C.

Paper number 97JD03300.
0148-0227/97/97JD-03300$09.00

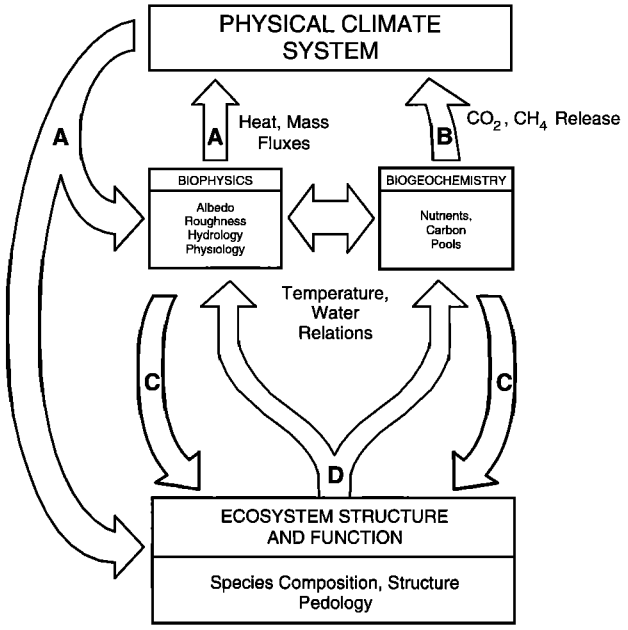

Figure 1. Important interactions between the boreal forest and the atmosphere with respect to global change. (a) Influence of changes in the physical climate system on biophysical processes. These may feedback to the atmosphere through changes in energy, heat, water, and CO_2 exchange; (b) changes in nutrient cycling rates; release of CO_2 and CH_4 from the soil carbon pool back to the atmosphere; (c) changes in biogeochemical processes and water and nutrient availability influence community composition and structure; (d) change in species composition results in changes in surface biophysical characteristics and biogeochemical process rates.

BOREAS data set will be initiated in late 1997. Other work from BOREAS has been published elsewhere, notably in a special issue of *Tree Physiology* [*Margolis and Ryan*, 1997]. This overview paper describes the BOREAS experiment, reviews the constituent papers of the special issue, summarizes the important results of work done to date, and identifies future research directions.

2. Science Background

The interactions between the boreal forest and the atmosphere can be grouped into physical climate system processes, carbon and biogeochemistry, and ecology (see Figure 1). These are discussed in turn below, with particular emphasis on the issues addressed by BOREAS.

2.1. Physical Climate System

At the present rate of increase, atmospheric CO_2 concentration will double before the end of the next century [*Houghton et al.*, 1995]. Climate simulations made with AGCMs point to large temperature increases in the northern high-latitude continental interiors [*Schlesinger and Mitchell*, 1987; *Houghton et al.*, 1995; *Sellers et al.*, 1996a], partly due to projected changes in the polar sea ice climatology and snow-albedo feedbacks. A significant warming trend was observed in the boreal zone during the 1980s and early 1990s, reaching 1.25°C per decade within the Canadian interior [*Chapman and Walsh*, 1993]. *Keeling et al.* [1996] analyzed time series of atmospheric CO_2 concentrations to show that this warming may have led to a lengthening of the approximately 150-day growing season by about 6 days at higher latitudes. *Keeling et al.*'s [1996] result has recently been supported by analysis of a global satellite data record which suggests that the growing season and photosynthetic activity increased over large areas of Europe, northern Eurasia, Alaska, and Canada for the same period [*Myneni et al.*, 1997].

The land surface parameterizations (LSPs) and surface parameter sets used in AGCMs have improved considerably over the last decade [*Sellers et al.*, 1997]. Climate models use many of the same formulations, submodels, and parameters as numerical weather prediction (NWP) models; the latter also benefit from a continuous process of operational verification. Recent experience has shown that the results of large-scale field experiments are usually transferred first to NWP models [*Betts et al.*, 1993, 1996, 1997, 1998] and later to climate models [*Sellers et al.*, 1995a, 1997]. In any case, if a process submodel is responsible for systematic errors in an NWP model, it will certainly lead to even larger biases in a climate model which is not reinitialized at short time intervals. Analyses have demonstrated that until very recently, even the best NWP models consistently overpredicted the evaporation rates and specified unrealistic winter albedo fields over the boreal region with serious consequences for forecasting skill [*Sellers et al.*, 1995b; *Betts and Ball*, this issue]. The reasons for these errors were directly connected to misrepresentations of important biophysical processes in LSPs, for example, controls on evapotranspiration, and inaccuracies in specifying model parameters, such as the extent, type, and density of forest biomes. The main aims of the physical climate system component of BOREAS were therefore to provide data which could be used (1) to improve and validate LSPs and (2) to enhance methods for deriving parameter fields from satellite observations, which are the only feasible, consistent means of providing global surface data sets. NWP models have already benefited from this work, and climate models are expected to benefit in due course.

2.2. Carbon and Biogeochemistry

The physical climate system is strongly coupled to the global carbon cycle. Temperature and precipitation anomalies have been compared with seasonal variations in atmospheric CO_2 concentration and isotopic analyses to show that warm years over the northern continents are associated with a net terrestrial carbon sink, while cold and/or dry years are associated with a net source of terrestrial carbon [*Keeling et al.*, 1995; *Ciais et al.*, 1995; *Denning et al.*, 1995; *Tans et al.*, 1990]. Together, these recent studies suggest that the northern continents acted as a large sink for atmospheric carbon, an average of 1–2 Gt C yr^{-1} over the 1980s, or about 15 to 30% of the anthropogenic CO_2 flux from fossil fuel burning. The exact biophysical mechanisms responsible for this sink are unclear, although the hypothesized lengthening of the growing season could be a factor [*Keeling et al.*, 1996; *Myneni et al.*, 1997]. The boreal ecosystem is vast, between 12 million km^2 [*Whittaker and Likins*, 1975] and 20 million km^2; the latter figure we compute from the classification of *DeFries and Townshend* [1994], as published by *Meeson et al.* [1995] and described by *Sellers et al.* [1996b]. Simple arithmetic implies then that on average, only 50–80 g C m^{-2} yr^{-1} need be sequestered to account for a 1 Gt C yr^{-1} global sink. As will be seen later in this paper, such a number is well within the range of annual carbon uptake values estimated from eddy correlation data acquired at the BOREAS tower sites. However, to extrapolate these measurements to

the entire boreal zone, or into the future from a couple of years worth of data, necessitates a deeper understanding of the climatological and physiological processes controlling carbon uptake, respiration, and fire frequency, how such processes depend on soil and land cover type, and how they might be affected by change. From the outset an important objective of BOREAS was to acquire the data needed to improve terrestrial carbon models for the boreal region. In particular, data are needed to improve our understanding of the dependence of carbon fluxes on physical climate variations and to develop methods for extracting useful parameters from satellite data.

2.3. Ecology

Carbon sequestration in the boreal ecosystem amounts to the relatively small difference between gains from photosynthesis and losses due to respiration in the plants, roots, and soils. For roughly the past 8000 years after the last glaciation, the boreal ecosystem has been accumulating carbon in its soils, particularly in deep layers of organic peat where soil organic matter accumulates under water-saturated conditions. *Harden et al.* [1992] place historical carbon accumulation rates in these peat soils in the range of 10–50 g C m^2 yr^{-1} through surface moss production, fine root turnover, and litter fall. On shorter timescales, primary carbon storage mechanisms appear to be in aboveground standing biomass. The progressive warming that occurred during the 1980s and early 1990s could have altered rates of photosynthesis, soil respiration, and fire frequency in the region. In addition to driving changes in the ecophysiology of the biome, continued warming could eventually alter the spatial structure of the boreal ecosystem. There have been several attempts to map the future extent of the northern biomes based on the projected warming and drying regime due to a "doubled-CO_2" climate. Some of these suggest that the North American boreal forest would move north and perhaps split into two halves: one in Alaska and the Canadian Northwest and the other in the Canadian Northeast [*Rizzo and Wiken*, 1992]. Such changes may themselves have significant feedbacks on the climate system through changes in winter albedos and energy fluxes over the altered land surfaces.

The earliest discussions about BOREAS recognized the importance of the issues reviewed above; they also recognized how these issues are mutually dependent and that an integrated experimental strategy that addressed all three disciplines offered the most profitable scientific approach (see Figure 1). BOREAS, however, has served to elaborate and sharpen the detailed questions related to these issues and has provided partial resolution to many of them.

3. Experimental Objectives

BOREAS was designed to bridge a wide range of spatial scales because some of the important governing processes can only be studied at very small spatial scales (e.g., the links among leaf biochemistry, spectral properties, and photosynthesis), but ultimately, the scientific gains must be applied within the context of AGCMs, carbon cycle models, or similar large-scale studies. A multi-scale-nested design was developed which permits knowledge at one scale to be translated and compared to that obtained or inferred at different scales (see Plate 1). The governing objectives of BOREAS can be stated as follows:

1. Improve the process models that describe the exchanges of radiative energy, water, heat, carbon, and trace constituents between the boreal forest and the atmosphere. The approach here was to measure the fluxes of energy (radiation, heat) and mass (water, CO_2, and radiatively important trace gases) at several scales along with observations of the ecological, biogeochemical, and atmospheric conditions controlling them. Data collection schemes were designed to support development and testing of process models that will be applied to the global change issues described above. The field observations that support process model development include measurements of water, CO_2, and trace gas fluxes at the small plot or leaf scale (chambers, porometers), the stand scale (tower-mounted eddy correlation and profile instrumentation), and the mesoscale and regional scales (airborne eddy correlation; meteorological measurements and analyses). At the smaller length scales, these measurements were coordinated with a series of ecological, meteorological, and edaphic observations to link these fluxes to appropriate state variables (see Plate 1).

2. Develop methods for applying the process models over large spatial scales using remote sensing and other integrative modeling techniques. The process studies described in objective 1 above were coordinated with remote sensing investigations using satellite, airborne, and surface-based instruments that focus on methods for quantifying critical state variables. These remote sensing studies, combined with mesoscale meteorological studies, will allow us to scale up and apply process models to regional and ultimately global scales. Some large-scale validation techniques were incorporated in the experiment design to test scale-integration methods directly; these techniques included airborne flux and profile measurements, meteorological observations, and modeling.

4. Experiment Design and Resources

The objectives of BOREAS relate to two spatial scales that had to be reconciled within the experiment design. The primary focus of objective 1 is most easily addressed by local-scale (a few centimeters to a few kilometers) process studies that involve detailed, coordinated in situ observations. These local-scale studies had to be connected to the larger-scale measurement and analysis tools associated with objective 2, which was directed toward defining regional-scale (10–1000 km) fluxes and states. In BOREAS, as in previous field experiments such as the First ISLSCP (International Satellite Land Surface Climatology Project) Field Experiment (FIFE) [*Sellers et al.*, 1992a; *Hall and Sellers*, 1995] and the Hydrological Atmospheric Pilot Experiment-Sahel, HAPEX-Sahel [*Goutorbe et al.*, 1994], the science team adopted a nested multiscale measurement strategy to integrate observations and process models over the scale range, as shown in Plate 1.

The resolution of global AGCMs, of the order of hundreds of kilometers, defined the largest spatial domain in BOREAS, the 1000 × 1000 km BOREAS region shown in Plate 1. This was the domain for meteorological and satellite data acquisition and large-scale modeling. Since it is impractical, even with aircraft, to measure surface-atmosphere fluxes over areas larger than a few tens of kilometers on a side, another scale of investigation was set at about 50 × 50 km which corresponds to the two BOREAS study areas (Plate 1 and Figure 2). These two study areas were placed near the northern and southern ecotones of the biome in order to study important processes associated with the controlling factors (temperature in the north, moisture in the south) which are most likely to undergo significant change within the biome as a whole. The northern study area (NSA) and the southern study area (SSA) were

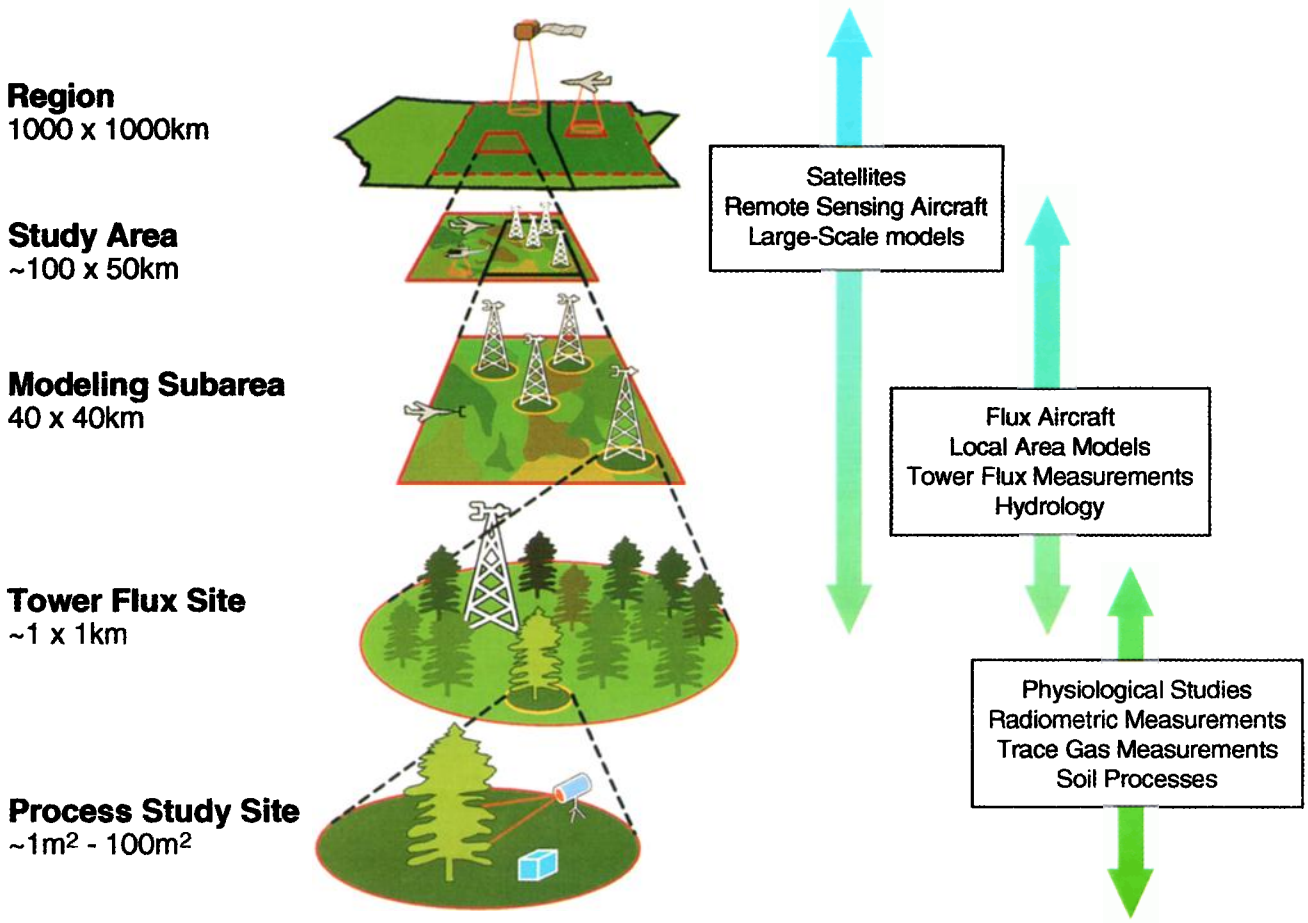

Plate 1. Multiscale measurement strategy used in BOREAS; see text.

located near Thompson, Manitoba, and Prince Albert, Saskatchewan, respectively. The study areas are about 500 km apart, sufficiently far apart to resolve the ecological gradient while permitting the routine ferry of research aircraft and people between them. The study areas themselves were small enough to be characterized by using surface and aircraft measurements, yet large enough to test scaling hypotheses using models and remote sensing imagery. Within each study area, water vapor, heat, and CO_2 fluxes were measured at the local scale (about 1 km) using eddy correlation equipment mounted on "flux" towers (five in the NSA, six in the SSA) which were located in patches of relatively homogenous vegetation and soils. Three boreal forest dominants were characterized by these tower flux (TF) measurements: black spruce, jack pine, and aspen. Two wetland fens, one in the NSA and one in the SSA, and beaver ponds in the NSA and SSA were equipped with smaller towers (Figure 2). The tower-based measurements have been compared with aircraft flux data (up one scale level) and with the biophysical characteristics of the constituent vegetation in the patch as defined by small-scale measurements made at small plots (down one scale level). Because these few TF sites could not capture the range of variability in the region, an additional 70 auxiliary sites (marked as category 3 sites in Figure 2) were selected, stratified by species type, productivity, and age. In these small (approximately 100 × 100 m) sites, biometry and optical techniques were used to measure biomass density, leaf area index, net primary productivity (NPP), litter fall, etc. While process models will be tuned by using primarily the tower flux data, the auxiliary sites can be used as independent test sites for process model and remote sensing algorithm validation. Some embedded plots (marked as category 2 auxiliary sites in Figure 2) were the focus of in situ measurement work which measured the variables needed to drive stand-level ecophysiological models, for example, site-level biomass, leaf photosynthetic rate, litter decomposition and quality, soil moisture, and temperature. Trace gas studies were conducted in both study areas with some specialized investigations in the NSA where some beaver pond sites and a collapsed palsa were instrumented to measure methane flux. (Palsas are common features in the boreal landscape; they are shallow depressions in the land surface caused by melting of subsurface permafrost and subsequent collapse of the surface. Usually, palsas have high water tables which support typical bog vegetation cover such as sphagnum moss, sedges, bog birch, etc.)

A remote sensing science program was implemented (see Table 4 and Plate 2) to characterize surface component optical properties from the leaf level (using laboratory spectroradiometers), to the canopy and stand level (using tower and helicopter-mounted spectrometers), to the study area and regional level (using aircraft and satellite platforms). Microwave scattering properties were determined at the canopy level using airborne radiometers and at the study area and regional levels using aircraft and satellite-based measurements.

A large multidisciplinary team of scientists was needed to cover the measurement and modeling requirements of the

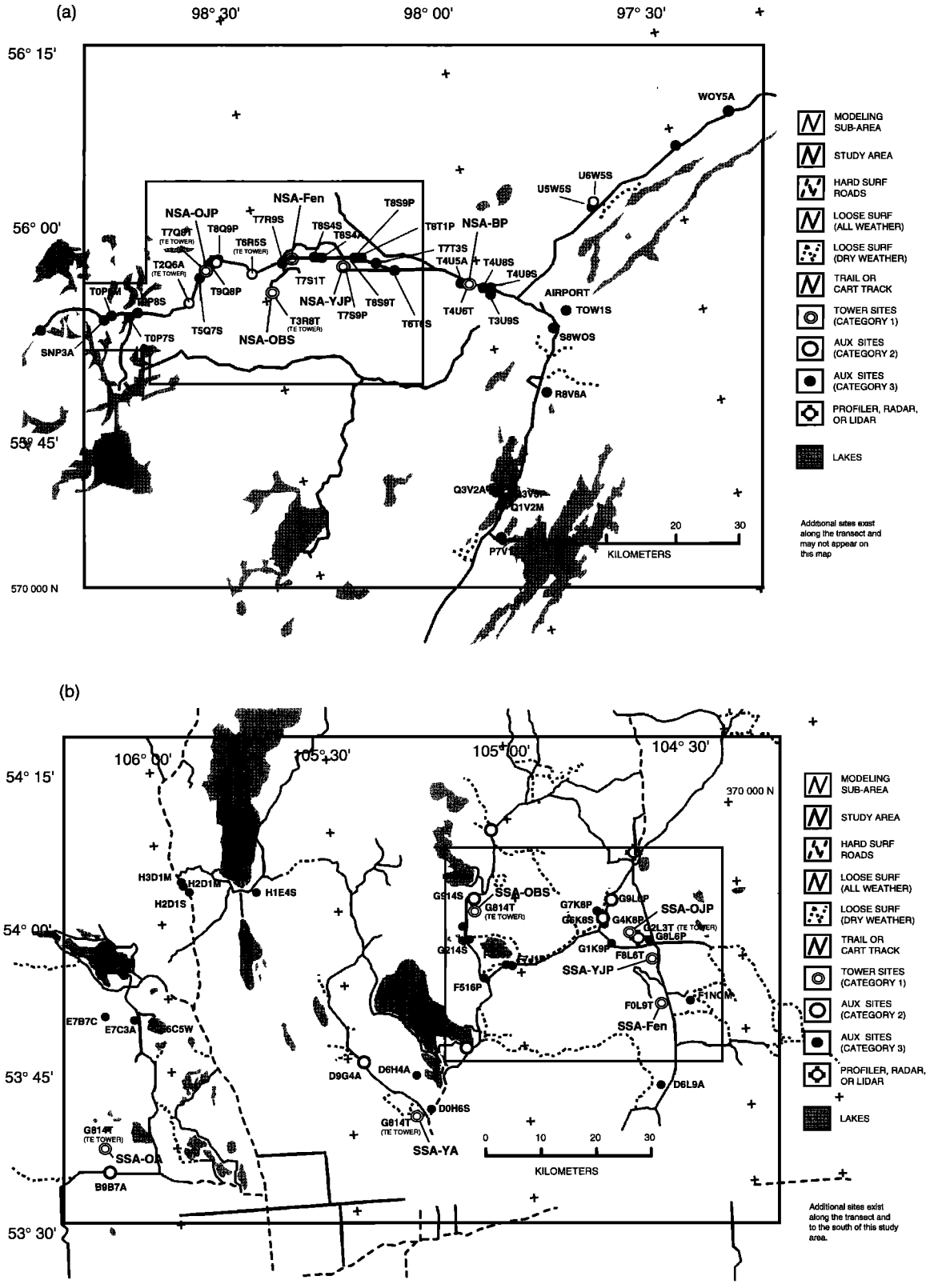

Figure 2. Maps of (a) the northern (NSA) and (b) southern (SSA) study areas of BOREAS. Tower flux (TF) sites, auxiliary sites, and modeling subareas are marked. TF sites are identified by a study area prefix (NSA or SSA) and a vegetation-type identifier (OA, old aspen; YA, young aspen; OBS, old black spruce; OJP, old jack pine; YJP, young jack pine; FEN, fen; BP, beaver pond). Auxiliary sites (category 2) were used for carbon modeling studies; category 3 sites were primarily used for remote sensing validation work.

project. In 1992, 85 science teams were selected from 229 proposals and other solicitations to take part in BOREAS. Most U.S. university investigators were funded by either the National Aeronautics and Space Administration (NASA), the National Oceanographic and Atmospheric Administration (NOAA), or the National Science Foundation (NSF). Canadian university investigators were funded through a collaborative special project grant from the Natural Sciences and Engineering Research Council (NSERC) and Canadian government investigators by their respective agencies. There was also significant participation by scientists and research organizations from the United Kingdom, France, and Japan. The individual projects were organized into six disciplinary groups to facilitate coordination during the field phase. The objectives of these six science groups are summarized below and the names of individual principal investigators are listed in Table 1.

4.1. Airborne Fluxes and Meteorology (AFM)

Four aircraft were used to measure turbulent fluxes; sounding lidars and radars were also deployed (see Figure 3 and Table 2). One other aircraft was used for operations support in 1994 and 1996 and for CO_2 concentration measurement work in 1996. Ten meteorological stations and a dense array of upper air radiosounding stations operated over the region during 1994, with their data being transmitted to operational meteorological centers for assimilation via the Global Telecommunications System. Several investigators, including some with close links to these centers, are using these data to improve mesoscale and global-scale atmospheric models. The surface network, a subset of the aircraft, and a few of the upper air stations also operated during 1996.

4.2. Tower Fluxes (TF)

The TF group's primary objective was to quantify the turbulent exchanges of energy and mass between the atmosphere and a variety of boreal forest surface covers and to investigate the processes controlling these fluxes. This work was designed to be complementary to chamber observations and other process-oriented studies on smaller scales (TE, TGB) and aircraft studies (AFM, RSS) covering larger scales. The TF towers operated almost continuously during the growing season of 1994, measuring radiation, heat, water, CO_2, and in some cases CH_4 and other trace gas fluxes; see Figure 2 for their location. Two of the sites, one in the NSA and one in the SSA, operated more-or-less continuously from the fall of 1993 onward to characterize the annual cycle of the energy fluxes. Six TF sites operated during the growing season in 1996; see Figure 3 for the operating schedules.

4.3. Terrestrial Ecology (TE)

Over 20 teams examined the biophysical controls on carbon, nutrient, water, and energy fluxes for the major ecosystems in the boreal landscape and are developing models and algorithms to scale chamber measurements to stand, landscape, and regional scales. Much of the work was carried out at plots within the footprints of the TF sites, i.e., within the surface zones that contribute fluxes measured by the TF instrumentation, typically within a 200 m radius of the TF tower. An important focus for the TE group was the measurement of carbon cycle components. A number of free-standing towers (TE towers in Figure 2) were installed in the study areas to facilitate access to the forest canopy for leaf/branch chamber measurements and other in situ work.

4.4. Trace Gas Biogeochemistry (TGB)

Ten TGB teams used chamber measurements and other techniques to characterize the flux of trace gases between the soil and the atmosphere, including CO_2, CH_4 and nonmethane hydrocarbons (NMHCs). The TGB group also studied the long-term accumulation of carbon in boreal soils.

4.5. Hydrology (HYD)

The HYD group consisted of eight teams. Five focused on the measurement of snow hydrology components to support remote sensing algorithm development; two worked on catchment hydrological processes in the SSA and NSA using precipitation gage networks, stream gages, and a rain radar; and one team operated a program of almost continuous soil moisture measurements at the TF sites during the 1994 and 1996 growing seasons.

4.6. Remote Sensing Science (RSS)

The RSS group developed linkages between optical and microwave remote sensing signatures and boreal zone biophysical parameters at scales that include leaf, canopy, and regional levels using field, aircraft and satellite-borne sensors, and radiative transfer models. The TE and RSS groups collaborated in gathering a wide range of biometric and radiometric data at the auxiliary sites (Figure 2). Several remote sensing aircraft were deployed in BOREAS 1994 and BOREAS 1996; see Table 4 and Figure 3.

4.7. Staff

The science teams were supported by a staff of scientists and support contractors from the National Aeronautics and Space Administration (NASA); the Atmospheric Environment Services (AES), Canada; the Canada Center for Remote Sensing (CCRS); Parks Canada; the School of Forestry, Laval University; the School of Forestry, University of Wisconsin; and the Canadian Forestry Service. The BOREAS staff oversaw the components of the project which required significant logistical effort, extended and/or routine monitoring work, or work that required the particular expertise and resources of one of the participating agencies. In the early stages of the project, the staff carried out the detailed site reconnaissance work and construction planning. During the field seasons, the staff dealt with the organization of the field logistics and the day-to-day management of field operations. The staff monitoring program included automatic meteorological station network; upper air network; hydrology, snow, and soil moisture; auxiliary site work; biometry and allometry; radiometric calibration; standard gases and gas calibration; thermal radiance intercomparison; global positioning system (GPS) facilities.

The NASA staff were also responsible for implementing the BOREAS Information System (BORIS) which serves as a data organization, distribution, and short-term archiving center for the project. All in all, some 300 people were working within or above the study areas in BOREAS 1994 and around 150 people participated in BOREAS 1996.

5. Experiment Execution

Many of the BOREAS measurements were taken continuously; for example, the 10 meteorological stations took 15-min

Table 1. Principal Investigators and Tasks Associated With Each BOREAS Science Group

Aircraft	Sounding/Networks	Models
	Airborne Fluxes and Meteorology (AFM),[a] 14 Teams	
AFM-1 Crawford	AFM-5 Atkinson	AFM-8 Betts
AFM-2 Kelly	AFM-6 Martner	AFM-9 Dickinson
AFM-3 Lenschow	AFM-7 Shewchuk	AFM-11 Mahrt
AFM-4 MacPherson/Desjardins		AFM-12 Pielke
		AFM-13 Schuepp
		AFM-14 Sellers
		AFM-15 Verseghy
Vegetation Type	**SSA**	**NSA**
	Tower Fluxes (TF),[b] 11 Teams	
Old aspen (OA)	TF-1 Black*	...
	TF-2 den Hartog	...
Old black spruce (OBS)	TF-7 Desjardins	TF-3 Wofsy*
	TF-9 Jarvis	
Old jack pine (OJP)	TF-5 Baldocchi	TF-8 Fitzjarrald
Young jack pine (YJP)	TF-4 Anderson	TF-10 Jelinsky/McCaughey
Fen (FEN)	TF-11 Verma	TF-11 Jelinsky/McCaughey
Soils, Forest Floor, Wetlands	**Ecophysiology and Ground Carbon**	**Models**
	Terrestrial Ecosystems (TE),[c] 22 Teams	
TE-1 Anderson	TE-2 Ryan	TE-13 Apps
	TE-4 Berry	TE-14 Bonan
	TE-5 Ehleringer/Flanagan	TE-15 Bukata
	TE-6 Gower	TE-16 Cihlar
	TE-7 Hogg	TE-17 Goward
	TE-8 Kharuk	TE-18 Hall
	TE-9 Margolis	TE-19 Harriss
	TE-10 Middleton	TE-20 Knox
	TE-11 Saugier	TE-21 Running
	TE-12 Walter-Shea	TE-22 Shugart
		TE-23 Rich
Methane	**Isotopes, Pesticides**	**NMHCs**
	Trace Gas Biogeochemistry (TGB),[d] 10 Teams	
TGB-1 Crill	TGB-6 Wahlen	TGB-8Monson
TGB-3 Moore	TGB-7 Waite	TGB-9 Niki
TGB-4 Roulet		TGB-10 Westburg
TGB-5 Zepp		TGB-12 Trumbore
Soil Moisture	**Snow Processes, Remote Sensing**	**Hydrological Modeling**
	Snow and Hydrology (HYD),[e] 8 Teams	
HYD-1 Cuenca	HYD-2 Chang	HYD-8 Band
	HYD-3 Davis	HYD-9 Soulis
	HYD-4 Goodison	
	HYD-5 Harding	
	HYD-6 Peck	
Optical	**Microwave**	**Algorithms/Modeling**
	Remote Sensing Science (RSS),[f] 20 Teams	
RSS-1 Deering	RSS-13 Gogenini	RSS-4 Curran
RSS-2 Irons	RSS-15 Ranson	RSS-5 Goel
RSS-3 Walthall	RSS-16 Saatchi	RSS-6 Williams
RSS-10 Holben	RSS-17 Way	RSS-7 Chen
RSS-11 Markham		RSS-8 Running
RSS-12 Wrigley		RSS-9 Strome
RSS-14 Smith		RSS-18 Green
		RSS-19 Miller
		RSS-20 Vanderbilt

Staff science support: infrastructure installation and maintenance, calibration of radiometric instruments, aircraft operations, satellite data acquisition program, BOREAS Information System (BORIS), operations management.

[a]Airborne eddy correlation profiling (5 aircraft), surface meteorological network (10 stations), upper atmosphere soundings (radiosondes), lower atmosphere profiling, modeling and analysis.

[b]Two long-term towers: *heat, H_2O, CO_2, some trace gases; eight growing season towers: heat, H_2O, CO_2, some trace gases.

[c]Porometry and chamber photosynthesis, canopy and soil respiration, biometry, nutrient cycling, modeling.

[d]Trace gas chamber measurements including methane and nonmethane hydrocarbons (NMHCs); studies of fire scars, beaver ponds, soil and moisture gradients; isotopes.

[e]Snow processes and snow remote sensing; catchment hydrology; soil moisture, canopy interception; hydrological modeling.

[f]Optical remote sensing (four aircraft), microwave/radar/gamma remote sensing (four aircraft), surface-based remote sensing studies, algorithm development

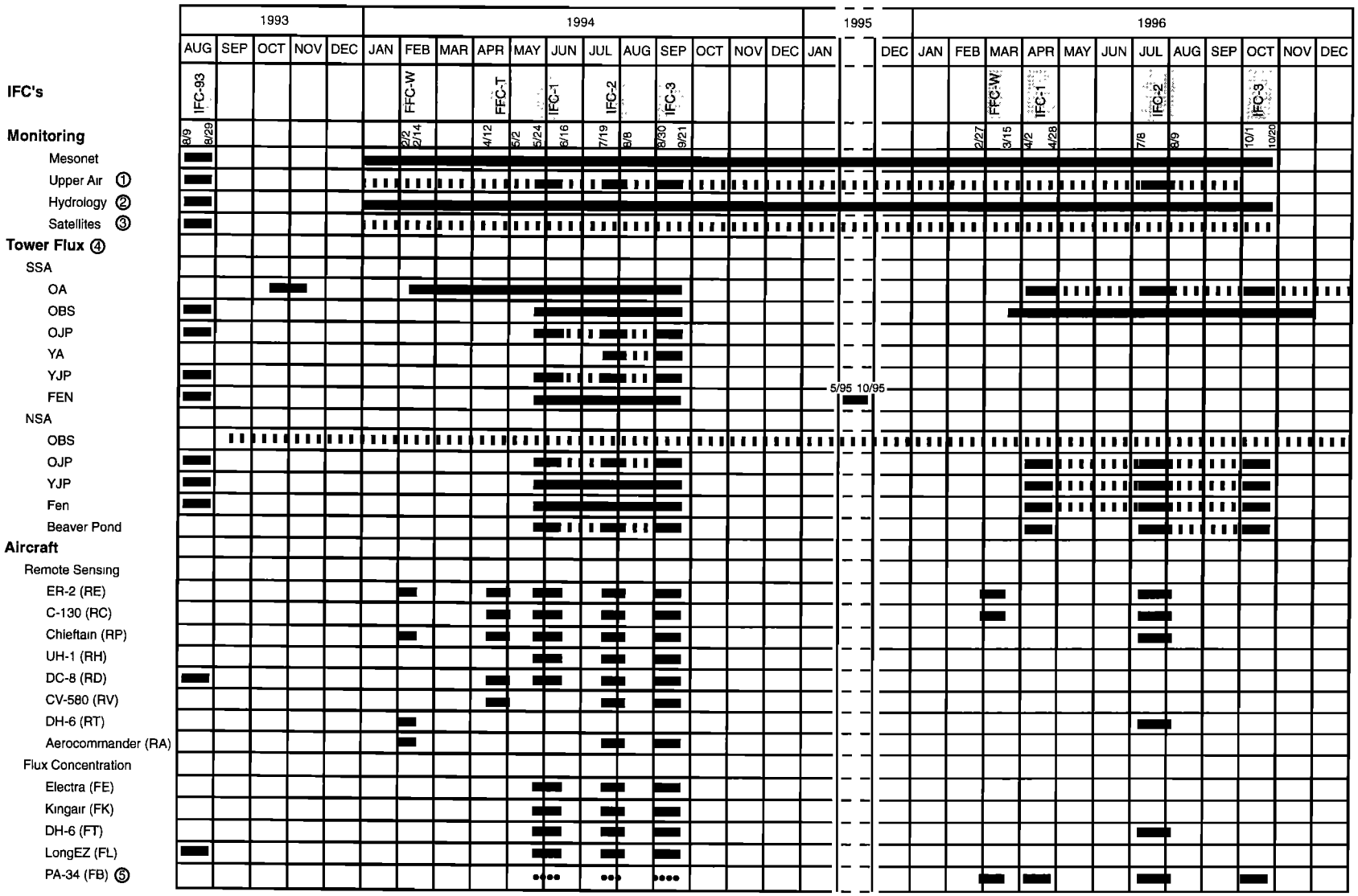

① Upper air measurements taken by the operational stations were archived. The operational network was significantly augmented during BOREAS IFCs

② Hydrological measurements were taken at subcatchments at NSA and SSA

③ GOES, NOAA 11, LANDSAT, SPOT, RADARSAT, SIR-C, ERS-1.

④ Dashed periods denote automated operations and/or on-site presence of investigators. Solid blocks denote TF team was present continuously during the IFC.

⑤ FB flew operations support missions in 1994 CO_2 measurements were taken by FB in 1996 field campaigns.

Figure 3. Master schedule for BOREAS, showing the timing of Intensive Field Campaigns (IFC's); monitoring activities, Tower Flux measurements and aircraft operations.

Table 2. Remote Sensing (R-Prefix) and Flux Measurement (F-Prefix) Aircraft Deployed in BOREAS

Aircraft Type	BOREAS Identifier	Science Team	Equipment	Primary Target/Role	Home Institution
			Remote Sensing Aircraft (R-Prefix on BOREAS Identifier)		
ER-2	RE	RSS-18	airborne visible infrared imaging spectrometer (AVIRIS)	vegetation properties	NASA Ames Research Center
		HYD-2	MODIS airborne simulator (MAS) in FFC-W	snow	
C-130	RC	RSS-2	advanced solid-state array spectroradiometer (ASAS)	vegetation properties, SART	NASA Ames Research Center
		staff	thematic mapper simulator (TMS), MODIS airborne simulator (MAS), airborne tracking Sun photometer (ATSP)		
		RSS-20	Polarization and Directionality of Earth's Radiation (POLDER)		
Piper Chieftain	RP	RSS-19	compact airborne spectrographic imager (CASI)	vegetation properties, SART	Ontario Remote Sensing Office, Canada
Helicopter (UH-1)	RH	RSS-3, 13, 20	Spectron Electronics-590, Barnes multiband modular radiometer, C-band scatterometer, ATSP, POLDER	vegetation and surface properties	NASA Wallops Flight Facility
DC-8	RD	RSS-15, 16, 17	airborne synthetic aperture radar (AIRSAR); P, L, C-band; fully polarimetric	vegetation and soil properties soil moisture	NASA Ames Research Center
CV-580	RV	TE-16	airborne synthetic aperture radar (CCRS-SAR); X and C-band, polarimetric	vegetation and soil properties soil moisture	Canada Centre for Remote Sensing (CCRS)
Twin Otter (DH-6)	RT	HYD-2	microwave radiometers; 18, 37, and 92 GHz; H and V	snow	National Research Council, Canada
Aerocommander	RA	HYD-6	gamma ray equipment	snow and soil moisture	NOAA National Weather Service
			Flux Measurement Aircraft (F-prefix on BOREAS Identifier)		
Electra	FE	AFM-3	flux, H, LE, CO_2, limited atmospheric chemistry lidar	local but mainly regional flux measurements, chemistry	National Center for Atmospheric Research, Colorado
Kingair	FK	AFM-2	flux; H, LE, CO_2	local and regional scale (5–600 km) flux measurements	University of Wyoming
Twin Otter (DH-6)	FT	AFM-4	flux; H, LE, CO_2, O_3	local and regional scale flux measurements	National Research Council, Canada
LongEZ	FL	AFM-1	flux; H, LE, CO_2	local scale (5–60 km) flux measurements	NOAA, Oak Ridge
PA-34	FB	AFM-14	CO_2 concentrations (1996 only)	profiles (0–10000'), regional gradients	NASA GSFC

See also Figure 3.

data from early in 1994 to the end of 1996, and satellite data were collected regularly over the same period (Figure 3). Some flux towers ran continuously and a few science teams were in the field during the entire growing seasons of 1994 and 1996, but for most investigations involving complex equipment and moderate-size teams, it was not practical or necessary to sustain a continuous presence in the field, so special periods, intensive field campaigns (IFCs), were defined for coordinated visits. The IFCs, each of which lasted about 20 days, were spaced to catch the major phenological events, including a snow hydrology/RSS campaign in the winter, spring thaw, green-up, peak greenness, and the beginning of senescence (Figure 3).

In August 1993, many of the BOREAS investigators and staff were in place in the study areas as part of the "shakedown" intensive field campaign, IFC-93. This 21-day IFC was used to test the experiment infrastructure and investigator's instruments as well as to refine coordination and communication procedures. All of these experiences were pooled to refine the four-volume experiment plan which served as the basis for running operations in 1994 [*Sellers et al.*, 1994]. During IFC-93 and the five BOREAS 1994 field campaigns, operations were coordinated out of two centers, one in the NSA and one in the SSA. Each center was equipped with FM ground-to-ground and VHF ground-to-air radio links, telephones, fax machines, etc., to maintain real-time management of the airborne operations and related surface work. Nightly meetings of the participating scientists, air crew, and managers analyzed the results of the day's completed operations and set up the next day's activities. Weekly science symposia provided a useful forum for sharing scientific results and reviewing recent progress. This continuous exchange of information and ideas between BOREAS staff and science team members permitted continuous refinement of the experiment design and operations and better integration of the various scientific components in the project.

The BOREAS 1994 fall field campaign, IFC-3, ended in September 1994, and the first science workshop was held in December of that year. On the basis of the results from early analyses presented at the workshop, it became apparent that

Table 3. Organization of Papers in This Special Issue

	Overview of Papers	No. of Papers
	Section 6.1: Carbon-Water-Energy Fluxes	
6.1.1	small-scale fluxes and physiological measurements (chambers and enclosures)	10
6.1.2	stand and plot-level fluxes and dynamics (flux towers)	17
6.1.3	landscape-scale fluxes and surface-boundary layer interactions (aircraft, sondes, profilers)	15
	Section 6.2: Trace Gas Fluxes	
6.2.1	small-scale fluxes (chambers and enclosures)	5
6.2.2	stand and plot-level fluxes and dynamics (flux towers)	4
	Section 6.3: Soil and Snow Moisture and Runoff	
6.3.1	point measurements and modeling of soil moisture dynamics	2
6.3.2	stand-level soil moisture and snow dynamics (models and measurements)	4
6.3.3	landscape-scale precipitation and soil moisture (models, radar estimates	1
	Section 6.4: Remote Sensing Science	
6.4.1	ground and aircraft measurements of biophysical and optical characteristics, and understory and canopy reflectance	8
6.4.2	radiative transfer models and algorithm development	3
6.4.3	landscape-scale land cover and biophysical characteristics algorithms	9
6.4.4	radiation and atmospheric effects	5

Each section is devoted to a specific science area and is further subdivided by spatial scale.

there were a number of gaps in the 1993–1994 data set, and in addition the meteorological record showed 1994 to be an unusual year: a new record had been set for the longest frost-free period at Prince Albert National Park, while the NSA had experienced the driest year on record. A full account of the BOREAS 1994 field campaigns may be found in the work of *Sellers et al.* [1995b].

During 1995 the decision was made to take additional field measurements during 1996 to fill the 1994 data gaps [*Sellers et al.*, 1996c]. The BOREAS 1996 campaigns involved fewer aircraft and scientists on the ground than BOREAS 1994 as the objectives were strictly defined by shortcomings in the BOREAS 1994 data sets and important findings from early analyses. Particularly important was the decision to start TF measurements earlier (in March) and end later (in October) in 1996, compared with 1994, to better cover the growing season (Figure 3). This was done because the BOREAS 1994 modeling and measurement results indicated that variations in spring thaw and fall temperatures were critical in determining interannual variability in ecosystem productivity.

6. Overview of Papers in This Special Issue

The 83 papers in this special issue were contributed by the science groups listed in Table 1. The papers have been organized into four major sections (see Table 3). The first three sections cover surface energy and mass exchange processes and the fourth final section is devoted to remote sensing science. The findings of these papers are summarized below.

6.1. Carbon-Water-Energy Fluxes

Carbon, water, and energy fluxes were measured in BOREAS using a comprehensive range of techniques ranging from leaf-scale observations made with chambers and porom-

Table 4. BOREAS RSS Ground, Aircraft, and Satellite Instruments With Measurements and Related Products

	Measurements	Products
	Ground-Based Sensors	
PARABOLA	3-band bidirectional radiance	BRDF, spectral albedo
Laboratory and field	spectral radiance spectroradiometers	understory and tree component reflectances
	Remote Sensing Aircraft/Sensor	
NASA DC-8/AIRSAR	radar backscatter	forest type, biomass density, canopy moisture
NASA ER-2/AVIRIS, MAS	spectral radiance	forest type, canopy moisture, atmospheric properties
Piper Chieftain/CASI	spectral radiance	BRDF
NASA C-130	TMS, ASAS, MAS, POLDER	spectral radiance, bidirectional radiance BRDF, albedo, forest type, FPAR
NASA helicopter	MMR, SE-590, POLDER	spectral radiance
Radar backscatter	C-band scatterometer	BRDF, FPAR canopy scattering profiles
	Remote Sensing Satellites	
AVHRR	spectral reflectance, emittance	land cover, FPAR
Landsat TM	spectral reflectance, emittance	land cover, FPAR, LAI, biomass density
SPOT	spectral reflectance	land cover
ERS-1, 2 SAR	radar backscatter	freeze/thaw
JERS-1 SAR	radar backscatter	land cover
Radarsat	radar backscatter	land cover
SIR-C/XSAR	radar backscatter	land cover, biomass density
GOES	spectral radiance	PAR, albedo, downwelling irradiance

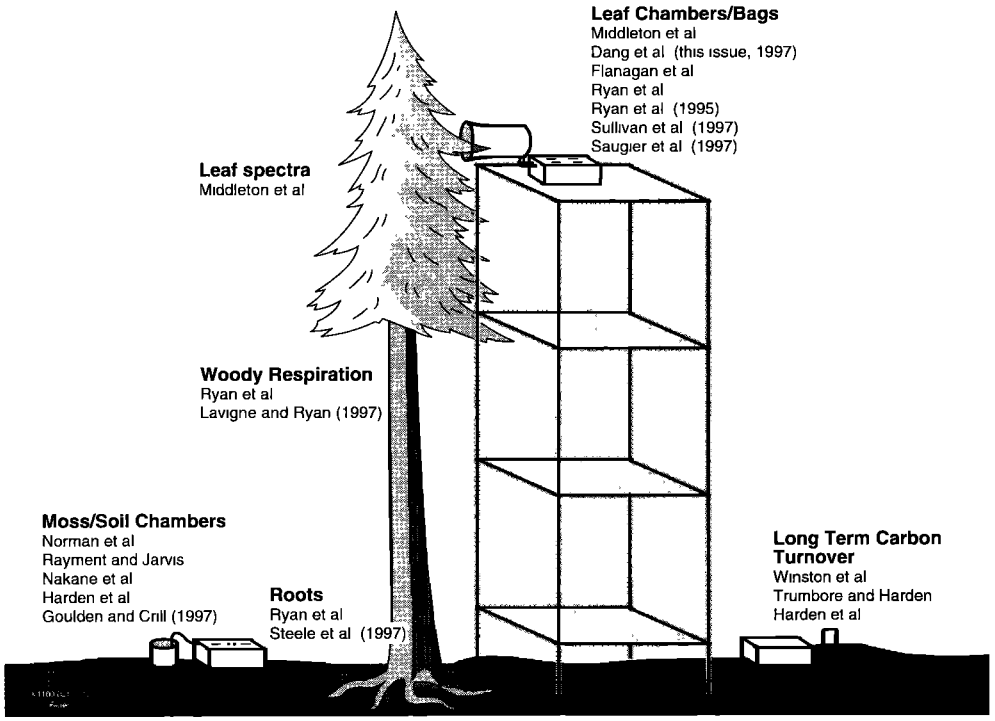

Figure 4. Schematic summarizing papers in section 6.1.1; small-scale fluxes and physiology with chambers and enclosures.

eters (section 6.1.1), through intermediate-scale studies conducted with flux towers and supporting measurements (section 6.1.2), up to regional-scale studies which used aircraft, meteorological arrays, and satellites (sections 6.1.3 and 6.4.4).

6.1.1. Small-scale fluxes and physiology with chambers and enclosures. Six papers describe soil fluxes and four papers describe leaf- and branch-scale measurements (Figure 4). A BOREAS special issue of *Tree Physiology* [*Margolis and Ryan*, 1997] has 10 papers that report on a variety of BOREAS ecophysiological studies; the results of some of these are discussed here for completeness.

Norman et al. [this issue] compared soil CO_2 fluxes measured by six different chamber methods as fielded by participants in BOREAS (Figure 5a). It was demonstrated that systematic differences exist between the measurement methods. Adjustment factors of between 0.8 and 1.4 are needed to bring all the data into agreement. These differences are actually smaller than were anticipated prior to the BOREAS intercomparison based on the disparate techniques used. Biases among the techniques were constant across the range of fluxes measured (1–8 μmol $m^{-2} s^{-1}$). *Rayment and Jarvis* [this issue] used an "open" chamber that maintained an interior pressure very close to external atmospheric pressure, thereby reducing mass flow effects on the soil CO_2 flux measurements. CO_2 fluxes were measured more or less continuously from a subplot on the floor of a black spruce forest (SSA-OBS) over a period of about 3 months in 1994; the fluxes were found to be strongly correlated with soil temperature at 5 cm depth. *Nakane et al.* [this issue] measured soil CO_2 fluxes at wet and dry subplots at the same black spruce site as *Rayment and Jarvis* [this issue]. They also measured carbon storage components (litterfall, soil carbon, etc.). The drier plot had decomposition rates that were roughly double those from the wet plot, presumably because of the much warmer soil temperatures and aerobic conditions at the drier subplot, which suggests that near-surface and surface decomposition rates could be significantly enhanced under a warmer, drier climate. *Winston et al.* [this issue], who worked mainly in the NSA, extended many of their CO_2 flux measurements through the winters of 1993–1994 and 1994–1995. The magnitude of observed wintertime CO_2 fluxes ranged from 0.5 to 1.0 g CO_2 $m^{-2} d^{-1}$. The lowest fluxes were correlated with the midwinter minimum temperatures. Accumulated over the long winter period, these fluxes contribute an important fraction of the annual carbon budget. The winter fluxes seem to agree well with the eddy correlation measurements taken at the northern black spruce site (NSA-OBS). *Goulden and Crill* [1997] used automated chambers at NSA-OBS to measure the CO_2 fluxes from the feathermoss and sphagnum moss covers and deeper soils beneath the black spruce canopy. Maximum net photosynthesis occurred between 5°C and 8°C, and moss and surface net photosynthesis was estimated to account for between 10 and 40% of whole ecosystem uptake and 50 to 90% of the whole ecosystem respiration from above-canopy eddy correlation measurements.

Winston et al. [this issue] report that the ^{14}C content of the CO_2 releases showed a progressive shift to lighter, that is older, carbon as the winter wore on, which suggests that the source material for the CO_2 flux changed from recently fixed, modern carbon to older organic material, presumably located deeper in the soil. *Harden et al.* [this issue] also used isotopes to investigate the sequestering of carbon by surface peats and mosses near the NSA-OBS site: these two surface types have sequestered an average of 40–60 g C $m^{-2} yr^{-1}$ over the last 90 years, and net decomposition in deeper soils released 20–50 g C $m^{-2} yr^{-1}$ over the same period leading to an average net exchange of soil carbon within the range of +10 (efflux) to −50 g C $m^{-2} d^{-1}$ (uptake) over the last century. *Harden et al.* [this issue] point out that site-to-site differences are due to (1) the rate of

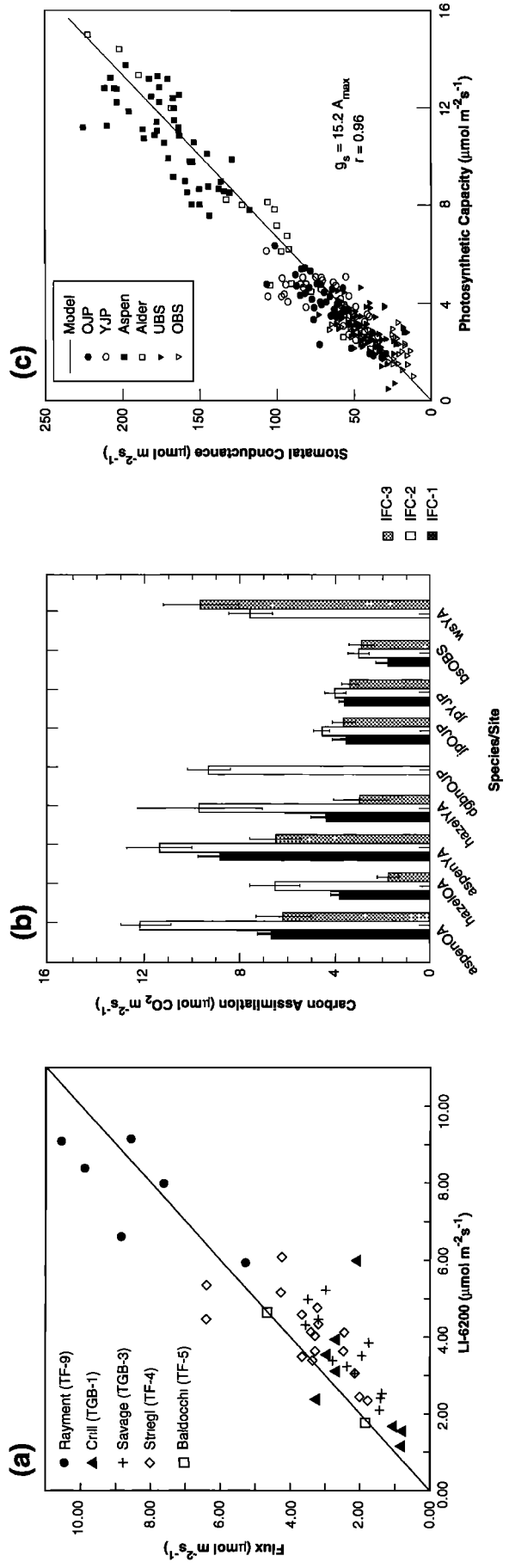

decomposition of surface peats, (2) rates and method of lateral spread of moss, and (3) the history and rate of decomposition in the deeper soil layers. Sites can therefore vacillate between source and sink status based on climate variability. The primary control on carbon accumulation in peats and moss is drainage, while deep carbon storage seems to be a function of respiration, decomposition, drainage, and fire history.

The isotopic record found in soil organic matter has been useful in determining decadal-scale carbon accumulation rates in the NSA soils. Analyses of soil carbon and its isotopic composition revealed differences in carbon dynamics between sites in the NSA [*Trumbore and Harden*, this issue]. The jack pine sites had the lowest soil carbon concentrations, and the fastest turnover occurred in the surface organic and mineral layers. Black spruce sites with moss surface layers were found mainly on clay soils with degrading permafrost. These sites had net carbon uptake rates that were similar to those at the jack pine sites (50–100 g C m^{-2} yr^{-1}), but they also had slower decomposition rates, due to high soil moisture contents and lower temperatures, which resulted in the accumulation of more carbon in their soils. The fen sites had the largest soil carbon stores (1.2×10^5 g C m^{-2}) and the highest productivities (200–400 g C m^{-2} yr^{-1}). Slow deep soil respiration offset about 15% of the carbon uptake rates in wetlands and about 45% in upland sites. Deep soil respiration/decomposition rates were observed to decrease with depth. Deep soil carbon decomposi rates as determined from ^{14}C and soil inventory work agree with the findings of *Winston et al.* [this issue].

Middleton et al. [this issue] acquired leaf-level measurements of gas exchange, chemistry, morphology, and spectral optical properties during the BOREAS 1994 IFCs at all of the SSA forest cover TF sites (Figure 5b). Leaf net photosynthetic rates were found to be comparable between the old (SSA-OA) and the young (SSA-YA) aspen sites, but leaf transpiration rates were significantly different; the SSA-YA leaves transpired about 30% more than the SSA-OA leaves. The black spruce shoots at SSA-OBS exhibited the lowest photosynthetic rates among all the forest types. The conifers (SSA-OBS, SSA-OJP, SSA-YJP) were observed to have peak photosynthetic rates in late summer to early fall, while the deciduous species peaked in midsummer (see also *Sullivan et al.* [1997] and *Saugier et al.* [1997]). *Dang et al.* [1997, this issue] examined the profiles of photosynthetically active radiation (PAR), leaf nitrogen, and photosynthetic capacity at two jack pine sites, an aspen site and two black spruce sites in the NSA. Beer's law descriptions (exponential extinction) fit the PAR profiles down through the canopy fairly well (r = 0.73–0.92) under both cloudy and clear-sky conditions. Leaf nitrogen decreased with the fraction of absorbed PAR in each of the forest stands (relationships were similar among the species except for an alder understory),

Figure 5. (opposite) (a) Comparison of soil CO_2 fluxes measured by different investigators and instruments at a common test site in the SSA in BOREAS 1994, from *Norman et al.* [this issue]; (b) leaf assimilation rates as measured by porometry for several species at the SSA TF sites, from *Middleton et al.* [this issue]. Note that understory (hazel, bog birch) as well as the dominant species (bs, black spruce; jp, jack pine, ws, white spruce) were sampled at each TF site (OA, old aspen; YA, young aspen; OJP, old jack pine; YJP, young jack pine; OBS, old black spruce); (c) plot of leaf stomatal conductance against photosynthetic capacity for several species in the NSA, from *Dang et al.* [this issue].

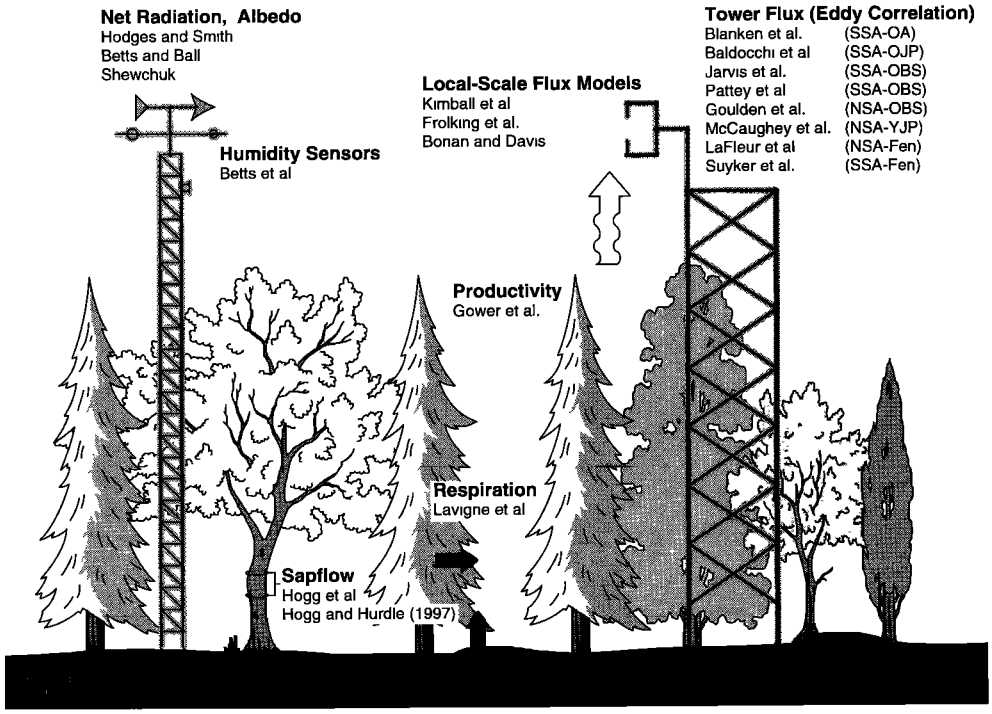

Figure 6. Schematic summarizing papers in section 6.1.2; stand and plot-level carbon-water-energy dynamics.

and photosynthetic capacity decreased significantly with leaf nitrogen except for the single case of jack pine during early leaf flush. Aspen leaves had higher photosynthetic capacities than conifers for the same leaf nitrogen. Good correlations were found between canopy photosynthetic capacity and remote sensing spectral vegetation indices (NDVI and simple ratio), but the relationships varied depending on the canopy scaling procedure. In all cases it was found that photosynthetic capacity correlated well with stomatal conductance (Figure 5c) but decreased less steeply than did PAR down through the canopy.

Flanagan et al. [this issue] correlated leaf isotopic contents, specifically ^{13}C to ^{12}C ratios, to infer the degree of stomatal restriction on photosynthesis. Despite the very low stomatal conductances observed among the forest species in BOREAS their results indicated that there was little stomatal limitation of photosynthesis, in agreement with gas exchange and meteorological data published by *Dang et al.* [1997]. Measurements of the carbon isotope concentration of cellulose from individual tree growth rings varied with summer precipitation and temperature, suggesting that tree ring carbon isotopes may be used to infer the effects of past environmental conditions on photosynthesis.

Ryan et al. [this issue] and *Lavigne and Ryan* [1997] estimated annual autotrophic respiration from chamber measurements of foliage, woody tissue, and fine roots of aspen, black spruce, and jack pine forests in the SSA and the NSA during the BOREAS 1994 growing season. Mean foliage respiration per unit leaf area was found to be similar among expanded leaves for all species at 10°C. Wood respiration was strongly seasonal, with high rates in midsummer that coincided with wood growth. Fine root respiration declined by about a factor of 3 throughout the season, but rates were similar among species. Annual costs of autotrophic respiration for the whole system were estimated to be 310–610 g C m^{-2}. Carbon use efficiency (CUE), the ratio of net production to net photosynthesis, averaged 0.44, 0.29, and 0.43 for aspen, black spruce, and old jack pine, respectively. Differences in CUE between the NSA and the SSA sites were small for the conifers but larger for aspen because of higher root respiration in the NSA.

6.1.2. Stand and plot-level carbon-water-energy dynamics. The first two papers in this section deal with radiation fluxes and albedo measurements measured over forested sites in BOREAS; most of the remaining 15 papers describe eddy correlation measurements from the flux towers (TF sites) and analyses of patch-scale carbon dynamics inferred from these and supporting observations taken within footprints of the TF sites (Figure 6).

Hodges and Smith [this issue] analyzed surface net radiation (R_n) distributions across the BOREAS region. Three calibrated net radiometers were compared with 22 R_n instruments at 21 sites in BOREAS; R_n fields generated from GOES observations were also compared with the in situ measurements. The results show that one make of radiometer, used at 15 out of the 21 sites, underestimated R_n by about 5% in the daytime and by about 45% at night. *Betts and Ball* [this issue] analyzed the BOREAS mesonet data (see note by *Shewchuk* [this issue]) to create time series of albedo estimates over the different cover types sampled in BOREAS throughout 1994 and 1995. Representative daily average albedos in summer ranged from 0.083 for coniferous sites, 0.15 for aspen, to 0.20 at grass (airport) sites; winter albedos were 0.13 for conifers, 0.21 for aspen, and 0.75 for the grass site (Figure 7a). The winter albedos of the forest sites varied with canopy closure and with solar diffuse/direct flux ratios but never exceeded 0.3. These numbers were significantly different from those used in the European NWP model which led to a systematic underestimation of the near-surface air temperature (Figure 7b). The note of *Betts et al.* [this issue] compared surface humidity measurements from the operational AES sensor at Meadow Lake, Saskatchewan, with a colocated BOREAS mesonet sensor,

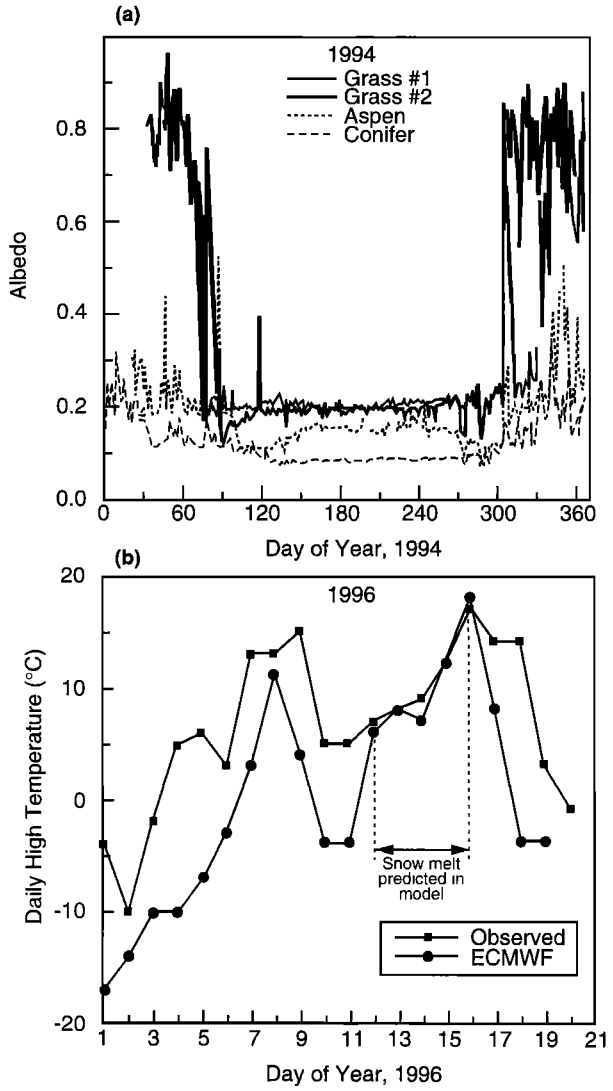

Figure 7. (a) Annual course of surface albedo over different BOREAS cover types during 1994, from *Betts and Ball* [this issue]. Note that the winter albedo over the grassland sites varies around 0.7, while the winter albedos over the forest sites are much lower, 0.12–0.30; see section 6.1.2; (b) effects of overestimating surface albedo on the performance of the European numerical weather prediction (NWP) model. The model assumed a winter surface albedo of about 0.8 over the boreal zone, while the true value was around 0.1–0.2; see Figure 7a. Shown here is the ECMWF (European Center for Medium-Range Weather Forecasting) model near-surface air temperature for the SSA site as predicted 24 hours ahead of the start of the model run, compared with the mean observations from the BOREAS meteorological towers for the same time. (The NWP runs were initialized with observed temperatures). Note how the (24 hour) predicted surface air temperature is always much lower than observations because the surface is calculated to absorb only a small fraction of the incident solar energy, except when the model predicts melting conditions (marked by horizontal bar in figure) in which case the calculated albedo is reset to a value representative of a snow-free surface, around 0.2, which is actually close to the observed winter albedo for the forest. ECMWF output are from Hollingsworth (personal communication, 1996) and the analysis and figure are from Huemmrich (personal communication, 1996).

showing that the operational instrument has significant biases that could be important to surface climate studies.

Figure 8 summarizes the flux data reported by the TF sites during BOREAS 1994; it can be seen that the coniferous vegetation is characterized by low evaporative fractions (ratio of latent heat to the sum of the latent and sensible heat fluxes) and low CO_2 uptake rates during the growing season. Boreal deciduous land cover, while showing larger transpiration and CO_2 uptake rates than its coniferous counterpart, is still much less active than deciduous forests in temperate North America [e.g., *Baldocchi and Vogel*, 1996; *Baldocchi and Harley*, 1995]. The papers summarized below provide more details on these results.

Blanken et al. [this issue] presented results from eddy covariance measurements of latent and sensible heat flux made above and below the aspen overstory at the SSA-OA site during 1994. Before leaf emergence, most of the available energy was converted to sensible heat flux, but latent heat flux dominated after leaf emergence. During the full leaf period, daytime mean dry leaf aspen and hazelnut canopy conductances were 330 and 113 mmol $m^{-2} s^{-1}$, respectively (Figure 9a). The canopy conductances of both species increased with increasing photosynthetic photon flux density and decreasing saturation deficit at the leaf surface and were not limited by soil moisture. Forest canopy conductance was directly proportional to forest leaf area index. The daytime average ratio of the latent heat flux to the equilibrium latent heat flux (the Priestley-Taylor alpha) suggests that the understory hazelnut transpiration was mainly energy controlled, while the overstory aspen canopy transpiration rate was more limited by stomatal conductance.

Hogg et al. [this issue] measured sap flows through aspen boles at the SSA-OA site in BOREAS 1994 using two different techniques (see also *Hogg and Hurdle* [1997]). Both techniques produced similar results and compared well with the eddy correlation measurements described above in terms of diurnal and seasonal patterns and magnitudes, although the sap flow time series lagged the eddy correlation data by about 1 hour due to water storage changes in the trees. All methods showed that as expected, transpiration increased with air vapor pressure deficit until about 1 kPa but then remained almost constant for higher vapor pressure deficits.

Baldocchi et al. [this issue] report on the variations of radiation, sensible, and latent heat fluxes above and below a boreal jack pine canopy (SSA-OJP) during the 1994 growing season. The sum of the measured hourly average sensible, latent and soil heat fluxes, and canopy heat storage was about 8% less than the net radiation, indicating a systematic underestimation of one or more of the measured energy fluxes. When the canopy was dry, daily evapotranspiration was less than 2.5 mm d^{-1} with most growing season values being much less than 1.5 mm d^{-1} (Figure 9b). This extremely low rate was attributed to the low LAI (1.9–2.2) and low stomatal conductances observed at the site. Factors restricting stomatal opening were low soil moisture supply, limiting atmospheric saturation deficits and the low photosynthetic capacity of the needles. Typically, 20–40% of the total energy exchanged originated at the forest floor underneath the sparse jack pine canopy.

Jarvis et al. [this issue] summarize eddy covariance measurements of CO_2, water vapor, and sensible heat fluxes above a black spruce (SSA-OBS) forest over a 120-day (May 23 to September 21) period in 1994 (Figure 9c). Average midday evaporative fractions (latent heat flux divided by the sum of the latent and sensible heat fluxes) for the three IFCs were 0.34–

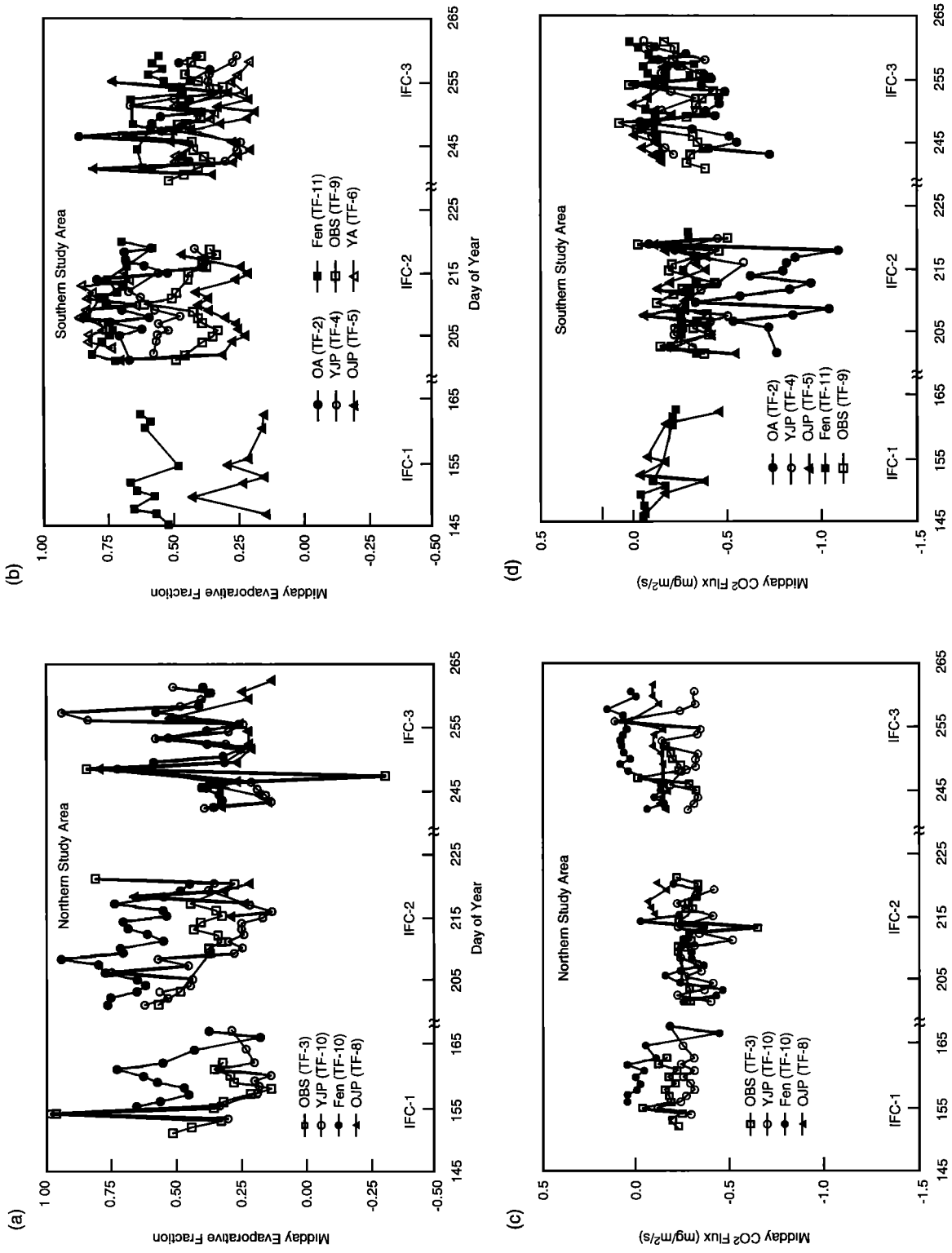

Figure 8. 1994 Time series of evaporative fraction (LE/(LE + H)) as reported by the site captains listed in Table 1 for (a) NSA and (b) SSA. These were calculated from preliminary analyses of flux measurements averaged over a 1-hour period centered on midday for each day of each IFC. Time series of total (above canopy) CO_2 flux as reported by the TF site captains for (c) NSA and (d) SSA. The samples were taken at same times as for Figures 8a and 8b above. Figure redrawn from *Sellers et al.* [1995b].

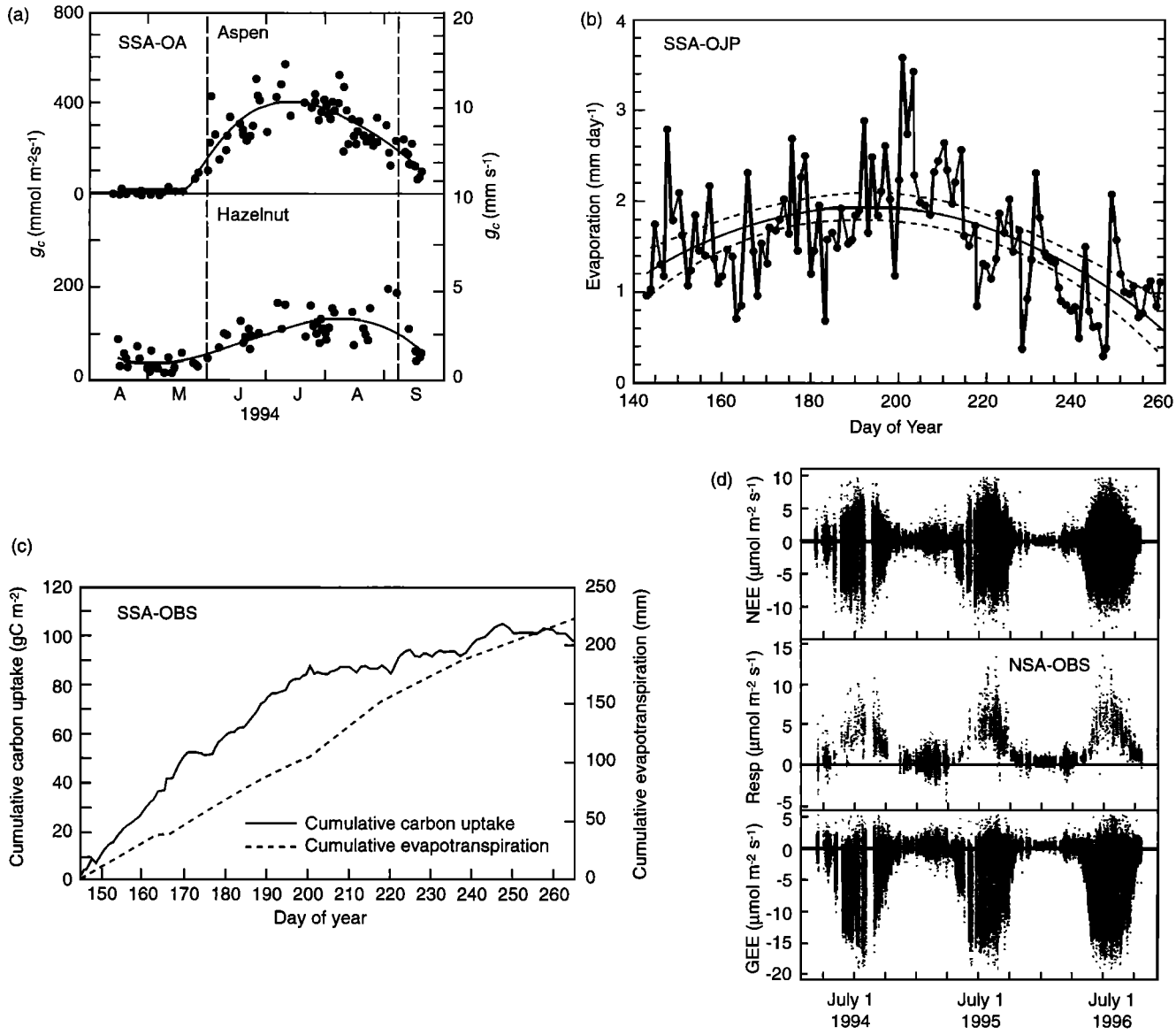

Figure 9. (a) Seasonal variation of midday canopy conductance calculated from eddy correlation measurements taken (top panel) above the SSA-OA aspen canopy and (bottom panel) the hazelnut understory, from *Blanken et al.* [this issue]; (b) daily evaporation rates calculated from eddy correlation measurements taken above the SSA-OJP jack pine canopy, from *Baldocchi et al.* [this issue]; (c) cumulative carbon uptake and evapotranspiration rates calculated from measurements made above the SSA-OBS black spruce canopy, from *Jarvis et al.* [this issue]; (d) three years of carbon exchange estimates made from continuous eddy correlation measurements made above the NSA-OBS black spruce site, from *Goulden et al.* [this issue]. Shown is (top) net ecosystem exchange (NEE); (middle) respiration; and (bottom) gross ecosystem exchange (GEE).

0.44, in contrast with values of 0.56–0.71 for the SSA-OA site. On a 24-hour basis, evapotranspiration accounted for about 43% of the net radiation during the growing season. Mean half-hourly net ecosystem exchange (NEE) reached -9 μmol m^{-2} s^{-1} (sink) during the daytime and 6 μmol m^{-2} s^{-1} (source) at night under unstable conditions. Storage of CO_2 in the air column beneath the eddy covariance instrumentation complicated the measurement of respiration during stable nights, so nighttime fluxes were modeled using a relationship between the eddy flux on windy ($u^* > 0.4$ m s^{-1}) nights and the temperature; 95 g C m^{-2} were stored and 237 mm of water were evapotranspired over the 120-day period (Figure 9c). The NEE was very susceptible to changes in PAR flux and temperature as evidenced by 31 days in the growing season for which there were net carbon losses.

Pattey et al. [this issue] present eddy correlation measurements taken at a height of 20 m above the ground at the same site (SSA-OBS) as *Jarvis et al.* [this issue], who measured at a height of 27 m. Comparisons of 120-min covariances with the means of the corresponding four 30-min covariances showed that the shorter time averages slightly underestimated (1–4%) fluxes of CO_2, momentum, sensible, and latent heat. The daytime evaporative fraction was 0.37–0.45, consistent with the findings of *Jarvis et al.* [this issue]; CO_2 fluxes agreed very well with those measured by *Jarvis et al.* [this issue].

Lavigne et al. [this issue] used relationships among woody

tissue, foliage, and soil respiration rates and temperature measurements to estimate half-hourly ecosystem respiration rates at six coniferous BOREAS sites. These were compared with nocturnal eddy correlation estimates. Soil surface respiration was the largest contributor (48–71%) to the total flux and foliar respiration was a significant contributor (25–43%) at all the sites. The nocturnal eddy correlation measurements (at $u^* > 0.25$ m s^{-1}) were poorly correlated to estimates obtained from scaling up chamber measurements; estimates of ecosystem respiration from chambers were 1.2–1.5 times greater than those from eddy correlation.

Goulden et al. [this issue] used eddy correlation equipment to measure CO_2 exchange between the atmosphere and the NSA-OBS site for 2 years (March 16, 1994 to February 19, 1996) (Figure 9d). This is the longest continuously running eddy covariance CO_2 flux record of the BOREAS TF teams. Nocturnal CO_2 fluxes on windy nights were used to develop a respiration versus temperature relationship for the forest which was then applied to separate net exchange into gross photosynthesis and respiratory fluxes. Gross photosynthesis was largely a function of PAR flux and air temperature with no apparent effects due to high evaporative demand or soil water content. Under moderate light levels, photosynthesis was higher under cloudy than under sunny conditions. A single set of regression relationships describing the response of gross photosynthesis to PAR flux and temperature and the response of respiration to temperature accounted for 72% of the variation in hourly CO_2 exchange. Maximum rates of photosynthesis at the NSA-OBS site were small compared to those measured at a deciduous Harvard forest site [*Wofsy et al.*, 1993].

McCaughey et al. [this issue] report on measurements of sensible and latent heat and CO_2 fluxes taken above the stand at the NSA-YJP site over 119 days in BOREAS 1994. The PAR and clear-sky solar albedos were approximately 0.054 and 0.136, respectively, during this time, and the average evaporative fraction during this period was about 0.3. Nighttime CO_2 fluxes were estimated by using a regression relationship between fluxes measured in neutral to near-neutral conditions and soil temperature at 10- and 75-cm depths. The regression estimates for June and July agreed quite well with the modeled values calculated by *Ryan et al.* [this issue]. It was estimated that the stand fixed 224 g C m^{-2} during this period.

Lafleur et al. [this issue] collected eddy covariance measurements of sensible and latent heat, and CO_2 fluxes and related climatic variables over a period of 124 days (April 9 to September 19) in 1994 over the NSA fen site. Albedos (solar and PAR) decreased dramatically after snowmelt; during full leaf, solar and PAR hemispheric reflectances were 0.18 and 0.055, respectively. Mean evaporative fractions increased from about 0.5, during the snowmelt period, to 0.59 at leaf-out, to 0.83–0.91 near midsummer, and then decreased to around 0.5 at senescence. The fen acted as a net sink for CO_2 only when vascular plants were actively photosynthesizing to give a daily mean flux of -0.81 g C m^{-2} d^{-1}. Over the 124-day period the fen lost 30.4 g C m^{-2} to the atmosphere. While the authors point out that there is considerable uncertainty in the latter figure, there is a marked contrast between this fen and the one in the SSA, which was relatively productive (i.e., acted as a carbon sink) during the June–August period; see *Suyker et al.* [this issue] who report on atmospheric CO_2 exchanges measured at the SSA-fen site from mid-May to early October 1994. Canopy photosynthesis at the SSA-fen site was calculated by adding the downward CO_2 exchange and the soil respiration measured by soil chambers. Midsummer photosynthesis approached light saturation above 1000–1200 μmol m^{-2} s^{-1} and decreased in response to increasing temperature and saturation deficit. Maximum midday photosynthetic rates, which occurred in early July, were 13 μmol m^{-2} s^{-1}. Mid-May to early October net ecosystem exchange (NEE) was -88 g C m^{-2} (sink). This substantial productivity is consistent with the observed high water table and is in marked contrast with the loss of carbon over the corresponding period measured at the drier NSA-fen site in the same year [*Lafleur et al.*, this issue]. *Roulet et al.* [this issue] report that their beaver pond site in the NSA was a strong source of CO_2 (183 g C m^{-2}) over the 120 growing season days of 1994 (section 6.2.2), which suggests that in some boreal landscapes, beaver ponds could make a significant contribution to the regional carbon budget.

Productivity and carbon allocation within an ecosystem are critically important for determining site carbon budgets. *Gower et al.* [this issue] analyzed their detailed measurements at the TF and auxiliary sites to show that aboveground net primary productivity (ANPP) for the BOREAS forest sites was 55–310 g C m^{-2} yr^{-1} for aspen, black spruce, and young and old jack pine covers, low values when compared to most temperate sites. Thirty to 40% of the ANPP, as estimated at the BOREAS forest sites, fell to the surface as detritus; only 60–70% was retained as biomass increment. Black spruce ecosystems contained the highest carbon stocks (39–48 kg m^{-2}), aspen was intermediate (16–18 kg m^{-2}), and jack pine was the lowest (5–8 kg m^{-2}). Leaf area indices ranged from a low value of 1.25 for jack pine sites to 5.6 for black spruce sites. Fine root NPP estimated with minirhizotrons ranged from 30 g C m^{-2} yr^{-1} at SSA-OA to 115 g C m^{-2} yr^{-1} at NSA-OBS [*Steele et al.*, 1997]. Root elongation was highly correlated with soil temperature (10 cm) for aspen, black spruce, and jack pine sites at both the NSA and the SSA [*Steele et al.*, 1997].

Three papers present stand-scale simulation modeling results which used TF flux data and supporting measurements for validation. *Kimball et al.* [this issue] discuss energy and water balance simulations performed with the BIOME-BGC model. In their model, total ET was calculated to be insensitive to ecosystem leaf area index, and canopy conductance to water vapor averaged 67% of its maximum (unstressed) value during the growing season, with low light and low temperatures (not low humidity) causing the reductions. This reduction in canopy conductance correlates with the stable carbon isotope work of *Flanagan et al.* [this issue]. *Frolking* [this issue] assessed the effect of climate anomalies on carbon dynamics at the NSA-OBS site with a black spruce-moss process model. Net ecosystem fluxes of carbon (sinks) were calculated to be 120 g C m^{-2} yr^{-1} in 1994 and 90 g C m^{-2} yr^{-1} in 1995. The effects of introducing climate anomalies, in the form of 2-month periods of warm, wet, cool, or dry conditions, into the model runs varied with the timing of the anomaly and were not anticipated from simple relationships of gross processes with climate. If the moss layer remained intact to insulate the soil, large differences in air temperature were simulated to have only a minor (5–10%) effect on decomposition. *Bonan and Davis* [this issue] assessed the ability of their land surface parameterization (NCAR LSM1) to reproduce the fluxes of energy and carbon as measured by eddy covariance at aspen and jack pine sites. Using generic vegetation parameters, their calculations generally matched the observed net radiation and eddy covariance CO_2 and sensible heat fluxes but overestimated the latent

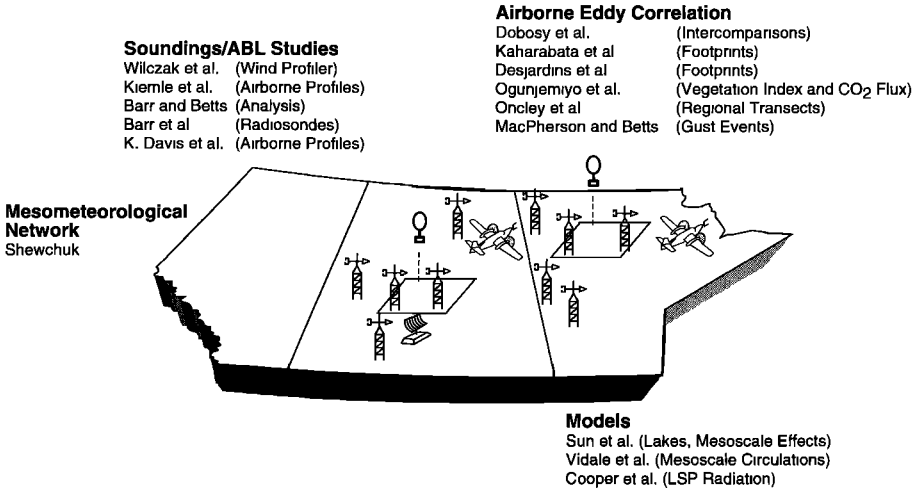

Figure 10. Schematic summarizing papers in section 6.1.3; landscape-scale carbon-water-energy dynamics and surface-atmosphere boundary layer interactions.

heat flux and did not capture real differences within vegetation types, for example between the jack pine sites in the NSA and SSA.

6.1.3. Landscape-scale carbon-water-energy dynamics and surface-atmosphere boundary layer interactions. Figure 10 summarizes the regional scale studies carried out in BOREAS using aircraft, sounding devices, meteorological networks, and coupled land-atmosphere models. *Shewchuk* [this issue] describes the mesoscale meteorological network that was deployed over the BOREAS 1000 × 1000 km region in 1994 and ran continuously through 1996. Two sites were located in the SSA, one in the NSA with another nearby, and the remaining six were placed at or near airfields in the region to allow for easy deployment and servicing. The BOREAS years of 1994 and 1995 showed warmer air temperatures than normal; 1994 was 0.7°C above the long-term mean. *Wilczak et al.* [this issue] present results obtained with a 915-MHz profiling radar located near SSA-OJP during BOREAS 1994. The device yielded profiles of wind velocity, virtual temperature, and atmospheric boundary layer (ABL) depth.

Several papers describe intercomparisons between airborne flux measurements, both aircraft to aircraft and aircraft to tower. *Dobosy et al.* [this issue] present extensive comparisons among the four flux aircraft involved in BOREAS, all based on wing-to-wing flights spaced throughout the BOREAS 1994 IFCs. Overall, the smallest correlations (most scatter) were between the LongEZ and the Twin Otter, while the Twin Otter-King Air and Electra-King Air pairings had higher correlations (less scatter). At least some of the reduced correlation for the LongEZ-Twin Otter comparison is because the air-motion equipment and techniques used on the LongEZ, with its small size and payload are different in many ways from the other three aircraft.

Significant efforts were devoted to determining the geometry of the surface source zones sampled by the airborne flux systems and in correlating the airborne fluxes with surface cover types. An encouraging study of aircraft flux footprints by *Kaharabata et al.* [this issue] made use of SF_6 releases to compute diffusion profiles within the lower boundary layer; their results indicate that the tower and low-level flux aircraft measurements can be expected to yield site-specific estimates of the surface fluxes. The work also explores the progressive decoupling of the boundary layer fluxes from surface features with increasing height. The differences in scale between aircraft- and tower-measured fluxes were also examined by *Desjardins et al.* [this issue], but the large difference in footprint size between those platforms makes it questionable to compare flux values directly. Among other things, it appears that the tower flux footprints (around 10^4–10^5 m^2 in unstable conditions) may have been drier than the aircraft flux footprints (around 10^7 m^2 for a 10-km pass), as evidenced by differences in sensible and latent heat fluxes. *Desjardins et al.* [this issue] compared fluxes measured by the Twin Otter, from short passes over specific TF sites (SSA-OA, SSA-OBS, SSA-OJP, NSA-OBS, NSA-OJP, NSA-YJP), with the TF measurements themselves (Figures 11a and 11b). The aircraft fluxes were on

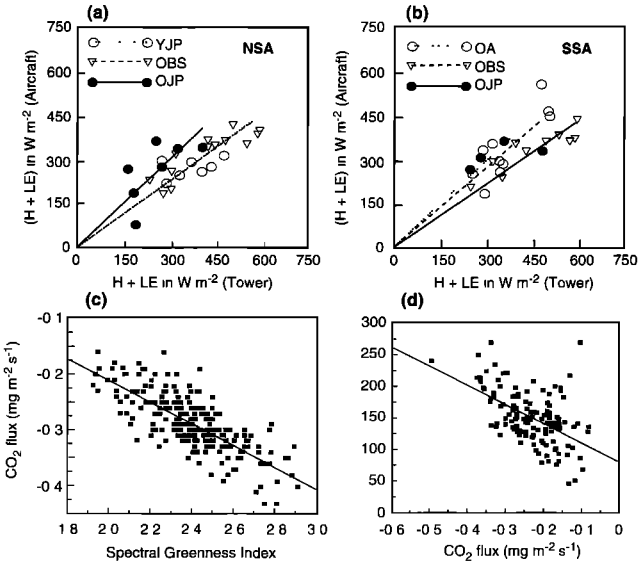

Figure 11. Comparison of the sum of sensible and latent heat fluxes measured by the Twin Otter (FT) aircraft over short runs close to several TF towers in (a) NSA and (b) SSA, from *Desjardins et al.* [this issue]. Comparison of aircraft-measured (FT) daytime (c) CO_2 fluxes with spectral greeness index and (d) latent heat fluxes with CO_2 fluxes as measured over a grid within the SSA; see *Ogunjemiyo et al.* [this issue].

average higher than the towers for latent heat, less than the towers for sensible heat, and comparable to the towers but with much more scatter for CO_2. The best comparisons (both in magnitude and in degree of scatter) were for momentum fluxes.

Two-dimensional patterns of surface-ABL coupling are presented by *Ogunjemiyo et al.* [this issue] for multiple grid flights in both study areas (Figures 11c and 11d). Strong correlations were observed between CO_2 flux and spectral greenness index, a very encouraging result for modelers trying to estimate large-scale surface fluxes over the boreal zone. These results concur with similar findings for grasslands [*Cihlar et al.*, 1992], leaf-scale studies in BOREAS [*Dang et al.*, 1997], and theory [*Sellers et al.*, 1992b]. At the same time, sensible heat fluxes were noticeably decoupled from the atmosphere-surface temperature difference (see also *Mahrt et al.* [this issue], *Vining and Blad* [1992], and *Hall et al.* [1992]).

Oncley et al. [this issue] documented seasonal and spatial flux changes along a regional transect, from just south of the SSA, up over the NSA, and into the tundra near Churchill, located near the southwest corner of Hudson Bay. Traces of CO_2 fluxes from three of these transects, in BOREAS 1994 IFC-1, IFC-2, and IFC-3, show changes with latitude, season, and land cover. There were also large-amplitude variations along each transect, superimposed on the other trends.

Airborne flux measurements taken over lakes highlight the complexity that must be addressed in modeling the regional surface energy budget. *Oncley et al.* [this issue] estimate that aircraft-level fluxes measured in their regional transects originated from surface areas (footprints) that were up to 40% water (lake surfaces). They also estimate that surface heat storage accounted for 30% (forests) to 40% (tundra) of the net radiation, with a large portion of the storage being assigned to the numerous lakes in the region. The length scales of the flight-level fluxes point to specific forcing mechanisms and to the difficulties faced in merging aircraft and tower flux data. A detailed analysis of flux fields over and around several lakes in the SSA by *Sun et al.* [this issue] indicates that the area-averaged sensible heat fluxes in the SSA were 12–24% lower than they would have been if no lakes were present. A well-defined divergent lake breeze circulation was observed over three lakes in the SSA during the day by the BOREAS flux aircraft with the circulation strength dependent on lake size and wind speed. The modeling study of *Vidale et al.* [this issue] investigates the contribution of mesoscale circulations to the large-scale surface-atmosphere fluxes of heat, water, and momentum. They conclude that these contributions can be significant under low-wind conditions and are generated by the differences between the energy balances associated with the different surface types found in the region, for example, lakes, dry uplands, and wet forested areas. They argue that these mesoscale effects should be parameterized in large-scale atmospheric models.

Aircraft measurements, radiosondes, surface measurements and analyses were all used to explore exchanges among the land surface, the boundary layer, and the free atmosphere. Inversion-level (ABL-top) entrainment, the capture of air from the free troposphere into the ABL, is an important factor which affects many of these exchanges. *Kiemle et al.* [this issue] used an airborne laser to remotely sense profiles of aerosols and water vapor that were used to build 2-D cross-sectional maps of entrainment structures and estimate entrainment-zone water vapor fluxes. They found good agreement with direct eddy-covariance measurements of the same fluxes. *Barr and Betts* [this issue] calculated area-wide estimates of entrainment rates from a budget analysis, based on data from the BOREAS radiosonde network. They found the entrainment parameter A_R above the boreal forest to be 0.21, which is in close agreement with the generally accepted value of 0.20. The surface available energy, calculated by summing the sensible and latent heat fluxes derived from the budget analysis, was within 4% of the independent estimate provided by the BOREAS meteorological network radiation measurements of *Shewchuk* [this issue]. They estimated the mean surface evaporative fraction over the forest during the summer to be 0.49, which can be compared with the value of 0.71 observed over the grassland FIFE site [*Smith et al.*, 1992].

Barr et al. [this issue] compared the surface fluxes derived from the radiosonde budget analysis with the eddy fluxes measured by the Twin Otter aircraft for the three growing season IFCs of BOREAS 1994. The sum of the aircraft-measured sensible and latent fluxes was 25% less than the radiation network estimate of available energy, in contrast to the 4% underestimate given by the budget analysis. However, the aircraft-derived estimate of the evaporative fraction was 0.52, which agrees well with the budget analysis figure of 0.49, which implies that the aircraft measurements may be systematically and proportionately underestimating the turbulent fluxes. The authors point out that both methods have value for the study of landscape-scale fluxes, with the budget analysis providing a large-area integral view, while the aircraft provide insight into spatial variations and associations between different surface flux regimes and land cover type. *Davis et al.* [this issue (a)] describe studies of the convective boundary layer based on aircraft measurements in BOREAS 1994. Convective boundary layer divergence during the midday period and early afternoon was often observed to dry out the atmospheric boundary layer; this drying may have had feedback effects on the vegetation which could have further reduced evapotranspiration, thus reinforcing the drying of the ABL; see also discussion by *Sellers et al.* [1995b]. *MacPherson and Betts* [this issue] document the structure of the strong ABL vortices seen by aircraft at low levels in 1994 in conditions of deep ABLs and low winds.

Cooper et al. [this issue] used the BOREAS meteorological observations, soil and vegetation parameters, and satellite-based estimates of radiation fluxes to drive a surface-atmosphere flux exchange model for an area covering most of the BOREAS domain. According to sensitivity analyses conducted with their model, root depth, soil moisture, and soil depth are the most important quantities in controlling transpiration fluxes. The radiation balance of the BOREAS region was studied by a number of BOREAS investigators using satellite data analyses (section 6.4.4).

6.2. Trace Gas Fluxes

Carbon exchange (CO_2, CH_4, and CO) was the principal focus of the TGB group, largely because of the great interest in the carbon balance of the boreal ecosystem but also because early measurements showed that the fluxes of nitrogen gases were small except in very recently burned areas. Most of the BOREAS trace gas studies were conducted within the NSA, which can be roughly divided into drained upland sandy soils usually dominated by jack pine and aspen; less well drained clay-rich soils dominated by black spruce; and wet peat soils dominated by sphagnum and sedges (Figure 12). TGB measurements were focused at the NSA tower sites, some landscape transects, a chronosequence of sites disturbed by fire,

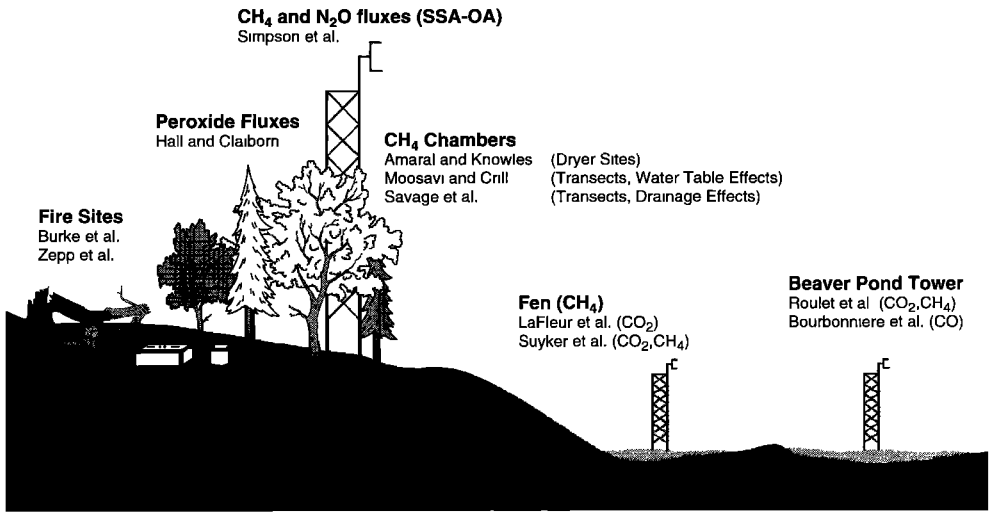

Figure 12. Schematic summarizing papers in Section 6.2; trace gas fluxes, principally CH_4 and CO. (CO_2 fluxes are covered in Section 6.1).

and a small tower at the NSA beaver pond. The CO_2 flux measurements of the TGB group are summarized in section 6.1.1; in this section we summarize the TGB CH_4 and CO research.

6.2.1. Small-scale fluxes with chambers and enclosures. *Amaral and Knowles* [this issue] found that drier sites, dominated by aspen, jack pine, or birch with a vascular plant ground cover and a thin (1–5 cm) surface organic layer, often acted as strong CH_4 sinks (Figure 13a). These sites were warmer and drier with faster nitrogen cycling and shorter path lengths to CH_4 oxidation layers. Consistent with early indications in temperate soils, *Amaral and Knowles* [this issue] determined that the location of CH_4 oxidation activity was near the surface of the mineral soil and at the base of the organic layer. A significant positive relationship between CH_4 uptake and surface C:N ratio was also observed. Their microbiological work demonstrates the potential for a near-surface organic layer of drained soils to produce CH_4 under anaerobic conditions. This effect is obvious on the macroscale but has not been well documented for well-drained soils.

Moosavi and Crill [this issue] observed CH_4 effluxes at all sites along their experiment transect which extended from some of the driest upland soils to inundated wetlands near the NSA beaver pond tower (NSA-BP) and the NSA-OBS site. Fluxes along this transect varied by 4 orders of magnitude; strong CH_4 sources require a consistent, high water table, as at the beaver pond mire (Figure 13b). Their work shows that upland sites might be converted from net sinks to net sources by minor changes in water table; also, low soil temperatures strongly inhibited methane flux rates even under saturated conditions.

Bubier et al. [1995] reported a large range in CH_4 fluxes (3 orders of magnitude) from different plant communities in the NSA fen complex, with the largest fluxes from open graminoid fens and the smallest from frozen peat plateaus and treed peatland areas. Temperature at the average position of the water table was the best predictor of seasonal average CH_4 fluxes, and floating peat sites maintained high fluxes during the dry late summer period in 1994. The correlations between CH_4 flux and plant community distribution may be useful for scaling fluxes from the chamber to the landscape using remote sensing.

Savage et al. [this issue] conducted a dark chamber measurement program and were able to model CH_4 fluxes using correlations with surface organic matter and the soil temperature at 20 cm in NSA upland soils. Weakly emitting sites were usually dominated by black spruce with a feather moss or

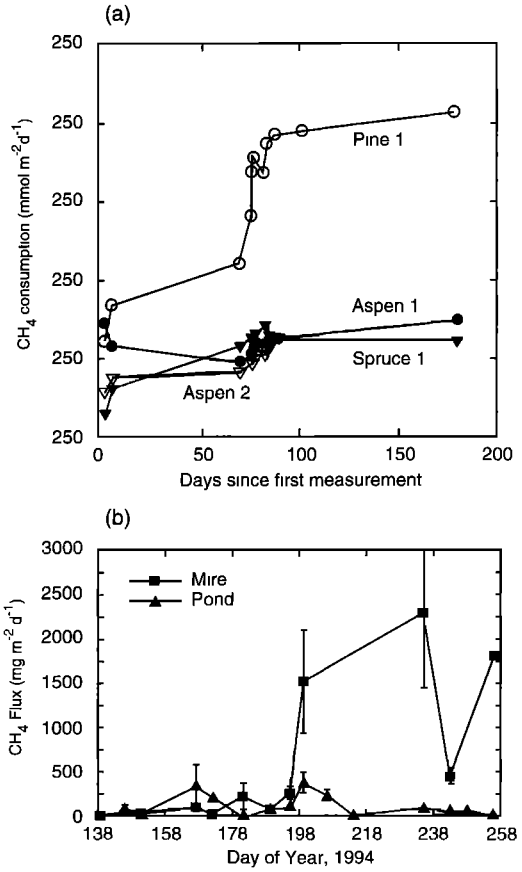

Figure 13. (a) Methane (CH_4) consumption by vegetation type in the NSA estimated from chamber measurements, from *Amaral and Knowles* [this issue]; (b) methane production as measured over a beaver pond site in the NSA, from *Moosavi and Crill* [this issue].

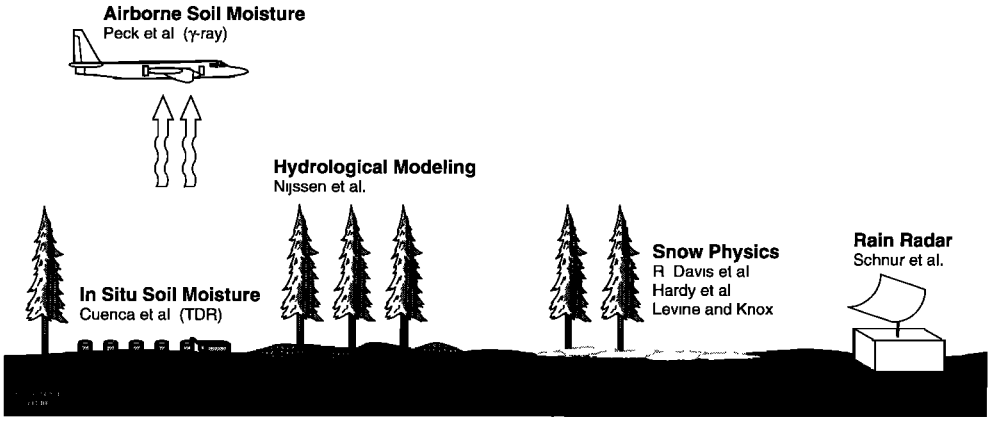

Figure 14. Schematic summarizing papers in section 6.3; soil and snow moisture and runoff.

sphagnum moss ground cover and a thick organic layer of 20–50 cm; these sites tended to be colder and wetter with long paths to the zone of CH_4 oxidation. Unlike other studies, the effects of H_2O on CH_4 uptake could not be observed in BOREAS because of limited variability in the soils over the season at most of the upland BOREAS sites. However, *Savage et al.* [this issue] observed that a single heavy precipitation event in early spring changed many of the jack pine sites from CH_4 sinks to sources for a short period of time. The problem of scaling the chamber measurements of these boreal wetlands to larger regions using remote sensing has been addressed in part by *Bubier et al.* [this issue] (section 6.3.1).

Fire disturbance is an important factor in the boreal forest. *Burke et al.* [this issue] measured fluxes of CO_2 and CH_4 across a chronosequence of burned sites on both clay (typical of less well-drained black spruce dominated sites) and sandy soils (typical of well-drained jack pine dominated sites). All of the sites were net sinks of atmospheric methane with median fluxes ranging from -0.3 to -1.4 mg C m^{-2} d^{-1}. Median fluxes of carbon dioxide from the forest floor to the atmosphere ranged between 1 and 2 g C m^{-2} d^{-1}. Both ecosystem characteristics (e.g., soil and vegetation type) and burning history (time since burn and fire intensity) appear to have some effect on atmospheric methane consumption and carbon dioxide emission by these forest soils. Their results suggest that soil CO_2 effluxes from upland black spruce stands may not be immediately impacted by fire. By 2 years postfire there appears to be a significant reduction in soil CO_2 flux, while soil respiration rates recover to preburn levels by 7 years postburn.

Carbon monoxide fluxes were slightly higher in more recently burned areas [*Zepp et al.*, this issue]. However, CO flux was shown to be affected by thermogenic and photogenic production as well as plant consumption and production.

6.2.2. Stand and plot-level trace gas dynamics with towers. The boreal forest is in a constant state of regeneration due to continuous disturbance by fire and beavers, insects, and to a lesser extent man. *Roulet et al.* [this issue] made continuous measurements of fluxes over a beaver pond in the NSA using a flux gradient method on a 1.25-m tower. It was discovered that the beaver pond was a strong and continuous source of both CO_2 and CH_4; 678 g m^{-2} CO_2 (183 g C m^{-2}) and 11.3 g m^{-2} CH_4 (8.3 g C m^{-2}) for the 120-day measurement period. Subsequent surveys of other beaver ponds in and near the NSA for surface emissions and near-surface CO_2 concentrations showed similar results, although *Staebler and Edwards* [1997] report lower values from a beaver pond in the SSA. This indicates that beaver ponds could be significant contributors to the boreal carbon cycle with source strengths 4 to 5 times larger than the sink strengths observed for boreal soils by *Harden et al.* [this issue] or as estimated for boreal peatlands by *Gorham* [1991].

The surface waters of the NSA beaver pond site were also shown to evolve CO, most likely from degradation by incident radiation of dissolved organic carbon [*Bourbonniere et al.*, this issue]. This illustrates some of the difficulties of estimating a regional flux of CO to the atmosphere.

Simpson et al. [this issue] measured CH_4 and N_2O fluxes above the SSA-OA stand using a tunable diode laser. Small emissions of both gases were observed for the measurement period (April 16–September 16, 1994), around 1.9–2.5 ng m^{-2} s^{-1} for N_2O and 21–28 mg m^{-2} s^{-1} for CH_4. The authors correlated the above-canopy measurements with some (below canopy) chamber measurements to conclude that CH_4 emission from scattered anoxic patches in the aspen forest overwhelmed CH_4 uptake by the larger drier areas. This result should be compared with the observations of *Amaral and Knowles* [this issue], described above, who found the drier areas to act as strong CH_4 sinks; however, they did not comment on the sign of the net CH_4 flux on intermediate (stand level) scales, as *Simpson et al.* [this issue] have done.

Understanding the sources and sinks of hydrogen peroxide (H_2O_2) and organic peroxides (ROOH) is important for understanding atmospheric chemistry in general and acid deposition in particular. *Hall and Claiborn* [this issue] used concentration gradient measurements from the tower of the SSA-OJP site to infer deposition velocities for these compounds. They report daytime and nighttime deposition velocities for hydrogen peroxide of 5 cm s^{-1} and 1 cm s^{-1} respectively, with much lower rates for organic peroxides. The highest deposition rates occurred from 1100 to 1500 LT, indicating that deposition rates are primarily turbulence limited. These rates are similar to values obtained over deciduous forests in the southern United States.

6.3. Soil and Snow Moisture and Runoff

Soil moisture and snow measurements in BOREAS ranged from point measurements in the vicinity of the TF sites to airborne measurements over the TF sites, along short transects within the study areas, and along an extended transect between the study areas (Figure 14). Traditional catchment hydrologi-

(a)

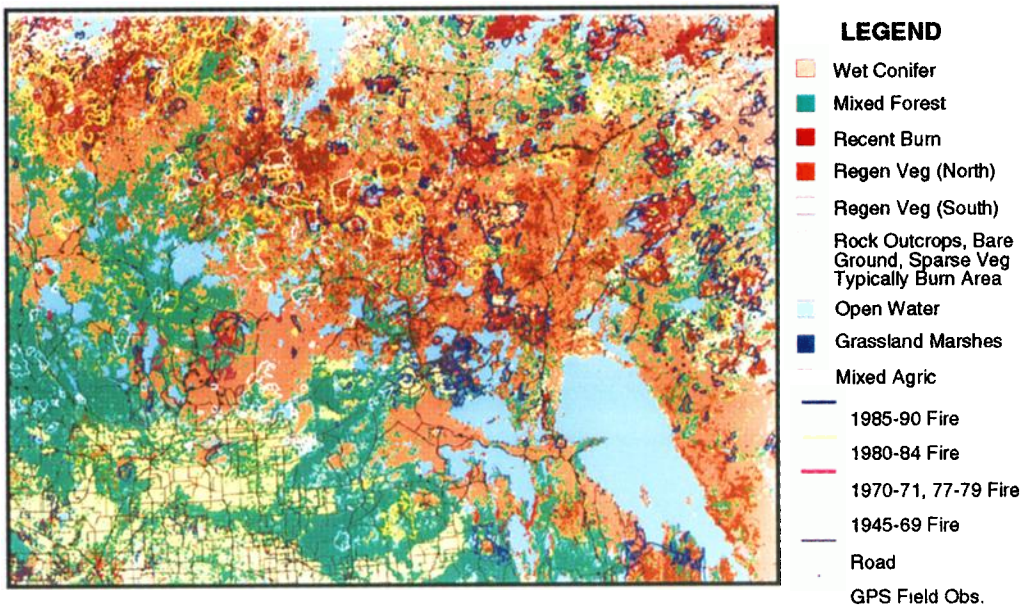

(b)

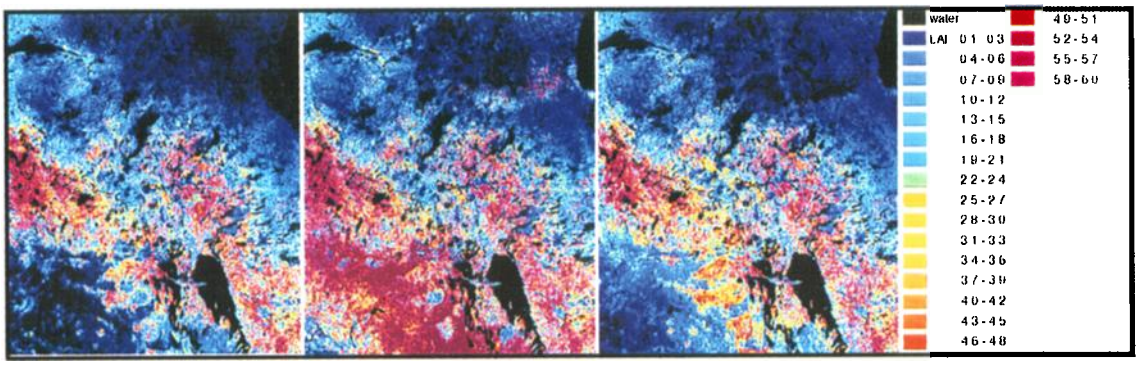

(c)

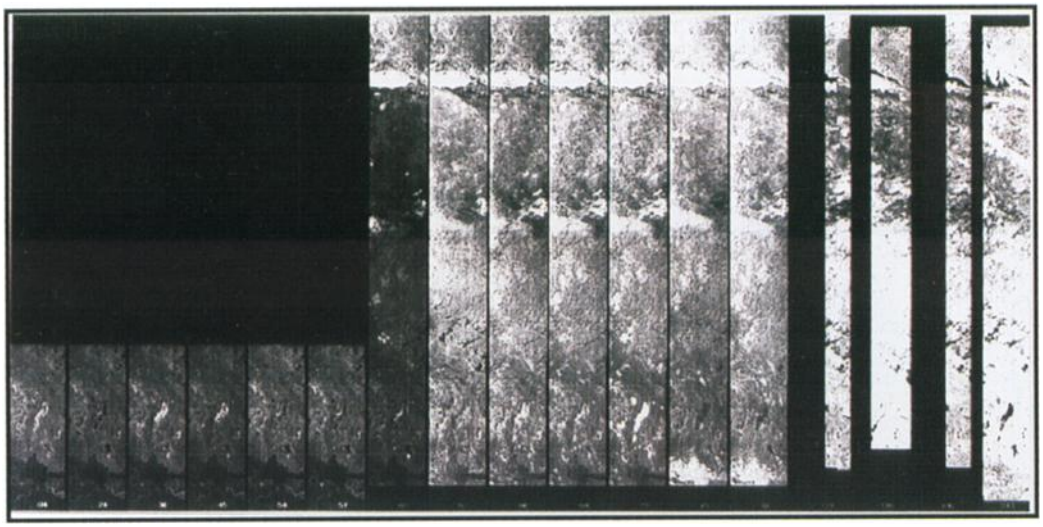

Plate 2. Use of regional remote sensing to monitor (a) land cover and fire disturbance from *Steyaert et al.* [this issue]; (b) regional FPAR from *Cihlar et al.* [this issue]; and (c) soils freeze-thaw status from *Way et al.* [this issue] (image brightness proportional to radar return rendering dark areas as frozen sites and light areas as thawed).

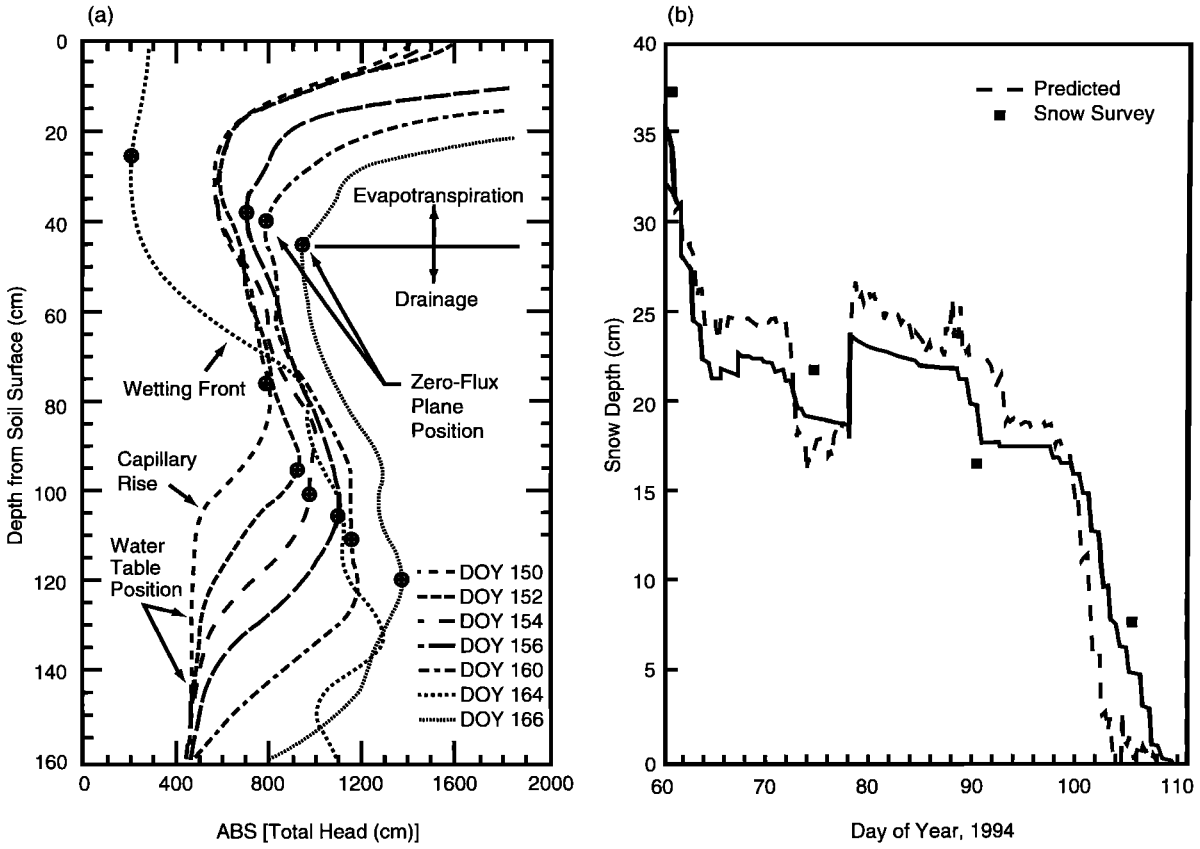

Figure 15. (a) Absolute value of total head (or soil water potential) as a function of depth measured using time-domain reflectrometry at a tube at the NSA-OJP site, from *Cuenca et al.* [this issue]; (b) comparison of modeled and observed (snow survey) snow depths for a plot at the SSA-OJP site; see *Hardy et al.* [this issue].

cal studies were performed in both the SSA and the NSA; also, in the SSA a precipitation radar was deployed during BOREAS 1994. A number of supporting modeling studies were made of soil moisture dynamics, snow physics, and catchment hydrology.

6.3.1. Point measurements and modeling of soil moisture dynamics. Soil moisture measurements were collected via in situ time domain reflectrometry (TDR) observations in the vicinity of the tower sites [*Cuenca et al.*, this issue] (Figure 15a). The typical measurement design used involved transects of five sites spaced 5–20 m apart. These transects provided a unique opportunity to study the space-time variability of soil moisture profiles over footprints representative of the immediate area surrounding the tower sites. In addition to the expected evolution of the depth profiles through the season, these measurement systems show that strong soil moisture variations in the near-surface level (depths to 20 cm) occurred even at spatial scales of less than the transect lengths. These variations were especially pronounced early in the season and following precipitation events. *Cuenca et al.* [this issue] also estimated evaporative fluxes in the vicinity of the NSA-OJP and SSA-OJP towers from changes in soil moisture profiles. Comparisons with tower-measured fluxes indicated that the evapotranspiration rates estimated from soil moisture observations were about two thirds of those measured by eddy correlation. Reasons for the discrepancies are not clear at this point.

Nijssen et al. [this issue] describe the testing of a distributed hydrological model, which will ultimately be applied to subcatchments in the SSA and NSA, and to smaller areas of 5 km × 5 km surrounding the tower sites. The model simulated the redistribution of soil moisture in the saturated zone due to local topographic effects. Model estimates of latent, sensible, and ground heat fluxes, and net radiation were compared with tower observations. The model-predicted heat fluxes agreed reasonably well with those observed for the NSA-OBS, SSA-OBS, and the SSA-OA sites after the model had been modified to incorporate moss moisture storage effects and temperature feedbacks to canopy resistance. A slight time lag in the diurnal cycles of latent and sensible heat was attributed to deficiencies in the ground heat flux representation.

6.3.2. Stand-level soil and snow moisture dynamics. Soil moisture transects were monitored via an airborne gamma ray sensor for selected dates from August 1993 to the fall of 1994 [*Peck et al.*, this issue]. Comparisons of the airborne observations with TDR probes at the SSA-OA site showed that the aircraft measurements consistently underestimated (by a factor approaching 2) the near-surface measurements taken by TDR. However, the flight line was some distance (almost 1 km) from the tower, so spatial variability may explain at least part of the difference. In the vicinity of the SSA-OJP site, the aircraft and in situ measurements agreed more closely. Especially during the dry periods, spatial variability of soil moisture in this area was quite low. Attempts to compare in situ and aircraft surface moisture observations at the SSA-OBS site were abandoned due to the periodic presence of surface water, and moisture storage in the moss and peat layer which are not measured by the TDR techniques. However, gravimetric surface soil and moss/peat moisture transects collected for calibration of the

aircraft measurements showed that large spatial differences in soil and other surface moisture (e.g., moss) contents exist within the "footprint" of the SSA-OBS site, which must be taken into account when relating the SSA-OBS tower flux measurements to ground data.

Davis et al. [this issue (b)] performed a sensitivity analysis to examine the effects of conifer height and canopy density on the timing and rates of snow ablation. The analysis assumed radiation to be the first-order cause of snowmelt consistent with the results of *Hardy et al.* [this issue]. Forest maps of tree height and canopy density combined with generic conifer canopy properties provided boundary conditions for the calculations, which showed that canopy density and tree height are of more or less equal importance in controlling snow ablation rates. The calculated time series of snow depth showed close agreement with survey data from jack pine sites, but measurements showed slower melting than the model calculations in black spruce stands.

Hardy et al. [this issue] compared model predictions of snow grain growth, compaction, and melting, with measurements of snow depth at the SSA-OJP site (Figure 15b). They adjusted meteorological measurements from *Shewchuk* [this issue] to mimic conditions at the forest floor and over a nearby open area. *Levine and Knox* [this issue] present results from a soil and snow physics simulation model that includes a description of the effects of the overlying vegetation canopy. The simulations were run for the SSA-OBS, SSA-OJP, and NSA-OJP sites. The results showed good fits to measured snowpack thickness and soil temperature profiles and also predicted the extended frozen period in the NSA and the formation of an ice lens at the SSA-OBS site.

6.3.3. Landscape-scale precipitation and soil moisture dynamics. An important cause of spatial variability in soil moisture, and hence in surface moisture and energy fluxes, is the space-time variability of precipitation. *Schnur et al.* [this issue] operated a truck-mounted C-band precipitation radar, located to the south of the SSA from May to September 1994. Comparisons of radar-derived precipitation fields with estimates from a gage network showed that in terms of area averages, the radar estimated slightly higher precipitation accumulations. Simulations performed by using a spatially distributed hydrology model showed that spatial averages as well as local estimates of surface energy fluxes were quite sensitive to the use of radar-based precipitation images as compared with a gage-only product. However, when the effects of spatial resolution were isolated (by using only the radar precipitation product at different spatial resolutions), the sensitivity of area-averaged (over the 40 × 50 km southern modeling subarea) energy fluxes to the precipitation product was generally less than about 10%. However, local differences were much more sensitive to the spatial resolution of the precipitation product.

6.4. Remote Sensing Science

Remote sensing served three critical roles in BOREAS. First, it provided local- to regional-scale land cover data and solar radiation forcings which allow us to investigate the processes governing forest-atmosphere interactions on timescales ranging from minutes, with the GOES satellite, to decades, with the Landsat series of satellites. Second, ground, aircraft, and satellite data (Table 4) were used to develop and test ecosystem-atmosphere process models. Finally, remote sensing images were processed to define the overall context and representativeness of the study regions with respect to the boreal forest biome as a whole (Figure 16 and Plate 2).

In support of these goals, RSS investigators acquired measurements of reflectance, emittance, and backscattering properties of forest canopies and background, and atmospheric scattering from the leaf to the regional scale. In parallel, a significant amount of ancillary validation data on forest stand and soil biophysical properties was acquired in situ (Table 4). These combined data sets are a valuable resource for developing and testing new algorithms for mapping terrestrial biophysical parameters; specifically, they will prepare the way for the next generation of Earth-observing satellite instruments such as MODIS, MISR, and RADARSAT. The data will be produced on CD ROM by the BOREAS Information System (BORIS) and eventually archived at the Oak Ridge Data Analysis and Archiving Center (DAAC).

The RSS investigators also engaged in algorithm development and testing and produced multiyear site-level, study area level, and regional-scale maps of radiation and biophysical parameters. A number of land cover parameter maps (Plate 2) have been produced as part of BOREAS to provide inputs for ecosystem or climate models and to evaluate the expected performance of future spaceborne sensors. The articles summarized below represent a significant cross section of BOREAS remote sensing science activities and range across the entire multiscale design of BOREAS.

6.4.1. Ground and aircraft measurements of biophysical and optical characteristics and understory and canopy reflectance. Remote sensing algorithm development, as with process model development, involves a scaling strategy from the leaf level, where electromagnetic properties can be carefully measured, to the pixel level (meters to kilometers) where ground-based measures are impractical and remote sensing algorithms must function autonomously. Translating data and knowledge among these scales involves a mix of measurement and modeling in the form of radiative transfer (RT) models that can accurately compute reflectance as a function of canopy structure, optical and biophysical characteristics, etc. The validated RT models are then used for algorithm development to infer canopy characteristics over larger areas given satellite reflectance values. The algorithms take the form of either simple functional relations between vegetation indices and biophysical characteristics developed by using RT simulations or more sophisticated direct inversion approaches. The BOREAS experiment was designed in the context of this general scaling and algorithm development strategy, and the remote sensing papers in this special issue reflect this approach.

An important unresolved issue going into BOREAS was the accurate in situ characterization of canopy biophysical parameters over plots large enough to validate process models and remote sensing algorithms. BOREAS staff and PIs designed and implemented an approach which combined destructive sampling, allometry, and optical methods (hemispherical photography, photosynthetically active radiation (PAR) sensors, multiband photography) to generate ground estimates of canopy architecture, leaf area index (LAI), biomass density (BMD), and the fraction of PAR absorbed by the vegetation canopy (FPAR) over 30 × 30 m plots and 100-m transects within the BOREAS tower and auxiliary sites (Figure 2). Several activities reported here deal with ground measurements of these biophysical characteristics.

Chen et al. [this issue] used direct and indirect techniques to estimate LAI for the BOREAS tower and auxiliary sites. They

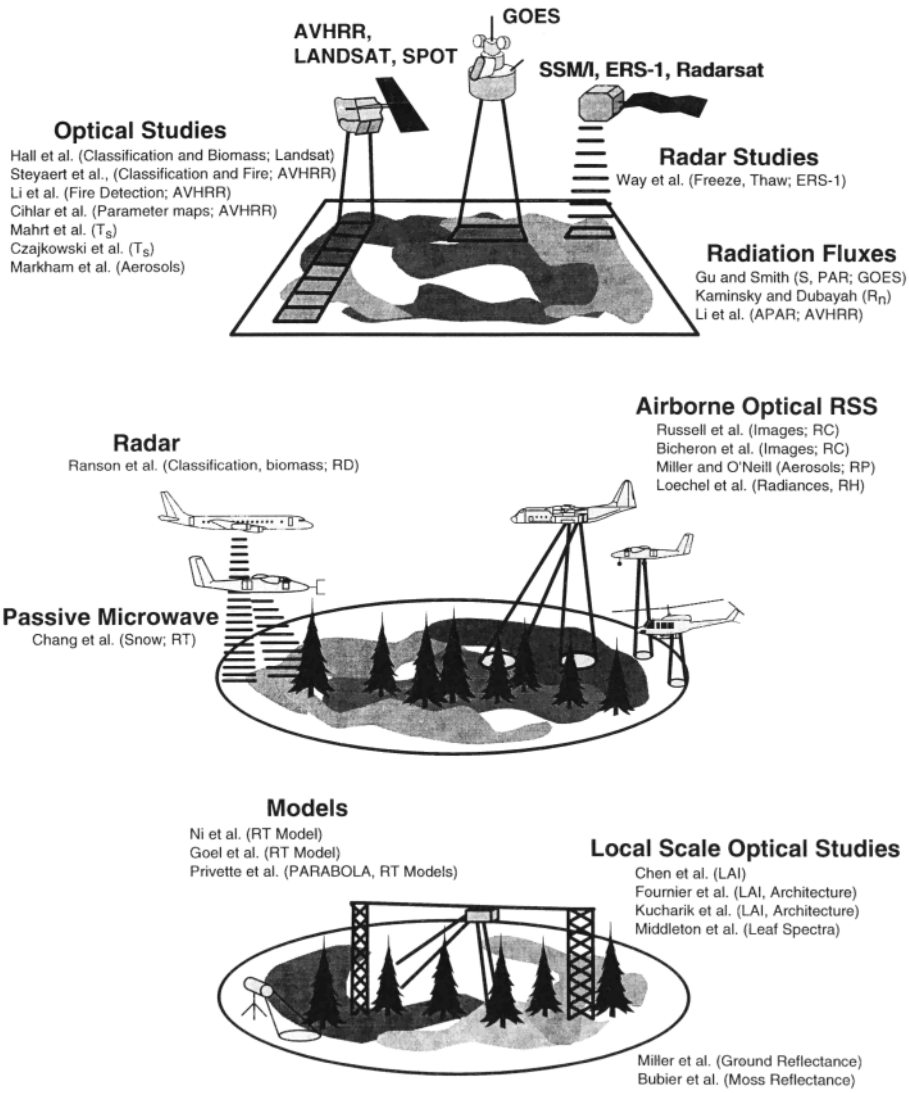

Figure 16. Schematic summarizing papers in section 6.4; remote sensing science. (RC, RD, RP, RH, RT refer to aircraft platforms; see Table 2).

compare results from their indirect optical technique with those from a similar manufactured instrument and estimates derived from direct destructive samples. They found that the manufactured LAI instrument underestimated the destructive sample estimates of LAI because its algorithm assumed a spatially random distribution of leaves to compute LAI as a function of canopy gap fraction. *Chen et al.* [this issue] developed a clumping index to correct for this error and used it to estimate the LAI of several BOREAS forest sites. *Chen et al.* [this issue] found that LAI ranged from 1 to 4 for jack pine and aspen stands and from 1 to 6 for black spruce. They also report errors of the order of 25%, a magnitude consistent with direct destructive sampling techniques. The difficulties with ground characterization of biophysical variables must be kept in mind when using them to evaluate satellite-based remote sensing algorithms.

Fournier et al. [this issue] combine hemispherical photography, stand mapping, destructive sampling and modeling to characterize the architecture of vegetated boreal landscape elements. They employ a variety of destructive and optical techniques to characterize the three-dimensional distribution of canopy elements and crown form, data which provide critical inputs for their and other RT models. With their model they are able to compute and validate architectural variables such as gap size as a function of view zenith. Their data sets will be used to explore the relationships among stand structure, light regimes, canopy reflectance, and ecological function in general.

Kucharik et al. [this issue] utilized a two-band visible and near-infrared (NIR) digital charge-coupled camera, the multiband vegetation imager (MVI), to map the nonrandomness of canopy gaps, i.e., the spatial "clumping" of leaves. As mentioned above, the spatial distribution of leaves is a key parameter for optical LAI-measuring devices which relate gap fraction to LAI; the distribution may also be critical to parameterizing canopy CO_2 assimilation models and RT models relating canopy reflectance to biophysical parameters. Aspen and balsam poplar canopies were imaged from below with the MVI to generate an NDVI image, which permitted the identification of sunlit and shaded foliage, discrimination among live foliage, twigs and branches, and sky-cloud discrimination. Analyses of the imagery showed that an assumption of

spatially random foliage leads to underestimates of LAI in aspen by about 45%, which then leads to underestimates in CO_2 assimilation rates by about 39%. In support of this, *Dang et al.* [this issue] show that the relationship between canopy photosynthetic capacity and spectral vegetation index can vary considerably depending on the scaling algorithm used.

An important and sometimes neglected component of forest remote sensing studies is the bidirectional reflectance of understory vegetation. *Miller et al.* [this issue] describe a multiteam effort to measure nadir understory reflectance for the tower flux sites. Shaded and sunlit reflectance measurements were made for black spruce and jack pine sites near solar noon throughout the year, capturing the variability due to species and seasonal phenology between and within the tower flux sites. Temporal-spectral variations were observed which correlated with changes in vegetation type and phenology. The data were shown to be useful for improving regression relationships between leaf area index and vegetation indices.

Multiband optical properties of mosses were found to be a critical input for understanding the relationship between canopy reflectance and biophysical properties. In addition to the leaf optical properties measured by *Middleton et al.* [this issue], discussed in section 6.1.1, *Bubier et al.* [this issue] conducted high spectral resolution measurements of moss ground cover on the BOREAS wetlands sites. They found that high spectral resolution reflectance data could be used to discriminate the brown and sphagnum mosses associated with bogs, fens, and water-saturated conifer stands from the feather mosses associated with more productive stands growing on mineral soils. Since *Harden et al.* [this issue] report that drainage class is a strong determinant of carbon storage rate, the results of *Bubier et al.* [this issue] provide a basis for designing remote sensing algorithms that can map these important classes over large areas.

Moving upscale from ground to aircraft, *Loechel et al.* [this issue] report on a series of helicopter-based reflectance measurements acquired over the BOREAS tower and auxiliary sites throughout the 1994 growing season. They compared red and NIR reflectance measurements to ground measures of overstory LAI. Their results show that reflectance in individual bands as well as common vegetation indices based on these bands are poorly correlated with LAI, confirming the results obtained by *Hall et al.* [1995] over similar species in the Superior National Forest in Minnesota. *Hall et al.* [1995] analyzed the difficulties found by *Loechel et al.* [this issue] and proposed and evaluated alternative approaches that demonstrate skill for those situations where vegetation indices perform poorly. *Hall et al.* [this issue] successfully applied these techniques to black spruce covers in BOREAS (section 6.4.2).

Bidirectional reflectance images similar to those to be obtained from the MISR sensor to be flown aboard EOS AM-1 were acquired over the BOREAS SSA and NSA sites from the airborne advanced solid-state array spectroradiometer (ASAS) mounted on the NASA C-130. *Russell et al.* [this issue] report on these spectral and bidirectional reflectance data acquired over the BOREAS SSA tower sites. They found that bidirectional reflectance distribution function (BRDF) measurements at 26° backscatter in the solar principal plane were best for discrimination among species. They also confirm a large number of previous studies showing view angle to significantly affect NDVI and its relationship to biophysical properties. Their measurements show that view angle effects are much more important for conifer stands than for aspen.

The advantages of multiangle observations for forest-type classification are also addressed by *Bicheron et al.* [this issue] who describe an analysis of bidirectional reflectance data acquired from the airborne POLDER (Polarization and Directionality of Earth Reflectances) instrument. The instrument was flown aboard the NASA C-130 aircraft over five vegetated areas representative of BOREAS land cover. Using multiple spectral bands and three view directions greatly improved the discrimination of forest cover.

6.4.2. Radiative transfer models and algorithm development. The most direct approach to using RT models in inferring biophysical characteristics of the land cover is through mathematical inversion of the RT model given a set of reflectance measures. However, this approach is often limited by the number of parameters in the RT model, which in many cases exceeds the number of remote sensing measurements necessary for inversion. To circumvent this problem, sensitivity analyses often reveal which parameters can be held fixed with minimum impact to the inversion, thereby reducing the number of bands required for inference.

BOREAS investigators and staff acquired validation data sets which are ideal for evaluating different direct inversion techniques. *Privette et al.* [this issue] describe some of the above-canopy measurements acquired in BOREAS with the PARABOLA instrument, a three-band radiometer capable of rapidly acquiring reflectance measurements over the entire viewing hemisphere. PARABOLA was used to collect BRDF data sets at the BOREAS SSA aspen, black spruce, and jack pine flux tower sites (SSA-OA, SSA-OBS, SSA-OJP) using a 100-m-long tram-mounted system elevated several meters above these canopies. The observed BRDFs were used to evaluate the performances of 10 different RT models in predicting albedo and nadir reflectance over nine land cover types ranging from grasslands at the FIFE site to the forest data sets of BOREAS. Their findings provide an important lesson for large-area remote sensing algorithms. They show that simpler RT models using fewer parameters may be both faster and more robust for inversion than complex RT models, even though the simpler models do not represent the BRDF as well. They attribute this to the fact that with simpler models, more accurate inversions are possible with sparse remote sensing data sets.

Goel et al. [this issue] demonstrate a computer-based simulation approach for investigating the utility of reflectance-based remote sensing algorithms and vegetation indices to infer canopy biophysical characteristics. They use a sophisticated computer graphics-based model to simulate the relationship between red and NIR reflectance and canopy biophysical characteristics at various view and illumination angles, including the "hot spot" where the view and solar illumination angles are identical. They varied the magnitudes of the biophysical characteristics used as parameters in the canopy reflectance model (crown dimensions, crown spacing, leaf size, etc.) over realistic ranges to simulate the covariance among these parameters and reflectance. This permits them to investigate how the relationship between reflectance and each of the canopy model parameters such as leaf size is affected by known variations in the remainder of the canopy model parameters. They show, for example, that for deciduous canopies, the ratio of NIR reflectance for a given view angle to hotspot reflectance at a high Sun zenith angle is the best index for estimating leaf size since it minimizes the effect of variability in the other model param-

eters. For conifers they show that leaf size is difficult to estimate except for sparsely spaced canopies.

Ni et al. [this issue] further develop geometrical optical canopy reflectance models to include light interception effects within tree crowns from the nonrandom spatial distributions of leaf material typical of needleleaf canopies [see *Chen et al.*, this issue; *Fournier et al.* this issue; *Kucharik et al.*, this issue]. For a specified canopy leaf area index, leaf clumping increases gap probability within a tree crown, increasing light transmission to the canopy floor; however, this is partially offset by reduced light transmissivity through the clumps. The primary motivation for the work of *Ni et al.* [this issue] was to improve the radiative computations for snowmelt models, an important problem for properly parameterizing albedo in weather forecast and climate models [see *Betts and Ball*, this issue], as well as in initiating photosynthesis in carbon models [see *Frolking et al.*, 1996]. Consistent with this motivation they test their model by comparing its estimates of downwelling solar flux through the canopy profile to measured values. These comparisons show their modified model to agree well with measured values; in addition, they show that the vertical distribution of radiation is quite different than would be predicted by Beer's law, pointing out the importance of proper representations of tree morphology to both photosynthesis and snowmelt models.

6.4.3. Landscape-scale land cover and biophysical characteristics algorithms. A number of BOREAS investigations developed and produced multiyear site-level, study area level, and regional-scale maps of radiation and biophysical parameters. This parameter set was defined by joint efforts between the BOREAS modeling group and the RSS investigators, identifying those land cover classes and radiation parameters considered to be essential as inputs to the process models and also spectrally separable using remote sensing multispectral, multidate reflectance measurements (see Figure 17).

Hall et al. [this issue] developed a physically based approach to integrated land cover classification and biophysical parameter estimation using Landsat Thematic Mapper (TM) data. They utilized geometric RT models to compute the expected spectral signatures of the land cover classes as a function of the distribution of biophysical parameters within each class. The algorithm does not depend on unrealistic statistical assumptions, such as multivariate normal distributions, to represent class signatures. Further, it can compute the signatures as a function of changing view and illumination conditions and other variables that give rise to global variations in the signatures, thus rendering the signatures more invariant to changing global conditions. Using this algorithm, they classify the BOREAS SSA and estimate the proportions of the land cover classes used in modeling. In addition, they estimate biomass density (BMD) for black spruce in the study area. BMD is an important parameter for ecosystem models since aboveground carbon is related to ANPP and litter fall [*Gower et al.*, this issue]. BMD is usually related to maintenance respiration, and in conifer wetlands, BMD may be related to below-ground drainage and age class. As *Harden et al.* [this issue] show, drainage and age class correspond to varying annual carbon storage rates. The *Hall et al.* [this issue] map for wetland conifers in the SSA shows BMD to be bimodally distributed with the lower mode (1–6 kg m^{-2}) consisting of poorly drained areas such as bogs and fens and the upper mode (8 to 10 kg m^{-2}) consisting of moderately to better drained areas with a slightly lower water table.

Steyaert et al. [this issue] mapped the 1000 × 1000 km BOREAS study region at 1 km resolution using an algorithm developed by *Loveland et al.* [1991] (Plate 2a). The algorithm utilized monthly composites of normalized difference vegetation index (NDVI) observations acquired by the advanced very high resolution radiometers (AVHRR) carried on the NOAA meteorological satellites. The resulting land cover product was evaluated by comparison to the *Hall et al.* [this issue] 30-m TM land cover product to investigate the effects of scale on land cover identification. The *Steyaert et al.* [this issue] map showed that wetland conifer dominates the BOREAS study region. Wetland conifer is an important landscape element in carbon sequestration [*Gower et al.*, this issue; *Harden et al.*, this issue]. *Steyaert et al.* [this issue] also discovered another result key to understanding the regional carbon flux; the boreal ecosystem is more fire prone than previously believed, with nearly 30% of the area having been cleared by fire in the last 25 years.

Ranson et al. [this issue] report on the results of using SIR-C, the *X*-band synthetic aperture radar carried aboard the NASA DC-8, and Landsat TM to classify the BOREAS SSA and map aboveground woody biomass. Plot-level measurements of leaf, branch, bole size, and angle distributions were used to develop relationships between backscatter coefficients in various bands, then the relationships were applied to imagery covering the SSA. Pixel-level BMD accuracies were estimated at 1.6 kg m^{-2} over a range of biomass from 0 to 15 kg m^{-2}. This technique could be a valuable mapping technique for the boreal ecosystem which is often obscured by clouds or smoke.

Li et al. [this issue (b)] used the 3.0-μm channel of AVHRR single-date images to detect fire events during 1994 in the BOREAS region. This work complements the historical fire-scar maps of *Steyaert et al.* [this issue]. The *Li et al.* [this issue (b)] 1994 fire map shows that 99 fires occurred in the BOREAS region during the summer of 1994, consuming about 20,000 km^2, or about 2% of the total BOREAS region. Their accuracy assessment showed that they detected 87% of the ground-detected fires and, in addition, identified many fires missed by conventional methods. Composited data were not effective in fire detection, which limits the usefulness of this technique when smoke from fire and clouds obscure the region.

Cihlar et al. [this issue] developed and applied an AVHRR preprocessing algorithm to the NOAA 11 1994 growing season AVHRR record to compute 10-day composites of surface reflectance in bands 1 and 2 and emittance in band 4 based on data with improved calibration, registration, and correction for atmospheric and angular reflectance effects. The composited data were also screened for cloud and snow contamination using the multidate algorithm developed by *Cihlar et al.* [this issue]. Clear-sky values in bands 1 and 2 were corrected for fixed and assumed densities of molecular, aerosols, and water vapor absorption and scattering. Band 4 was corrected for atmospheric water vapor effects to generate surface temperatures using split-window techniques [*Coll et al.*, 1994]. Where no clear-sky pixels existed in a 10-day period during the growing season, replacement pixels for bands 1 and 2 were substituted from adjacent composited periods using linear interpolation. Because the composited data set consists of observations at multiple view angles, *Cihlar et al.* [this issue] also apply land-cover-dependent corrections to bands 1 and 2 for view-angle variations in surface reflectance. The preprocessed, composited data set was then evaluated by using TM data and further processed using algorithms developed at the Canadian Centre for Remote Sensing (CCRS) to produce regional maps of seasonal multidate NDVI, surface temperature,

LAI, green FPAR, PAR, albedo, and APAR (absorbed PAR) over the 1000 × 1000 km BOREAS study region. These parameter maps are being used in various process studies but need further validation and comparison with other products (see also Plate 2b).

Two papers deal with the combined use of satellite thermal and optical data to infer certain thermodynamic properties of the vegetated land surface and environmental variables in the atmospheric boundary layer. *Mahrt et al.* [this issue] examine the use of radiometric temperature to infer aerodynamic temperature, a key variable in sensible heat transfer between the surface and the atmosphere. In essence, their work confirms similar research done in other ecosystems [e.g., *Vining and Blad*, 1992; *Hall et al.*, 1992], in that radiometric temperature cannot be used to accurately infer aerodynamic temperature for sensible heat computation when using Monin-Obukhov similarity theory. In the boreal environment the warm sphagnum moss background contributes significantly to radiometric temperature but insignificantly to sensible heat transfer (aerodynamic temperature). They show, however, that the difference in these two temperatures decreases with red reflectance corresponding to denser canopies and, subsequently, low visible background fraction. *Czajkowski et al.* [this issue] used the AVHRR surface NDVI versus radiometric temperature in an attempt to infer surface air temperature. They found that most of the air temperature values inferred in this way fell within ±5 K of ground-measured temperatures, but there were observed differences as large as ±15 K. They conclude that there is a consistent bias of 3.2 K caused by errors in the split-window estimates of surface temperatures and subpixel clouds and standing water. The main advantage of this approach would be more explicit spatial information on surface air-temperature distribution; however, the frequent presence of clouds and smoke in the region limits opportunities for applying this technique.

The final two papers in this section deal with the remote sensing of snow and soil temperatures, two important variables that other BOREAS studies have shown strongly influence interannual variations in carbon uptake by wetland conifers [e.g., *Frolking et al.*, 1996]. Timing of snowmelt is critical in determining the course of surface albedo, subsequent soil thawing, and the initiation of photosynthesis by wetland conifer. *Chang et al.* [this issue] use brightness temperature differences in the 18- and 37-GHz bands from microwave multiband radiometers flown aboard the Twin Otter to determine snow water equivalent (SWE) and lake ice thickness. They evaluate two algorithms that differ primarily in the parameterization of mean snow grain size. In nonforested areas the two algorithm's SWE estimates differ by from 4 to 10 mm from ground measures for a snowpack of about 40 mm SWE. In forested areas the differences are larger with estimated SWE values generally lower than ground observations. Overall, differences in observed and inferred SWE in the SSA with its denser forests are larger than for the NSA, indicating the importance of correcting SWE estimates for forest cover.

Completing the picture of the beginning of active photosynthesis, *Way et al.* [this issue] exploit the sensitivity of microwave backscattering cross section to dielectric differences between frozen and liquid moisture to map soil and canopy freeze/thaw boundaries in the boreal springtime. Currently, soil and canopy temperatures are modeled as a function of soil and canopy thermal properties, moisture, and air temperature. These variables are not easily obtained at the landscape scale; thus augmenting model predictions with direct measures of the water state will be a valuable adjunct to landscape-scale carbon flux prediction. From ground measures, *Way et al.* [this issue] showed that transitions in soil and stem thawing relate directly to the state of soil respiration and canopy photosynthesis, respectively. Using ERS-1 satellite radar images, they showed that shifts in backscattering cross section correlate well to soil thaw and possibly to canopy thaw as two independent transitions (Plate 2c).

6.4.4. Radiation and atmospheric effects. Five papers focus on radiative components of the surface energy balance and the effects of atmospheric aerosols on downwelling and upwelling radiation retrieved from satellite observations. The net radiation R_n absorbed by the surface through radiative exchange with the atmosphere is a critical parameter in carbon, water, and energy cycling. To infer R_n, the components of the surface shortwave and longwave radiation balance must be quantified.

$$R_n = S\{1 - a\} + L_{wd} - L_{wu}, \quad (1)$$

where S is the downwelling shortwave radiation energy flux (W m^{-2}), a is the albedo, and L_{wd} and L_{wu} are the incident and emitted longwave radiation at the surface (W m^{-2}), respectively. In addition to S the downwelling photosynthetically active radiation flux (PAR) is also a key variable in the surface energy balance of vegetative surfaces since it regulates photosynthesis and the stomatal control of evapotranspiration.

Gu and Smith [this issue] describe the modification and evaluation of a published algorithm for inferring S and PAR fluxes from GOES 7 imagery. Their maps were generated for the entire BOREAS study region at 30-min intervals and at 1 km resolution. Their modified algorithm incorporates a radiative transfer model to estimate aerosol transmittance and reflectance and accounts for column water vapor. Satellite results were compared with measurements acquired in situ from ground-based radiometers and agreed to within about 2 to 7% for S and PAR fluxes respectively, with a relative precision of around 20% over clear, cloudy, and smoky days.

Kaminsky and Dubayah [this issue] explore the relationship between R_n and surface shortwave fluxes using 1 year of 15-min surface flux data from nine BOREAS surface stations to determine how effectively R_n could be inferred from a knowledge of the shortwave component alone. Their analysis shows that if the term $S(1 - a)$ in (1) was known precisely, then R_n could be estimated with an rms error of from 18 to 36 W m^{-2}. A multifrequency radiometer, the TIROS N vertical sounder (TOVS), was used to obtain atmospheric temperature and water vapor profiles over the FIFE site for input to atmospheric radiative transfer models to estimate L_{wd} [*Breon et al.*, 1990]. The satellite-derived estimates were compared to ground measures of L_{wd}. *Breon et al.* [1990] estimated the error on a pixel level to be about 20 W m^{-2}, under both clear and cloudy conditions.

Li et al. [this issue (a)] apply an algorithm to process AVHRR red and NIR reflectance data to infer the amount of photosynthetically active radiation absorbed by the surface, $APAR_{sfc}$, a key variable in both surface energy balance and photosynthesis calculations. They compare their estimates to flux tower measurements and determine their estimates to have a bias of about 10 W m^{-2}. They map $APAR_{sfc}$ for the 1000 × 1000 km BOREAS region and show that surface variations in cloudiness and surface albedo cause significant spatial variation in $APAR_{sfc}$.

Miller and O'Neill [this issue] used the compact airborne spectrographic imager (CASI) instrument to measure shortwave upwelling and downwelling irradiance at multiple altitudes to examine the effects of airborne smoke from forest fires on downwelling radiation. They report on an episode where smoke from wildfires reduced surface insolation at noon from 800 to 680 W m^{-2} and PAR from 320 to 250 W m^{-2}. They found also that smoke from distant fires, consisting primarily of sulfate aerosols, had much higher single-scattering albedos and lower attenuation coefficients than aerosols from nearby fires from which the soot had not settled out.

Markham et al. [this issue] also verified the important impact of forest fire on atmospheric opacity from analysis of aerosol optical depth measurements acquired by a network of solar radiometers scattered throughout the BOREAS region. They also report on water vapor column abundance estimates. Their results show a dramatic interannual variation in atmospheric opacity due to smoke. In 1994 and 1995 the numerous fires in the BOREAS region reported by *Li et al.* [this issue (b)] and *Steyaert et al.* [this issue] resulted in a much wider variation in aerosol optical depths across the region than in 1996 where few fires were detected. Atmospheric optical depth varied widely over the area from as low as 0.02 (at 500 nm) under clear-sky conditions to as much as 4.5 (at 500 nm) because of smoke. Data from *Markham et al.*'s [this issue] measurements are used widely in atmospheric correction algorithms to correct satellite-measured radiance to surface reflectance. Such corrections are critical for use in physically based classification and biophysical parameter retrieval algorithms of the types developed by *Hall et al.* [this issue].

7. Scientific Summary and Future Research Directions

Planning for BOREAS was initiated in 1990. Starting in 1993, the science team and staff set in place a significant infrastructure in the Canadian wilderness and mounted 10 major intensive field campaigns (IFCs): one in late 1993, five in 1994, and four in 1996. The campaigns were complemented by a monitoring program of data acquisition which spanned the period 1993–1996. Each IFC, and the BOREAS experiment as a whole, was conducted according to detailed experiment plans which translated scientific goals into operational realities. 1994 saw the most intense and wide-ranging activities in the field, including over 350 airborne science flights; 1995 was a year of analysis, assessment, and planning; and 1996 saw the redeployment of many field teams to fill critical gaps in the 1994 data set.

In terms of the personnel and resources involved, BOREAS is roughly 3 times the size of the FIFE experiment [*Sellers et al.*, 1992; *Hall and Sellers*, 1995] and was also conducted over a much larger, sparsely populated area. Operations often involved coordinated activities by over 200 people and up to 10 aircraft at a time over the two study areas. The BOREAS data set is estimated to be roughly 5 times the size of the FIFE data set and is considerably more complex. Likewise, the science in BOREAS spans a wider range of disciplines than in FIFE. However, the management and staff head count for BOREAS is almost the same as it was for FIFE, which was possible due to the experience of many of the veteran staffers and scientists involved, improved procedures, and the use of better technology for communications, data collection, and data compilation. Of these factors, experience was probably the most significant in terms of augmenting efficiency.

BOREAS is a large enterprise and therefore inevitably serves as a test case for what "big science" (i.e., large-scale, interdisciplinary, coordinated) projects can and cannot do. So far, the indications are that as in FIFE and similar projects, the sum will be much greater than the parts in terms of scientific dividends. A data set is being constructed which will link our understanding of small-scale biological processes to zonal climate variations and the global carbon cycle. The multiscale design of the experiment will permit rigorous testing of the scale-integration techniques that will be employed in the process.

Most of the papers in this special issue report on data acquisitions, data analyses, or the results of preliminary modeling studies. On the basis of previous experience (see, for example, *Sellers and Hall* [1992] and *Hall and Sellers* [1995]), another couple of years will see integrated studies carried out using multiple data sets from all the contributing disciplines in BOREAS. These follow-on studies are expected to directly address the goals of BOREAS and are discussed in section 7.5. However, even at this early stage in the analysis phase of the project, some important scientific findings have emerged.

The papers in this special issue and the synopses of chapter 6 are organized by scientific subdiscipline and spatial scale. The scientific review in this final section reverts to the structure outlined in the introduction and in Figure 1, namely, physical climate system, carbon and biogeochemistry, and ecology, with an additional discussion of progress made in remote sensing science.

7.1. Physical Climate System

BOREAS results have already had a direct impact on climate modeling and numerical weather prediction (Figure 17). Observations from the mesoscale meteorological network and tower flux sites have provided new insight into the radiation and energy budgets of the forest and how these affect the regional climate.

When snow free, the BOREAS coniferous sites were observed to have the lowest growing season albedos for any vegetated surface that we know of, about 8%. The winter albedo of the forest was measured to be much lower than the value used by a number of AGCMs. Most NWP models treat snow albedo effects over the forest in the same way as for grass-covered or agricultural surfaces where the vegetation can be completely covered by snow to give a very high surface reflectance. In fact, forest vegetation usually projects above the snow, and even bare deciduous trees can present a very dark surface to the solar flux, which is also incident at a glancing angle for much of the winter (Figure 7a) [*Betts and Ball*, this issue]. Shortwave radiation is therefore efficiently intercepted by the forest and largely converted into sensible heat flux and outgoing longwave radiation during the winter. Omission of this effect in the European NWP model, which carried a winter albedo of around 0.80 as opposed to a value of around 0.25 as observed in the field, resulted in the systematic underestimation of near-surface winter air temperatures by up to 15°C during the BOREAS 1996 winter field campaign (Figure 7b). Since then, the model has incorporated more representative winter albedo values which has resulted in great improvements in the prediction of the near-surface air temperature, reduced lower tropospheric temperature biases, and improved forecast scores over the North Pacific and North Atlantic. As of December 1996, the European NWP model included these changes in its operational forecasts, and there are plans to use

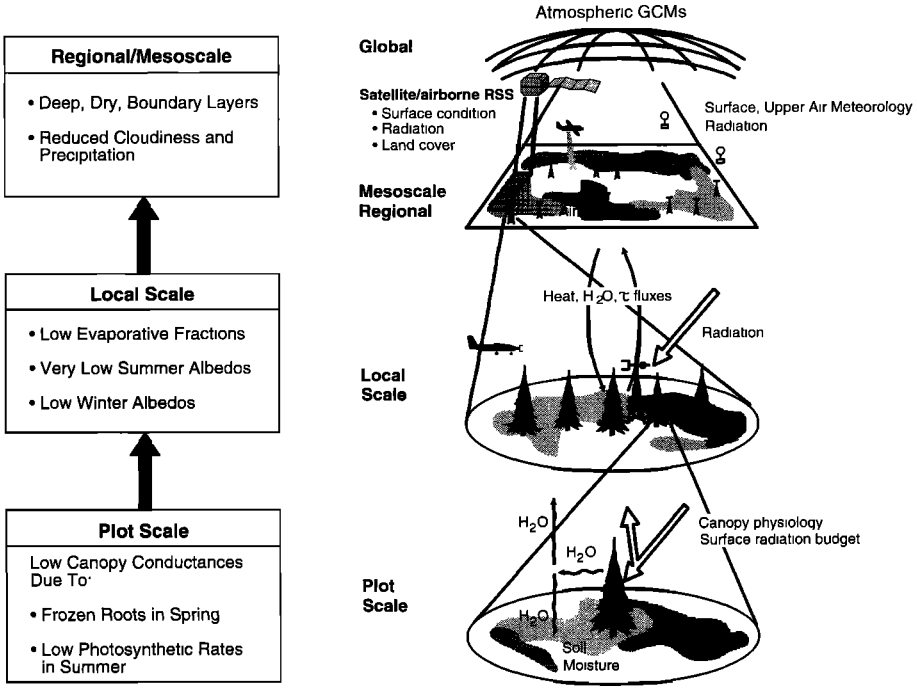

Figure 17. Schematic summarizing gains in the physical climate system science area due to BOREAS; see section 7.1.

satellite data to track snow-related albedo dynamics during the spring and fall.

The low evapotranspiration rates observed at the BOREAS forest sites, particularly the coniferous covers, are not represented correctly in most atmospheric models. In the middle of the growing season, the depressed evapotranspiration rates are due to low stomatal conductances associated with the low photosynthetic rates of these species, which are adapted to nutrient-poor environments. In the spring the very high sensible heat fluxes observed over the forest seem to be due to late thawing of the soil, so the root systems remain frozen and canopy transpiration is cut off. In wetland areas the forest canopy intercepts and processes almost all of the available energy, so the wet soil or moss-covered surface plays only a minor role in the surface energy balance. Interception and partitioning of most of the radiation flux by the forest canopy thus delays the warming and thawing of the underlying soil, so the bulk of net radiation is shunted into sensible heat flux. Airborne flux measurements in BOREAS have also shown how the thermal inertia of the lakes greatly reduces their contribution to the surface heat fluxes. All these effects combine to make the boreal forest, which includes large proportions of lakes, wetlands, and fens, a surprisingly strong source of sensible heat and a weak source of latent heat, compared with temperate grassland sites [*Sellers and Hall*, 1992] and tropical forests [*Shuttleworth et al.*, 1984a, b]. This situation often results in the generation of a very dry warm lower troposphere with a deep and turbulent atmospheric boundary layer over the forest during the growing season, more typical of a lower-latitude arid zone than would be expected for a high-latitude biome supplied with plentiful water. These phenomena were directly apparent to flux aircraft crews in BOREAS 1994 who, in making the transit from the agricultural region near Prince Albert northward into the forest, often encountered greatly increased turbulence, deeper boundary layers (sometimes up to 3000 m), and reduced cloudiness. In the European NWP model, the systematic overestimation of the latent heat flux over the boreal forest resulted in overprediction of precipitation and cloudiness within the region during the BOREAS 1994 growing season [*Sellers et al.*, 1995b]. Again, BOREAS results have had an immediate impact on NWP modeling, and it is expected that the BOREAS data will be extensively used to improve land surface parameterizations in climate models in the near future [*Sellers et al.*, 1997].

The flux aircraft provided a mesoscale picture of the surface-atmosphere fluxes which complements that provided by the tower flux measurements. In general, aircraft-to-aircraft and aircraft-to-tower comparisons were very encouraging and reinforce the perception that the region gives off much less latent heat than previously thought. As in other field experiments, the flux aircraft seem to systematically underestimate the surface fluxes, most likely because of problems with capturing very long wavelength turbulent structures; see *Desjardins et al.* [this issue] and papers cited by *Sellers and Hall* [1992]. Aircraft-measured CO_2 and water vapor fluxes were found to be closely related to spectral vegetation indices [*Ogunjemiyo et al.*, this issue], which concurs with previous findings for grasslands [*Cihlar et al.*, 1992] and with theory [*Sellers et al.*, 1992b]. This latest result for boreal forest holds considerable promise for future modeling work. Lakes were seen to act as important players in the regional energy balance, and more attention needs to be paid to their role in the regional climate. It seems that the lakes act as large stores for heat and give off little sensible heat flux during the growing season. They may also be associated with generating mesoscale circulations during periods of weak synoptic flow.

A number of BOREAS investigations deal with the problems of modeling snow interception and snowmelt in the forest; the results of these will doubtless improve the realism of winter-spring transitions as modeled in AGCMs. Also, satel-

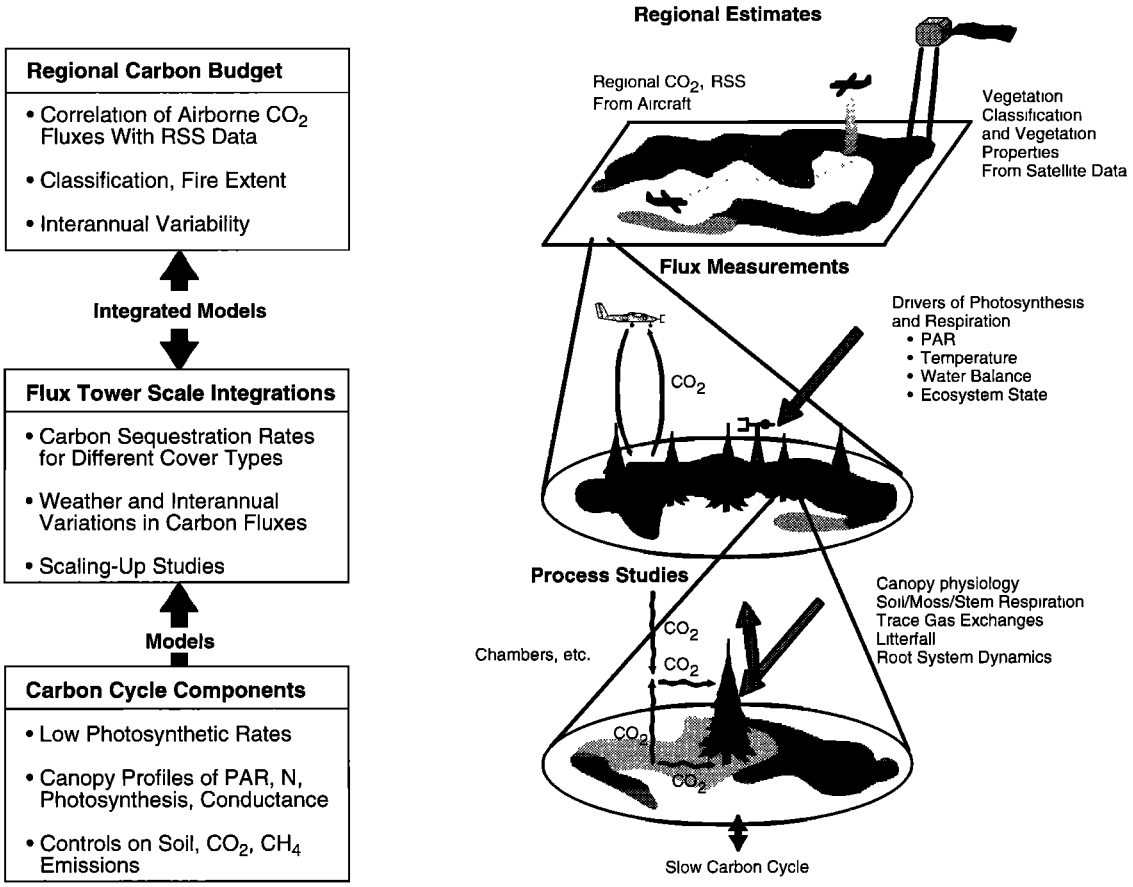

Figure 18. Schematic summarizing gains in the carbon cycle science area due to BOREAS; see section 7.2.

lite-borne radar has been shown to provide useful information about these transitions which are important for both climate and carbon models. Correct representation of soil moisture and surface hydrological processes in AGCMs and regional hydrological models is obviously crucial, and it has been observed that small variations in the hydrology of this biome can have significant effects on the carbon and trace gas budgets. The BOREAS hydrological studies were well integrated with tower flux measurements and have been used as an independent check on the growing season latent heat fluxes as well as furthering our understanding of soil moisture controls on evapotranspiration.

The radiation budget of the forest can be estimated with good accuracy from satellite observations processed by algorithms which were refined using BOREAS data. However, the in situ measurement of net radiation fluxes over the forest was shown to be more difficult than first thought; the radiometer intercomparison effort of *Hodges and Smith* [this issue] showed that a commonly used instrument systematically underestimates the net radiation flux as its transparent dome cover deteriorates over time (see also *Smith et al.* [1992]). Surface measurements have shown that smoke and associated aerosols are important factors in reducing the incident solar flux during the growing season. The large-scale vegetation classification products generated from satellite data will also be essential to correctly define the contributions of different surface types to the regional fluxes of heat, water, momentum, as well as carbon, discussed below. The BOREAS albedo data have already been used to partially validate global data sets generated for global models [*Meeson et al.*, 1995; *Sellers et al.*, 1996b].

7.2. Carbon and Biogeochemistry

The BOREAS field program has provided us with a comprehensive data set covering almost all components of the plant and soil physiological controls related to the energy, water, and carbon cycles in the region (Figure 18). BOREAS results have already shed considerable light on some aspects of the missing global carbon problem. Could the boreal ecosystem with its low productivities be sequestering a significant portion of the 1–3 Gt C yr^{-1} which is unaccounted for in the annual global carbon budget?

The deciduous and coniferous forests of the boreal ecosystem occupy 12–20 million km^2, depending on the data sources used [see *Whittaker*, 1975; *DeFries and Townshend*, 1994; *Sellers et al.*, 1996b]. Depending on which estimate of the boreal forest area we use, the global boreal forest need only sequester between 50 and 80 g C m^{-2} yr^{-1} to explain a 1 Gt C yr^{-1} global sink, and this does not include carbon uptake by high northern latitude tundra, which has been implicated as a carbon sink by *Myneni et al.* [1997].

What do the BOREAS plot-level carbon flux measurements of canopy and soils indicate with respect to these flux magnitudes? Measured annual NEE values at the BOREAS tower sites range from 130 g C m^{-2} yr^{-1} (a moderate sink) in the southern old aspen (SSA-OA) site [*Black et al.*, 1996] to a weak carbon source of 50 g C m^{-2} yr^{-1} at the northern old black

spruce (NSA-OBS) site for 1996 [*Goulden et al.*, this issue]. A number of chamber measurements [*Trumbore and Harden*, this issue] show that the boreal wetland peats have accumulated up to 50 g C m^{-2} yr^{-1} over the last century. Model simulations for conifer wetlands for the years 1968 to 1989 yield a calculated variation in carbon flux from a loss (source) of 50 g C m^{-2} yr^{-1} to a gain (sink) of -140 g C m^{-2} yr^{-1} [*Frolking et al.*, 1996]. His 1994 model value of -51 g C m^{-2} yr^{-1} for the NSA-OBS site agrees well with the measured value of *Goulden et al.* [this issue].

Thus although the boreal forest is characterized by low aboveground productivity of between 50 and 100 g C m^{-2} yr^{-1} [e.g., *Gower et al.*, this issue], equal or greater annual rates of fine root production combined with long carbon turnover rates of 500 years [*Trumbore and Harden*, this issue] in the cold anaerobic soils of the boreal forest wetlands appear to be sufficient to explain a significant sink of global carbon when extrapolated over the large area occupied by the circumpolar boreal ecosystem.

It should be emphasized that at this early stage in the analysis, inferences of boreal carbon flux at the global scale from the BOREAS sites can only serve to show that we cannot rule out the boreal ecosystem as an important global carbon sink. Clearly, the dynamics and strength of carbon sequestration differ by land cover type, climate, soils, topography, and many other factors that are more aptly captured using satellite extrapolations combined with ecosystem process models. For example, small chamber measurements highlighted the large spatial variability in soil and moss carbon effluxes which appear to be highly dependent on soil moisture content and litter quality. Beaver ponds were observed to be very strong sources of CO_2. The observed lags between carbon uptake by photosynthesis, which is confined to the short growing season, and carbon loss by respiration, which continues throughout most of the year, emphasize the need to correctly model the different controls on carbon sinks and sources in large scale models. *Cihlar et al.* [this issue] used satellite data analyses to show that fires burned over 3% of the BOREAS region during 1994. *Steyaert et al.* [this issue] show that nearly one third of the BOREAS study area has been burned within the last 25 years. Carbon contributions from fire disturbance must be factored into global estimates. A more reliable estimate of the magnitude of the global sink will be made after scaling studies in the BOREAS follow-on program has been completed.

By partially elucidating the mechanisms underlying atmosphere-biosphere carbon exchange, BOREAS tower flux and chamber measurements are also leading to a better understanding of the magnitude, trends, and interannual variation in global carbon flux. For example, measurements and modeling have shown that interannual variation in the timing of snowmelt is a major factor in determining annual carbon uptake rate. BOREAS measurements have shown that carbon uptake does not begin until the snow melts and the root zone thaws. Other measurements show that carbon respiration loss is not appreciable below about 17°C; thus immediately after snowmelt and soil thaw, cool air temperatures are conducive to rapid carbon uptake. However, as the soil warms up and air temperatures rise above 17°C, soil respiration is enhanced and the net ecosystem carbon loss increases rapidly. These observations are supported by BOREAS modeling studies which indicate that years with early springs and cool, wet summers are associated with stronger annual carbon uptake rates [*Frolking et al.*, 1996].

The trace gas studies in BOREAS showed that drier sites (aspen, jack pine) with fast nitrogen cycling in the soils could act as strong sinks for CH_4, while many of the wetter sites were strong sources, particularly the beaver ponds and fens. Some intermediate sites switched from source to sink status based on variations in the water table. Surprisingly, chamber measurements made at fen sites were found to scale up well to match eddy correlation measurements of CH_4. CO fluxes from a range of fire sites were measured, but more work needs to be done before an estimate of regional CO fluxes can be made.

The meteorological trends for 1961–1990 analyzed by *Chapman and Walsh* [1993] show that air temperature increases are most rapid over high-latitude continental interiors, with documented temperature trends as high as 1.25°C per decade. These observed trends are also consistent with AGCM simulations showing high-latitude seasonal air temperature increases with increasing atmospheric CO_2 concentrations and inferences about the extension of the boreal growing season by about six days over the last 15 years (see also *Keeling et al.* [1996] and *Myneni et al.* [1997]). If the increased winter and spring temperatures are coupled with relatively cool summers, as it would appear, global warming could initially lead to increased productivity, hence increased carbon sequestration at these latitudes. However, BOREAS soil carbon flux data show that longer warmer growing seasons could also lead to more rapid loss of older deeper soil carbon stores which would partially offset gains from productivity increase.

The biometric studies showed that the aboveground net primary productivity (ANPP) of the boreal forest is relatively small and the aboveground carbon stocks are low compared with temperate and tropical ecosystems. However, large amounts of carbon are stored in wetlands, and these stores are sensitive to climate change. With regard to the annual carbon balance, we are presented with a picture of an ecosystem operating very close to the margins of carbon profit and loss, with growing season length and summertime temperatures perhaps being the deciding factors. Sequestration of carbon by any ecosystem is a nonequilibrium process. In the longer term, changes in fire frequency, climate regime and vegetation succession patterns, and warming and drying of boreal soils with associated increases in respiration could greatly alter or even reverse the "boreal carbon sink" scenario described above. Follow-on analyses of ecological data collected during BOREAS will provide valuable insight into the mechanisms driving future changes.

7.3. Ecology

The future course of carbon dynamics in the boreal zone is thought to depend on variations in the physical climate in the near term and on ecological responses in the midterm and long term. Will warming drive the boreal ecosystem to a higher productivity state, populated by plant communities that can sequester higher levels of carbon than the present boreal communities, or will a new low-productivity equilibrium be achieved limited by the paucity of the boreal soils? Paleoclimate studies reveal that this ecosystem migrated to much more southerly latitudes during the last glaciation, then retreated to its present northerly position as the ice receded. Will the anticipated rapid warming induce ecological instabilities, resulting in rapid carbon loss from the great reserves of carbon in the largely anaerobic conifer wetlands before other plant forms can either fix the carbon in their living biomass or act as agents in stabilizing the soil? To understand these longer-term dy-

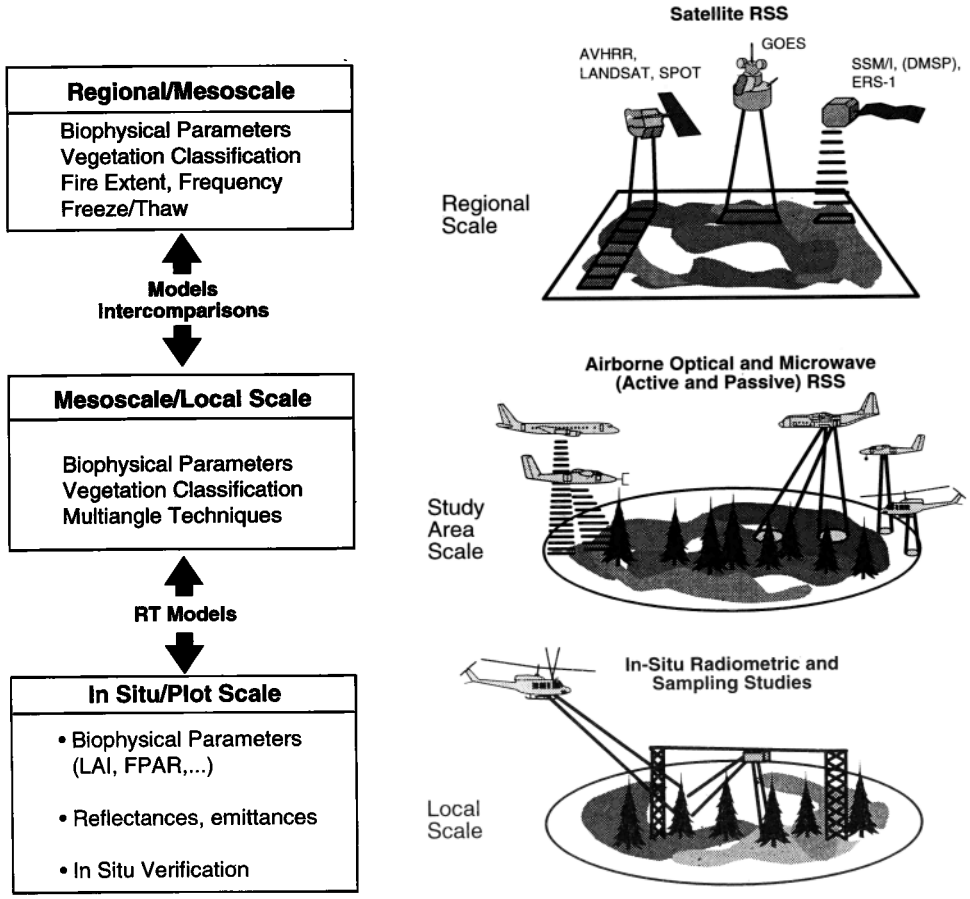

Figure 19. Schematic summarizing gains in ecology and remote sensing science due to BOREAS; see sections 7.3 and 7.4.

namics, a number of questions must be addressed. Where is the carbon being sequestered: in the canopy, litter or below ground by fine root turnover? What is the relative importance of the various boreal land cover types in this process? How will the source/sink strength depend on climate, particularly growing season length, and will respiration begin to dominate over photosynthesis in response to global warming, rendering the ecosystem a net source rather than a net sink of carbon? Would increasing fire frequency lead to increased or decreased carbon sink strengths overall? Data collected during BOREAS will be used to address these questions.

The ecophysiological studies in BOREAS clarified many of the links between vegetation type and state and the carbon, energy and water budgets of the region, while biometric and remote sensing studies have laid the groundwork for carrying out regional surveys of ecosystem state using remote sensing data (Figure 19). The ecophysiological work has been covered already, so this discussion is limited to a review of progress made in understanding ecological processes on relatively long timescales and over large spatial scales.

The leaf-scale and canopy-scale measurements conducted in BOREAS present us with a consistent picture of an ecosystem operating at a relatively low level: the deciduous canopies were observed to have much lower photosynthetic capacities than their temperate counterparts, and the coniferous species were observed to have even lower capacities, about half those of the deciduous species. Clearly, large-scale replacement of the conifers by deciduous species, which is likely to occur in a warming and drying climate, could have an enormous effect on the carbon and water budgets of the region. This speculation is supported by the tower flux and flux aircraft measurements carried out at larger spatial scales, both of which reconfirmed the tight links between evapotranspiration and photosynthesis during the growing season. The flux aircraft observations showed that mesoscale patterns of photosynthetic carbon uptake were closely related to spectral vegetation index information, which can also be used to estimate large-scale canopy conductances. The highest transpiration and carbon uptake rates were observed over the deciduous stands near the southern edge of the biome, which were also characterized by the highest spectral vegetation index values. The tower flux measurements showed a wide variation in carbon fluxes among the different cover types studied in BOREAS, but most of them seemed to be weak sinks on an annual basis. Given that up to 3% of the boreal forest is consumed by natural fire each year, it is entirely reasonable for an equilibrium boreal carbon budget to consist of weak sinks covering most of the region countered by catastrophic fire events within relatively small areas, their recovering to a stronger sink as new growth develops. It should also be borne in mind that in a warming and drying climate, fire frequency would change along with physiological and species changes.

7.4. Remote Sensing Science

Remote sensing research and development during BOREAS produced results that are key to investigating the

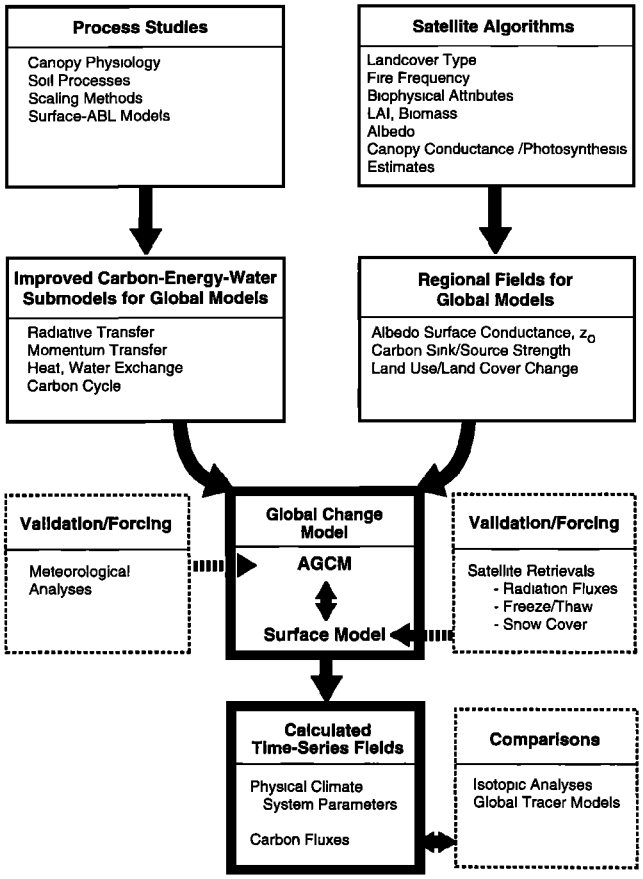

Figure 20. Schematic showing how different elements of BOREAS science could combine to improve the performance and realism of global change models; see section 7.5. The results of the BOREAS process studies have led to better land surface parameterizations for AGCMs and also improved carbon cycle submodels; see two boxes in top left of the figure. The remote sensing science and ecological research will lead to better classification schemes and more accurate specification of biophysical parameters over the entire boreal zone; see two boxes in top right of figure. The combination of improved models, global parameter fields, and large-scale validation data sets will result in greatly enhanced simulations of physical climate system fields (temperature, precipitation, etc.) and carbon cycle flows for the biome. These spatially resolved fields can be area integrated and compared to zonal-scale inferences about the boreal carbon cycle provided by atmospheric isotopic analyses and CO_2 tracer models; see bottom half of figure. In this way we hope to bridge the gap that currently exists between our understanding of small-scale physiological processes and global-scale inferences about the carbon cycle.

role of the boreal ecosystem in global change (Figure 19). Considerable progress was made casting remote sensing algorithms into a more physically based framework [e.g., *Hall et al.*, this issue], progress that should ultimately result in more robust global classification and biophysical parameter mapping techniques. The improved radiative transfer models developed during BOREAS should also provide more reliable components in numerical snowmelt models, a key to forecasting the effects of climate warming on the timing of snowmelt, which we saw was crucial to determining interannual variation and longer-term trends in carbon sequestration. In addition, *Way et al.* [this issue] demonstrated that radar can be used to monitor soil and bole thaw, also critical in initiating photosynthesis in the models. Remote sensing also showed that the role of fire in the boreal ecosystem is even more important than was known previously. *Steyaert et al.* [this issue] used AVHRR visible and near-infrared data to show that about one third of the study region has undergone fire over the last 25 years, a much larger proportion than previously believed; *Cihlar et al.* [this issue], using AVHRR data showed that 3% of the ecosystem burned during 1994 alone. Importantly, both of these efforts showed that AVHRR data can be used to reliably map the major land cover types, making it possible for a careful assessment of the global boreal biome. *Myneni et al.* [1997] showed how the 15-year AVHRR record can be used to monitor the response of the biome to climate warming. Finally, remote sensing was used during BOREAS to develop seasonally varying, regional-scale parameter maps for all the major driving variables governing carbon/water and energy processes (Figure 16). These maps should prove to be invaluable in scaling models and hypotheses from the plot level to the region.

7.5. Future Research Directions

Over the next few years, BOREAS data sets will be used to improve many of the critical process submodels needed for land-atmosphere models and carbon balance calculations. In particular, the BOREAS follow-on program will encompass efforts to improve radiative transfer models, leaf- and canopy-scale photosynthesis-conductance models, canopy, root and soil respiration models, soil moisture and surface hydrological schemes, and surface-atmosphere turbulent transfer models. The integrated nature of the BOREAS data sets will permit rigorous testing of the performance of these process models, together and in isolation from each other, over the diurnal and seasonal cycles (Figure 20).

With respect to weather and climate models, a critical short-term task is to apply the BOREAS data set to further improve numerical weather forecasting by improving land surface-atmosphere transfer codes. Tests of coupled photosynthesis-conductance models against BOREAS data have indicated that these schemes are robust and will lead to improved surface evapotranspiration estimates for the AGCMs. Incorporation of better albedo values has already improved the performance of a leading operational forecast model; further performance improvements are expected when satellite-based estimates of albedo are incorporated, permitting these models to respond seasonally to the effects of snow and vegetation phenology. BOREAS provided new data on the effects of smoke and associated atmospheric aerosols on the surface radiation balance. These effects were more widespread and severe over the biome than was previously thought (see also *Sellers et al.* [1995b]). GCM radiation codes may need to include this effect. A final area of improvement in weather and climate forecasting should result from incorporating improved parameterizations of boundary layer dynamics utilizing BOREAS radiosonde and aircraft measurements.

In carbon models the long-term trends and interannual variability in carbon dynamics for the biome appear to be driven primarily by the timing of snowmelt and the summer air temperatures. Incorporation of improved snowmelt models into regional and global carbon balance models should help us to understand these dynamics and thus better simulate the annual atmospheric CO_2 signal. In terms of growing season carbon fluxes the photosynthesis models seem to be realistic, but it is essential to improve the respiration models not only for the

aboveground components but also for the roots, litter, and soils. Finally, the effects of fire and disturbance are important to understand. Scaling studies involving point models and remote sensing will be key to gaging the effects of disturbance at the regional scale.

BOREAS has catalyzed several advances in remote sensing algorithm development which now enable us to monitor boreal vegetation by type and state and to track changes that may be due to fire, direct human activity, or climate change. Algorithm developments due to FIFE and BOREAS have already led to the production of AVHRR-derived global vegetation maps for the years 1987 and 1988 [see *Meeson et al.*, 1995; *Sellers et al.*, 1996a, b, 1997; *Randall et al.*, 1996]. These pilot products will be expanded to cover the 15-year AVHRR record and will allow us to develop time series fields of land cover, biophysical parameters, phenology, and snow cover. All these can be compared with the physical climate record and to seasonal and interannual variations in atmospheric CO_2 concentration. AVHRR data will also be used to monitor changes in the fire disturbance regime over the same period. The radiometric quality of the AVHRR data series will have to be enhanced to meet these tasks; this requires the development of techniques for improving long-term calibration and atmospheric correction of the data. The MODIS/MISR and other sensors to be launched aboard the EOS-AM platform in mid-1998 should provide significant additional capability for monitoring land vegetation and should be merged with the AVHRR data stream to produce a seamless monitoring data set into the 21st century. Finally, the use of radar satellites such as ERS-1 and JERS-1 will be used to monitor the interannual variability in the freeze-thaw boundary in the boreal ecosystem, shown to be a key factor in the interannual variability of the carbon flux. To take advantage of the different attributes of optical and radar sensors, further remote sensing research and development is required; in particular, data fusion algorithms, which combine optical and microwave sensors as well as other data such as topographic data, could be developed to provide richer information about the biome.

Enhancement of land-atmosphere process models and large-scale parameter quantification using satellite data would be considerable achievements for BOREAS. Success in these two areas is almost certain, based on the early results and work in progress. However, the real prize for BOREAS would be to incorporate the improved process models and remote sensing data sets within large-scale energy-water-carbon models to calculate surface-atmosphere fluxes of these quantities for the biome over the period of record of the earth-observing satellites, say from 1980 to the present day (see the bottom half of Figure 20). For this calculation the surface state should be constrained by satellite data, while the atmospheric conditions are specified from meteorological analyses or via direct coupling with an AGCM. Incorporating the role of fire in a carbon cycle model represents a real challenge, particularly when it comes to predicting changes in fire frequency, areal extent, and intensity as a result of climate change; the satellite and meteorological data records of the last 25 years are essential resources for addressing this problem. Initially, it is very unlikely that these integrative models will correctly simulate the value or even the sign of the net carbon flux for the biome, but they should be capable of reproducing interannual variations in the flux, superimposed on a relatively invariant bias. The time series of calculated interannual variations in the net carbon flux can then be compared with equivalent numbers inferred from global tracer and isotopic analyses to shed light on which processes are responsible for perturbations in the terrestrial carbon budget and where, geographically and biologically, they operate. In this way we hope that BOREAS will help us to bridge the huge gap that currently exists between global-scale inferences about the changing terrestrial carbon budget and our local-scale understanding of the controlling ecophysiological processes. When this is done, we can see our way toward constructing useful predictive models that can anticipate future interactions between the global physical climate system and the carbon cycle.

Notation

ABL	atmospheric boundary layer.
AES	Atmospheric Environment Services.
AFM	airborne fluxes and meteorology.
AGCM	atmospheric general circulation model.
ANPP	above-ground net primary productivity.
APAR	absorbed photosynthetic active radiation.
A_R	entrainment parameter.
ASAS	advanced solid-state array spectroradiometer.
AVHRR	advanced very high resolution radiometer.
BAHC	biospheric aspects of the hydrological cycle.
BMD	biomass density.
BOREAS	Boreal Ecosystem-Atmosphere Study.
BORIS	BOREAS Information System.
BP	beaver pond.
BRDF	bidirectional reflectance distribution function.
CCRS	Canada Centre for Remote Sensing.
DAAC	Data Analysis and Archiving Center.
ECMWF	European Center for Medium-Range Weather Forecasting.
EOS AM-1	Earth Observation System-AM-1 platform.
ET	evapotranspiration.
FIFE	First ISLSCP Field Experiment.
FM	frequency modulation.
FPAR	fraction of PAR absorbed by the canopy.
GCM	general circulation models.
GCTE	global change and terrestrial ecosystems.
GEE	gross ecosystem exchange.
GOES	Geostationary Operational Environmental Satellite.
GPS	Global Positioning System.
HAPEX-Sahel	Hydrological Atmospheric Pilot Experiment-Sahel.
HYD	hydrology.
IFC	intensive field campaign.
IGAC	International Global Atmospheric Chemistry.
IGBP	International Geosphere Biosphere Program.
ISLSCP	International Satellite Land Surface Climatology Project.
LAI	leaf area index.
LSP	land surface parameterizations.
MISR	multiangle imaging spectroradiometer.

MODIS	moderate resolution imaging spectrometer.
MVI	multiband vegetation imager.
NASA	National Aeronautics and Space Administration.
NCAR	National Center for Atmospheric Research.
NDVI	normalized difference vegetation index.
NEE	net ecosystem exchange.
NIR	near infrared.
NMHC	nonmethane hydrocarbon.
NOAA	National Oceanographic and Atmospheric Administration.
NSERC	Natural Sciences and Engineering Research Council.
NSA	northern study area.
NWP	numerical weather prediction.
OA	old aspen.
OBS	old black spruce.
OJP	old jack pine.
PAR	photosynthetically active radiation.
PARABOLA	portable aparatus for rapid acquisition of bidirectional observations of land and atmosphere.
POLDER	Polarization and Directionality of Earth Reflectances.
R_n	surface net radiation.
RSS	remote sensing science.
RT	radiative transfer.
SART	surface-atmosphere radiative transfer.
SIR-C	shuttle imaging radir.
SSA	southern study area.
SWE	snow water equivalent.
TDR	time domain reflectrometry.
TE	terrestrial ecology.
TF	tower flux.
TGB	trace gas biogeochemistry.
TIROS-N	multi-frequency radiometer.
TM	thematic mapper.
TOVS	multi-frequency vertical sounder.
VHF	very high frequency.
WCRP-GEWEX	World Climate Research Program-Global Energy and Water Cycle Experiment.
YA	young aspen.
YJP	young jack pine.

Acknowledgments. All the BOREAS scientists and staff contributed to this paper in one way or another. Scientists who contributed preliminary data sets are identified in the text and figure captions. The BOREAS operations group responsible for the design and oversight of the field experiment consisted of Piers Sellers, Forrest Hall, Dennis Baldocchi, Joseph Berry, Andrew Black, Josef Cihlar, Barry Goodison, Hank Margolis, Michael Apps, Bob Kelly, Gerry den Hartog, Tom Gower, Mike Ryan, Patrick Crill, Dennis Lettenmaier, and Jon Ranson. The BOREAS principal investigators are listed in Table 1; many of them provided data and written contributions for this paper. Almost all investigators took on project-related duties in addition to their own research tasks during the field year. The BOREAS and BORIS staff members are Valerie Corey, Shelaine Curd, Laura East, Carla Evans, Scott Goetz, Sara Golightley, Saera Haque, Dan Hodkinson, Fred Huemmrich, Fred Irani, David Knapp, David Landis, Elissa Levine, Beth McCowan, Blanche Meeson, John Metcalfe, Karen Mitchell, Amy Morrell, Theresa Mulhern, Alan Nelson, Ross Nelson, Jeffrey Newcomer, Jaime Nickeson, Paula Pacholek, Carey Noll, Don Rinker, Adam Rosenbaum, Al Schmidt, Richard Strub, Tracey Twine, Anthony Young, Barrie Atkinson, Mary Dalman, Tom Gower, David Halliwell, John Martin, Joe Niederleitner, John Norman, Paul Rich, Sandra Schussel, D'Arcy Snell, Sarah Steele, John Stewart, Karl Spence, David Terroux, Gillian Traynor, and Jason Vogel. Dave Dalman and Michael Fitzsimmons of Prince Albert National Park also provided much needed help to BOREAS. All are warmly thanked. Darrel Williams, branch head of 923, NASA/GSFC, is also thanked for maintaining his tolerance, good humor, and good sense throughout the entire project. The research aircraft crews and management performed their tasks with unflagging professionalism and patience. Special thanks go to George Alger, Chris Jenison, and Richard Rose (C-130); Gary Shelton (ER-2); Willie Dykes, Charlie Walthall, Charles Smith, Jeff Sigrist, Ed Melson, Pete Bradfield, and John Schaefer (helicopter); Larry Hill, Lawrence Gray, Ted Senese (chieftain); Chris Scofield and Michele Vogt (DC-8); Charles Livingstone and Brian Spicer (CV-580); Tom Carrol and Rob Posten (aerocommander); Paul Spyers-Duran, Henry Boynton, and Jerry Tejcek (Electra); John Aitken, Brian Bertrand, Murray Morgan, John Croll, and Charles Taylor (Twin Otter); George Bershinsky and Ernest Gasaway (Kingair); and Ed Dumas and Robert McMillen (for LongEZ). While these (generally unsung) heroes are specifically mentioned, we are fully aware that a tremendous job was done by many other people under frequently trying conditions. In addition, the crews of the Saskatoon, Prince Albert, and Thompson Flight Service Stations and the staff of ECMWF and NMC who provided BOREAS with invaluable weather prediction products during the field campaigns are warmly thanked. BOREAS benefited immensely from a series of independent external reviews conducted by the Science Advisory Group (SAG): Mike Unsworth (chairman), Pat Matson, Tzvi Gal-Chen, Joe Landsberg, Jim Ritchie. BOREAS is deeply indebted to these people. BOREAS contributes to both the U.S. and the Canadian Global Change Research Programs. For the United States the effort is being led by the National Aeronautics and Space Administration Mission to Planet Earth, with participation from the National Oceanic and Atmospheric Administration, the National Science Foundation, the U.S. Geological Survey, the U.S. Forest Service, and the Environmental Protection Agency. Participating Canadian agencies include the Canada Centre for Remote Sensing, Environment Canada, Natural Sciences and Engineering Research Council, Agriculture and Agri-Food Canada, National Research Council, Heritage Canada (Parks), Canadian Forest Service, the Institute for Space and Terrestrial Science, and the Royal Society of Canada. The BOREAS project was overseen by program managers from the participating agencies who made up the BOREAS Coordinating Committee (BCC). The membership of the BCC is Micheal Allen, Richard Asselin, Carmen Charette, Michael Coughlan, Bruce Hicks, Hank Margolis, Gordon Miller, Jarvis Moyers, Leo Sayn-Wittgenstein, Mac Sinclair, Lowell Smith, Robert Stewart, John Stone, Jeffrey Watson, and Diane Wickland. BOREAS is an element of the International Satellite Land Surface Climatology Project (ISLSCP) which is part of the World Climate Research Program-Global Energy and Water Cycle Experiment (WCRP-GEWEX). BOREAS is also contributing to three International Geosphere Biosphere Program (IGBP) core projects; Biospheric Aspects of the Hydrological Cycle (BAHC), Global Change and Terrestrial Ecosystem (GCTE), and International Global Atmospheric Chemistry (IGAC).

References

Amaral, J. A., and R. Knowles, Localization of methane consumption and nitrification activities in some boreal forest soils and the stability of methane consumption on storage and disturbance, *J. Geophys. Res.*, this issue.

Baldocchi, D. D., and C. Vogel, A comparative study of water vapour, energy and CO_2 flux densities above and below a temperate broadleaf and a boreal pine forest, *Tree Physiol.*, *16*, 5–16, 1996.

Baldocchi, D. D., and P. C. Harley, Scaling carbon dioxide and water vapour exchange from leaf to canopy in a deciduous forest: Model testing and application, *Plant Cell Environ.*, *18*, 1157–1173, 1995.

Baldocchi, D. D., C. A. Vogel, and B. Hall, Seasonal variation of energy and water vapor exchange rates above and below a boreal jack pine forest canopy, *J. Geophys. Res.*, this issue.

Barr, A. G., and A. K. Betts, Radiosonde boundary layer budgets above a boreal forest, *J. Geophys. Res.*, this issue.

Barr, A. G., A. K. Betts, R. L. Desjardins, and J. I. MacPherson, Comparison of regional surface fluxes from boundary layer budgets and aircraft measurements above a boreal forest, *J. Geophys. Res.*, this issue.

Betts, A. K., and J. H. Ball, Albedo over the boreal forest, *J. Geophys. Res.*, this issue.

Betts, A. K., J. H. Ball, and A. C. M. Beljaars, Comparison between the land surface response of the European Centre model and the FIFE-1987 data, *Q. J. R. Meteorol. Soc.*, *119*, 975–1001, 1993.

Betts, A. K., S.-Y. Hong, and H.-L. Pan, Comparison of NCEP/NCAR reanalysis with 1987 FIFE data, *Mon. Weather Rev.*, *124*, 1480–1498, 1996.

Betts, A. K., F. Chen, K. Mitchell, and Z. Janjic, Assessment of land-surface and boundary layer models in 2 operational versions of the Eta Model using FIFE data, *Mon. Weather Rev.*, *125*, 2896–2916, 1997.

Betts, A. K., J. H. Ball, B. J. Smith, and S. R. Shewchuk, Comparison of BOREAS and Atmospheric Environment Service humidity sensors at Meadow Lake, Saskatchewan, *J Geophys. Res.*, this issue.

Betts, A. K., P. Viterbo, and A. C. M. Beljaars, Comparison of the land-surface interaction in the ECMWF reanalysis model with the 1987 FIFE data, *Mon. Weather Rev.*, *126*, 186–198, 1998.

Bicheron, P., M. Leroy, O. Hautecoeur, and F. M. Bréon, Enhanced discrimination of boreal forest covers with directional reflectances from the airborne POLDER instrument, *J. Geophys. Res.*, this issue.

Black, T. A., et al., Annual cycles of water vapor and carbon dioxide fluxes in and above a boreal aspen stand, *Global Change Biol.*, *2*, 219–229, 1996.

Blanken, P. D., T. A. Black, P. C. Yang, H. H. Neumann, Z. Nesic, R. Staebler, G. den Hartog, M. D. Novak, and X. Lee, Energy balance and canopy conductance of a boreal aspen forest: Partitioning overstory and understory components, *J. Geophys. Res.*, this issue.

Bonan, G. B., and K. J. Davis, Comparison of the NCAR LSM1 land surface model with BOREAS aspen and jack pine tower fluxes, *J. Geophys. Res.*, this issue.

Bourbonniere, R. A., W. L. Miller, and R. G. Zepp, Distribution, flux and photochemical production of carbon monoxide in a boreal beaver impoundment, *J. Geophys. Res.*, this issue.

Bréon, F., R. Frouin, and C. Gautier, Satellite estimates of downwelling longwave irradiance at the surface during FIFE, in *Proceedings at the AMS Symposium on the First ISLSCP Field Experiment (FIFE)*, Am. Meteorol. Soc, Boston, Mass., 1990.

Bubier, J. L., T. R. Moore, L. Bellisario, N. T. Comer, and P. M. Crill, Ecological controls on methane emissions from a northern peatland complex in the zone of discontinuous permafrost, Manitoba, Canada, *Global Biogeochem. Cycles*, *9*, 455–470, 1995.

Bubier, J. L., B. N. Rock, and P M. Crill, Spectral reflectance measurements of boreal wetland and forest mosses, *J. Geophys. Res.*, this issue.

Burke, R. A., R. G. Zepp, M. A. Tarr, W. L. Miller, and B. J. Stocks, Effect of fire on soil-atmosphere exchange of methane and carbon dioxide in Canadian boreal forest sites, *J. Geophys Res.*, this issue.

Chang, A. T. C., J. L. Foster, D. K. Hall, B. E. Goodison, A. E. Walker, J. R. Metcalfe, and A. Harby, Snow parameters derived from microwave measurements during the BOREAS winter field campaign, *J Geophys. Res.*, this issue.

Chapman, W. L., and J E. Walsh, Recent variations of sea ice and air temperature in high latitudes, *Bull. Am. Meteorol. Soc.*, *74*, 33–47, 1993.

Chen, J. M., P. M. Rich, S. T. Gower, J. M. Norman, and S. Plummer, Leaf area index of boreal forests: Theory, techniques, and measurements, *J. Geophys. Res.*, this issue.

Ciais, P., P. P. Tans, J. W. C. White, M. Trolier, R. J. Francey, J. A. Berry, D. R. Randall, P. J. Sellers, J. G. Collatz, and D. S. Schimel, Partitioning of ocean and land uptake of CO_2 as inferred by $\delta^{13}C$ measurements from the NOAA Climate Monitoring and Diagnostics Laboratory Global Air Sampling Network, *J. Geophys. Res.*, *100*, 5051–5070, 1995.

Cihlar, J., P. H. Caramori, P. H. Schuepp, R. L. Desjardins, and J. I. MacPherson, Relationships between satellite-derived indices and aircraft-based measurements, *J. Geophys. Res.*, *97*, 18,515–18,522, 1992.

Cihlar, J., J. Chen, and Z. Li, Seasonal AVHRR multichannel data sets and products for studies of surface-atmosphere interactions, *J. Geophys. Res.*, this issue.

Coll, C., V. Cassels, J. A. Sobrino, and E. Valor, On the atmospheric dependence of the split-window equation for land surface temperature, *Int. J. Remote Sens.*, *15*, 105–122, 1994.

Cooper, H. J., E. A. Smith, J. Gu, and S. Shewchuk, Modeling the impact of averaging on aggregation of surface fluxes over BOREAS, *J. Geophys. Res.*, this issue.

Cuenca, R. H., D. E. Stangel, and S. F. Kelly, Soil water balance in a boreal forest, *J. Geophys. Res.*, this issue.

Czajkowski, K. P., T. Mulhern, S. N. Goward, J. Cihlar, R. O. Dubayah, and S. D. Prince, Biospheric environmental monitoring at BOREAS with AVHRR observations, *J. Geophys. Res.*, this issue.

Dang, Q.-L., H. A. Margolis, M. R. Coyea, M. Sy, and G. J. Collatz, Regulation of branch-level gas exchange of boreal trees: Roles of shoot water potential and vapor pressure difference, *Tree Physiol.*, *17*, 521–536, 1997.

Dang, Q.-L., H. A. Margolis, M. Sy, M. R. Coyea, G. J. Collatz, and C. L. Walthall, Profiles of PAR, nitrogen, and photosynthetic capacity in the boreal forest: Implications for scaling from leaf to canopy, *J. Geophys. Res.*, this issue.

Davis, K. J., D. H. Lenschow, S. P. Oncley, C. Kiemle, G. Ehret, A. Giez, and J. Mann, Role of entrainment in surface-atmosphere interactions over the boreal forest, *J. Geophys. Res.*, this issue (a).

Davis, R. E., J. P. Hardy, W. Ni, C. Woodcock, J. C. McKenzie, R. Jordan, and X. Li, Variation of snow cover ablation in the boreal forest: A sensitivity study on the effects of conifer canopy, *J. Geophys. Res.*, this issue (b).

DeFries, R. S., and J. R. G. Townshend, NDVI-derived land cover classifications at a global scale, *Int. J. Remote Sens.*, *15*, 3567–3586, 1994.

Denning, A. S., I. Fung, and D. A. Randall, Strong simulated meridional gradient of atmospheric CO_2 due to seasonal exchange with the terrestrial biota, *Nature*, *376*, 240–243, 1995.

Desjardins, R. L., et al., Scaling-up flux measurements for the boreal forest using aircraft-tower combinations, *J. Geophys. Res.*, this issue.

Dobosy, R. J., T. L. Crawford, J. I. MacPherson, R. L. Desjardins, R. D. Kelly, S. P. Oncley, and D. H. Lenschow, Intercomparison among the four flux aircraft at BOREAS in 1994, *J. Geophys. Res.*, this issue.

Flanagan, L. B., J. R. Brooks, and J. R. Ehrlinger, Photosynthesis and carbon isotope discrimination in boreal forest ecosystems: A comparison of functional characteristics in plants from three mature forest types, *J. Geophys. Res.*, this issue.

Fournier, R. A., P. M. Rich, and R. Landry, Hierarchical characterization of canopy architecture for boreal forest, *J. Geophys. Res.*, this issue.

Frolking, S., Sensitivity of spruce/moss boreal forest net ecosystem productivity to seasonal anomalies in weather, *J. Geophys. Res.*, this issue.

Frolking, S., et al., Modeling temporal variability in the carbon balance of a spruce/moss boreal forest, *Global Change Biol.*, *2*, 343–366, 1996.

Goel, N. S., W. Qin, and B. Wang, On the estimation of leaf size and crown geometry for tree canopies from hotspot observations, *J. Geophys. Res.*, this issue.

Gorham, E., Northern peatlands: Role in the carbon cycle and probable response to global warming, *Ecol. Appl.*, *1*, 182–195, 1991.

Goulden, M. L., and P. M. Crill, Automated measurements of CO_2 exchange at the moss surface of a black spruce forest, *Tree Physiol.*, *17*, 537–542, 1997.

Goulden, M. L., B. C. Daube, S.-M. Fan, D. J. Sutton, A. Bazzaz, J. W. Munger, and S. C. Wofsy, Physiological responses of a black spruce forest to weather, *J. Geophys. Res.*, this issue.

Goutorbe, J. P., et al., A large scale study of land-atmosphere interactions in the semi-arid tropics (HAPEX-Sahel), *Ann. Geophys.*, *12*, 53–64, 1994.

Gower, S. T., J. Vogel, J. Norman, C. Kucharik, S. Steele, and T. Stow, Carbon distribution and aboveground net primary production in aspen, jack pine, and black spruce stands in Saskatchewan and Manitoba, Canada, *J. Geophys. Res.*, this issue.

Gu, J., and E. A. Smith, High-resolution estimates of total solar and PAR surface fluxes over large-scale BOREAS study area from GOES measurements, *J. Geophys. Res.*, this issue.

Hall, B., and C. Claiborn, Measurements of the dry deposition of peroxides to a Canadian boreal forest, *J. Geophys. Res.*, this issue.

Hall, F. G., and P. J. Sellers, First International Satellite Land Surface Climatology Project (ISLSCP) Field Experiment (FIFE) in 1995, *J. Geophys. Res.*, *100*, 25,383–25,395, 1995.

Hall, F. G., K. F. Huemmrich, S. J. Goetz, P. J. Sellers, and J. E. Nickeson, Satellite remote sensing of surface energy balance: Suc-

cess, failures and unresolved issues in FIFE, *J Geophys. Res.*, *97*, 19,061–19,089, 1992.

Hall, F. G., Y. E. Shimabukuro, and K. F. Huemmrich, Remote sensing of forest biophysical structure in boreal stands of Picea mariana using mixture decomposition and geometric reflectance models, *Ecol. Appl.*, *5*, 993–1013, 1995.

Hall, F. G., D. E. Knapp, and K. F. Huemmrich, Physically based classification and satellite mapping of biophysical characteristics in the southern boreal forest, *J. Geophys. Res.*, this issue.

Harden, J. W., E. Sundquist, R. Stallard, and R. Mark, Dynamics of soil carbon during deglaciation of the Laurentide ice sheet, *Science*, *258*, 1921–1924, 1992.

Harden, J. W., K. P. O'Neill, S. E. Trumbore, H. Veldhuis, and B. J. Stocks, Moss and soil contributions to the annual net carbon flux of a maturing boreal forest, *J. Geophys. Res.*, this issue.

Hardy, J. P., R. E. Davis, R. Jordon, X. Li, C. Woodcock, W. Ni, and J. C. McKenzie, Snow ablation modeling at the stand scale in a boreal jack pine forest, *J. Geophys. Res.*, this issue.

Hasselman, K., Are we seeing global warming?, *Science*, *276*, 914–915, 1997.

Hodges, G. B., and E. A. Smith, Intercalibration, objective analysis, intercomparison, and synthesis of BOREAS surface net radiation measurements, *J. Geophys. Res.*, this issue.

Hogg, E. H., and P. A. Hurdle, Sap flow in trembling aspen: Implications for stomatal responses to vapor pressure deficit, *Tree Physiol.*, *17*, 501–510, 1997.

Hogg, E. H., et al., A comparison of sap flow and eddy fluxes of water vapor from a boreal deciduous forest, *J Geophys Res.*, this issue.

Houghton, J. T., et al., (Eds.), *Climate Change, Science of Climate Change, Technical Summary*, pp. 9–97, Cambridge Univ Press, New York, 1995.

Jarvis, P. G., J. M. Massheder, S. E. Hale, J. G. Moncrieff, M. Rayment, and S. L. Scott, Seasonal variation of carbon dioxide, water vapor, and energy exchanges of a boreal black spruce forest, *J. Geophys. Res.*, this issue.

Kaharabata, S. K., P. H. Schuepp, S. Ogunjemiyo, S. Shen, M. Y. Leclerc, R. L. Desjardins, and J. I. MacPherson, Footprint considerations in BOREAS, *J. Geophys. Res.*, this issue.

Kaminsky, K. Z., and R. Dubayah, Estimation of surface net radiation in the boreal forest and northern prairie from shortwave flux measurements, *J. Geophys. Res.*, this issue.

Keeling, C. D., T. P. Whorff, M. Wahlen, and J. van der Plicht, Interannual extremes in the rate of rise of atmospheric carbon dioxide since 1980, *Nature*, *375*, 666–670, 1995.

Keeling, C. D., J. F. S. Chin, and T. P. Whorf, Increased activity of northern vegetation inferred from atmospheric CO_2 measurements, *Nature*, *382*, 146–149, 1996.

Kiemle, C., G. Ehret, A. Giez, K. J. Davis, D. H. Lenschow, and S. P. Oncley, Estimation of boundary layer humidity fluxes and statistics from airborne DIAL, *J. Geophys. Res.*, this issue.

Kimball, J. S., M. A. White, and S. W. Running, BIOME-BGC simulations of stand hydrologic processes for BOREAS, *J. Geophys. Res.*, this issue.

Kucharik, C., J. M Norman, L. M. Murdock, and S. T. Gower, Characterizing canopy nonrandomness with a multiband vegetation imager (MVI), *J. Geophys. Res.*, this issue.

Lafleur, P. M., J. H. McCaughey, and D. E. Jelinski, Seasonal trends in energy, water, and carbon dioxide fluxes at a northern boreal wetland, *J. Geophys. Res.*, this issue.

Lavigne, M. B., and M. G. Ryan, Growth and maintenance respiration rates of aspen, black spruce and jack pine stems at northern and southern BOREAS sites, *Tree Physiol.*, *17*, 543–552, 1997.

Lavigne, M. B., et al., Comparing nocturnal eddy covariance measurements to estimates of ecosystem respiration made by scaling chamber measurements at six coniferous boreal sites, *J. Geophys. Res.*, this issue

Levine, E. R., and R. G. Knox, Modeling soil temperature and snow dynamics in northern forests, *J. Geophys Res.*, this issue.

Li, Z., L. Moreau, and J. Cihlar, Estimation of the photosynthetically active radiation absorbed at the surface, *J Geophys. Res.*, this issue (a).

Li, Z., J. Cihlar, L. Moreau, F. Huang, and B. Lee, Monitoring fire activities in the boreal ecosystem, *J. Geophys. Res.*, this issue (b).

Loechel, S. E., C. L. Walthall, E. Brown de Colstoun, J. Chen, B. L. Markham, and J. Miller, Variability of boreal forest reflectances as measured from a helicopter platform, *J. Geophys. Res.*, this issue.

Loveland, T. R., J. W. Merchant, D. O. Ohlen, and J. F. Brown, Development of land cover characteristics data base for the conterminous U S., *Photogramm. Eng. Remote Sens.*, *57*(11), 1453–1463, 1991.

MacPherson, J. I., and A. K. Betts, Aircraft encounters with strong coherent vortices over the boreal forest, *J. Geophys. Res.*, this issue.

Mahrt, L., J. Sun, J. I. MacPherson, N. O. Jensen, and R. L Desjardins, Formulation of surface heat flux: Application to BOREAS, *J. Geophys Res.*, this issue.

Margolis, H. A., and M. G. Ryan, A physiological basis for biosphere-atmosphere interactions in the boreal forest: An overview, *Tree Physiol.*, *17*, 491–500, 1997.

Markham, B. L., J. S. Schafer, B. N. Holben, and R. N. Halthore, Atmospheric aerosol and water vapor characteristics over north central Canada during BOREAS, *J. Geophys. Res.*, this issue.

McCaughey, J. H., P. Lafleur, D. Joiner, P. A. Bartlett, A. M. Costello, D. Jelinski, and M. Ryan, Magnitudes and seasonal patterns of energy, water, and carbon exchanges at a boreal young jack pine forest in the BOREAS northern study area, *J. Geophys. Res.*, this issue.

Meeson, B. W., F. E. Corprew, D. M. Myers, J. W. Closs, K.-J. Sun, and P. J. Sellers, ISLSCP Initiative I-Global Data Sets for Land-Atmosphere Models, 1987–1988; CD-ROMs available from Blanche Meeson, NASA/GSFC, Code 902.2, Greenbelt, Md., 1995.

Middleton, E. M., J. H. Sullivan, B. D. Bovard, A. J. DeLuca, S. S. Chan, and T. A. Cannon, Seasonal variability in foliar characteristics and physiology for boreal forest species at the five Saskatchewan tower sites during the 1994 Boreal Ecosystem-Atmosphere Study (BOREAS), *J. Geophys Res.*, this issue.

Miller, J. R., and N. T. O'Neill, Multialtitude airborne observations of the insolation effects of forest fire smoke aerosols at BOREAS: Estimates of aerosol optical parameters, *J. Geophys. Res.*, this issue.

Miller, J. R., et al., Seasonal change in understory reflectance of boreal forests and influence on canopy vegetation indices, *J. Geophys. Res.*, this issue.

Mitchell, J. F. B., The seasonal response of a general circulation model to changes in CO_2 and sea temperature, *Q. J. R Meteorol Soc.*, *109*, 113–152, 1983.

Moosavi, S. C., and P. M. Crill, Controls on CH_4 and CO_2 emissions along two moisture gradients in the Canadian boreal zone, *J. Geophys. Res.*, this issue.

Myneni, R. B., C. D. Keeling, C. J. Tucker, G. Asrar, and R. R. Nemani, Increased plant growth in the northern high latitudes from 1981 to 1991, *Nature*, *386*, 698–702, 1997.

Nakane, K., T. Kohno, T. Horikoshi, and T. Nakatsubo, Soil carbon cycling at a black spruce (Picea mariana) forest stand in Saskatchewan, Canada, *J. Geophys. Res.*, this issue.

Ni, W., X. Li, C. E. Woodcock, J. L. Roujean, and R. E. Davis, Transmission of solar radiation in boreal conifer forests: Measurements and models, *J. Geophys. Res.*, this issue.

Nijssen, B., I. Haddeland, and D. P. Lettenmaier, Point evaluation of a surface hydrology model for BOREAS, *J. Geophys. Res.*, this issue.

Norman, J. M., C. J. Kucharik, S. T Gower, D. D. Baldocchi, P. M. Crill, M. Rayment, K. Savage, and R. G. Striegl, A comparison of six methods for measuring soil-surface carbon dioxide fluxes, *J Geophys. Res.*, this issue.

Ogunjemiyo, O. S., P. H. Schuepp, J. I. MacPherson, and R. L. Desjardins, Analysis of flux maps versus surface characteristics from Twin Otter grid flights in BOREAS 1994, *J Geophys Res.*, this issue.

Oncley, S., D. Lenschow, T. Campos, K Davis, and J. Mann, Regional-scale surface flux observations across the boreal forest during BOREAS, *J. Geophys. Res.*, this issue.

Pattey, E., R. L. Desjardins, and G. St-Amour, Mass and energy exchanges over a black spruce forest during key periods of BOREAS 1994, *J. Geophys. Res.*, this issue.

Peck, E. L., T. R. Carroll, R. Maxson, B. Goodison, and J. Metcalfe, Variability of soil moisture near flux towers in the BOREAS southern study area, *J. Geophys. Res* , this issue.

Privette, J. L., T. F. Eck, and D W. Deering, Estimating spectral albedo and nadir reflectance through inversion of simple BRDF models with AVHRR/MODIS-like data, *J Geophys. Res.*, this issue.

Randall, D. A., et al., A revised land surface parameterization (SiB2) for atmospheric GCMs, 3, The greening of the CSU GCM, *J. Clim.*, *9*(4), 738–763, 1996.

Ranson, K. J., G. Sun, R. H. Lang, G., N. S. Chauhan, R. J. Cacciola, and O. Kilic, Mapping of boreal forest biomass from spaceborne synthetic aperture radar, *J. Geophys. Res.*, this issue

Rayment, M. B., and P. G. Jarvis, An improved open chamber system for measuring soil CO_2 effluxes in the field, *J. Geophys. Res.*, this issue.
Rizzo, B., and E. Wiken, Assessing the sensitivity of Canada's ecosystems to climatic change, *Clim. Change*, *21*, 37–55, 1992.
Roulet, N. T., P. M. Crill, N. T. Comer, A. Dove, and R. A. Bourbonniere, CO_2 and CH_4 flux between a boreal beaver pond and the atmosphere, *J. Geophys. Res.*, this issue.
Russell, C. A., J. R. Irons, and P. W. Dabney, Bidirectional reflectance of selected BOREAS sites from multiangle airborne data, *J. Geophys. Res.*, this issue.
Ryan, M. G., M. B. Lavigne, and S. T. Gower, Annual carbon costs of autotrophic respiration in boreal forest ecosystems in relation to species and climate, *J. Geophys. Res.*, this issue.
Saugier, B., A. Granier, J. Y. Pontailler, E. Dufrêne, and D. D. Baldocchi, Transpiration of a boreal pine forest measured by branch bag, sapflow and micrometeorological methods, *Tree Physiol.*, *17*, 511–520, 1997.
Savage, K., T. R. Moore, and P. M. Crill, Methane and carbon dioxide exchanges between the atmosphere and the northern boreal forest soils, *J. Geophys. Res.*, this issue.
Schlesinger, W. H., *Biogeochemistry: An Analysis of Global Change*, Academic, San Diego, Calif., 1991.
Schlesinger, M. E., and J. F. B. Mitchell, Climate model calculations of the equilibrium climatic response to increased carbon dioxide, *Rev. Geophys.*, *25*(4), 760–798, 1987.
Schnur, R., T. W. Krauss, F. J. Eley, and D. P. Lettenmaier, Spatiotemporal analysis of radar-estimated precipitation during the BOREAS summer 1994 field campaigns, *J. Geophys. Res.*, this issue.
Sellers, P. J., and F. G. Hall, FIFE in 1992: Results, scientific gains, and future research directions, *J. Geophys. Res.*, *97*, 19,091–19,019, 1992.
Sellers, P. J., F. G. Hall, G. Asrar, D. E. Strebel, and R. E. Murphy, An overview of the First ISLSCP Field Experiment, *J. Geophys. Res.*, *97*, 18,345–18,372, 1992a.
Sellers, P. J., J. A. Berry, G. J. Collatz, C. B. Field, and F. G. Hall, Canopy reflectance, photosynthesis and transpiration, III, A reanalysis using enzyme kinetics-electron transport models of leaf physiology, *Remote Sens. Environ.*, *42*, 187–216, 1992b.
Sellers, P. J., et al., *Experiment Plan. Boreal Ecosystem-Atmosphere Study*, version 3.0, NASA Goddard Space Flight Cent., Greenbelt, Md., 1994.
Sellers, P. J., et al., Remote sensing of land surface for studies of global change: Models-Algorithms-Experiments, *Remote Sens Environ.*, *51*(1), 3–26, 1995a.
Sellers, P. J., et al., The Boreal-Ecosystem-Atmosphere Study (BOREAS): An overview and early results from the 1994 field year, *Bull. Am. Meteorol. Soc.*, *76*(9), 1549–1577, 1995b.
Sellers, P. J , et al., Comparison of radiative and physiological effects of doubled atmospheric CO_2 on continental climate, *Science*, *271*, 1402–1406, 1996a.
Sellers, P J., et al., The ISLSCP Initiative I Global Data Sets: Surface boundary conditions and atmospheric forcings for land-atmosphere studies, *Bull. Am. Meteorol. Soc.*, *77*(9), 1996b.
Sellers, P J., et al., *Field Operations in BOREAS in 1996*, version 2.0, NASA Goddard Space Flight Cent., Greenbelt, Md., 1996c.
Sellers, P. J., et al., Modeling the exchanges of energy, water, and carbon between continents and the atmosphere, *Science*, *275*, 502–509, 1997.
Shewchuk, S. R., Surface mesonet for BOREAS, *J. Geophys. Res.*, this issue.
Shuttleworth, J. W., et al., Eddy correlation of energy partition for Amazonian forest, *Q. J. R. Meteorol Soc.*, *110*, 1143–1162, 1984a.
Shuttleworth, J. W., et al., Observations of radiation exchange above and below Amazonian forest, *Q. J. R. Meteorol. Soc.*, *110*, 1163–1169, 1984b.
Simpson, I. J., G. C. Edwards, G. W. Thurtell, G. den Hartog, H. H. Neumann, and R. M. Staebler, Micrometeorological measurements of methane and nitrous oxide exchange above a boreal forest, *J. Geophys. Res.*, this issue.
Smith, E. A., et al., Area averaged surface fluxes and their time-space variability over the FIFE experimental domain, *J. Geophys. Res.*, *97*, 18,599–18,622, 1992.
Staebler, R. M., G. C. Edwards, S. Lee, G. den Hartog, H. H. Neumann, G. W. Thurtell, and G. Dias, Measurements of the methane flux from a pond in the boreal forest by eddy covariance, *Global Biogeochem. Cycles*, in press, 1997.
Steele, S. J., S. T. Gower, J. Vogel, and J. M. Norman, Root mass, net primary production and turnover in aspen, jack pine and black spruce forests in Saskatchewan and Manitoba, Canada, *Tree Physiol.*, *17*, 577–588, 1997.
Steyaert, L. T., F. G. Hall, and T. R. Loveland, Land cover mapping, fire regeneration, and scaling studies in the Canadian boreal forest with 1-km AVHRR and Landsat TM data, *J. Geophys. Res.*, this issue.
Sullivan, J. H., B. Bovard, and E. M. Middleton, Variability in leaf-level CO_2 and water fluxes in Pinus banksiana and Picea mariana in Saskatchewan, *Tree Physiol.*, *17*, 553–562, 1997.
Sun, J., D. H. Lenschow, L. Mahrt, T. L. Crawford, K. Davis, S. P. Oncley, J. I. MacPherson, Q. Wang, R. J. Dobosy, and R. L. Desjardins, Lake-induced atmospheric circulations during BOREAS, *J. Geophys. Res.*, this issue.
Suyker, A. E., S. B. Verma, and T. J. Arkebauer, Season-long measurement of carbon dioxide exchange in a boreal fen, *J. Geophys. Res.*, this issue.
Tans, P. P., I. Y. Fung, and T. Takahashi, Observational constraints on the global atmospheric CO_2 budget, *Science*, *247*, 1431–1438, 1990.
Trenberth, K. (Ed.), *Climate Systems Modeling*, 788 pp., Cambridge Univ. Press, New York, 1992.
Trumbore, S., and J. Harden, Accumulation and turnover of carbon in organic and mineral soils of the BOREAS northern study area, *J. Geophys. Res.*, this issue.
Vidale, P. L., R. A. Pielke Sr., L. T. Steyaert, and A. Barr, Case study modeling of turbulent and mesoscale fluxes over the boreas regions, *J. Geophys. Res.*, this issue.
Vining, R. C., and B. L. Blad, Estimation of sensible heat flux from remotely sensed canopy temperatures, *J. Geophys. Res.*, *97*, 18,951–18,954, 1992.
Way, J., R. Zimmermann, E. Rignot, K. McDonald, and R. Oren, Winter and spring thaw as observed with imaging radar at BOREAS, *J. Geophys. Res.*, this issue.
Whittaker, R. H., and G. E. Likens, *Primary Production of the Biosphere*, Springer-Verlag, New York, 1975.
Wilczak, J. M., M. L. Cancillo, and C. W. King, A wind profiler climatology of boundary layer structure above the boreal forest, *J. Geophys. Res.*, this issue.
Winston, G. C., E. T. Sunquist, B. B. Stephens, and S. E. Trumbore, Winter CO_2 fluxes in a boreal forest, *J. Geophys. Res.*, this issue.
Wofsy, S. C., M. L. Goulden, J. W. Munger, S.-M. Fan, P. S. Bakwin, B. C. Daube, S. L. Bassow, and F. A. Bazzaz, Net exchange of CO_2 in a mid-latitude forest, *Science*, *260*, 1314–1317, 1993.
Zepp, R. G., W. L. Miller, M. A. Tarr, R. A. Burke, and B. J. Stocks, Soil-atmosphere fluxes of carbon monoxide during early stages of postfire succession in upland Canadian boreal forests, *J. Geophys. Res.*, this issue.

D. Baldocchi, National Oceanographic and Atmospheric Administration, Oak Ridge, TN 37831.
A. Black, University of British Columbia, Vancouver, British Columbia, Canada.
J. Berry, Carnegie Institution, Stanford, CA 943015-1297.
J. Cihlar and F. E. Guertin, Canada Center for Remote Sensing, Ottawa, Ontario, Canada.
P. M. Crill, University of New Hampshire, Durham, NH 03824.
D. Fitzjarrald, Atmospheric Sciences Resource Center, Albany, NY 12205.
B. Goodison, Atmospheric Environment Service, Downsview, Ontario, Canada.
S. T. Gower, University of Wisconsin, Madison, WI 53706.
F. G. Hall, J. Newcomer, K. J. Ranson, P. J. Sellers, and D. Williams, NASA Goddard Space Flight Center, Code 923, Greenbelt, MD 20771. (e-mail: fghall@tpmail.gsfc.nasa.gov)
D. Halliwell, Forestry Canada, Edmonton, Alberta, Canada.
P. G. Jarvis, University of Edinburgh, Edinburgh, Scotland, UK.
R. D. Kelly, University of Wyoming, Laramie, WY 82070.
D. P. Lettenmaier, University of Washington, Seattle, WA 98195.
H. Margolis, Centre de Recherche en Biologie Forestière, Sainte-Foy, Quebec, Canada.
M. Ryan, United States Department of Agriculture, Fort Collins, CO 80526-2098.
D. E. Wickland, NASA Headquarters, Washington, D.C. 20546.

(Received September 10, 1997; revised November 17, 1997; accepted November 17, 1997.)